CHAPTER 5

RESULTS AND DISCUSSION

Numerical simulations have been carried out for multiple hemispherical, flat and flat-triangular disk spiked blunt body at a hypersonic Mach number of 6.2. The aerospike contain either one, two or three aerodisks wherein the radius of the front aerodisk is the smallest and the radii of the rear aerodisks increase progressively with the rear most aerodisk being the largest one. The radius of the front disk is varied from 2 *mm* to 8 *mm* for single aerodisk, from 2 *mm* to 6 *mm* for the two disk aerospike and from 2 *mm* to 4 *mm* for the three disk aerospikes. The *l/D* ratio, which is the ratio of the length of aerospike to the diameter of the base configuration, is varied from 1 to 2.5. The length of the aerospikes is measured between stagnation point of the base configuration without aerospike and the stagnation point of the front aerodisk along the spike axis. Besides the *l/D* ratio, the ratios l_1/l, which is the location of the rear aerodisk in terms of the percentage of total spike length, is also varied between 0.25, 0.5 and 0.75. For three aerodisk, configurations an additional ratio l_2/l' appears, which represents the location of the mid aerodisk in terms of the percentage of spike length between the stagnation points of the front aerodisk and rear aerodisk.

The flowfield around spiked blunt body a single aerodisk has been exhaustively studied in the literatures and its effect on drag reduction is well established. Despite this single aerodisk spiked configurations are studied in the present investigation for a better comparison between configurations with one aerodisk, two aerodisk and three aerodisk of varying sizes. The details of flowfield around single aerodisk spike configurations are thus not presented here.

5.1. Effect of Disk Size on Drag for Single Disk Aerospike

Numerical simulations have been carried out for hemispherical, flat and flat-triangular disk spiked blunt body. The 2 *mm* aerodisk is just an aerospike while 4 *mm* is a proper aerodisk which results stronger detached shock wave resulting in high stagnation pressure and larger region of recirculating flow behind the disk. The flow detached from the aerodisk reattaches on the main body which causes the formation of a reattachment shock wave and hence a peak reattachment pressure. As can be seen in Fig. 5.1, the peak reattachment pressure on the main body, for the bigger aerodisk is significantly lower than that for 2 *mm* aerospike hence a reduced drag.

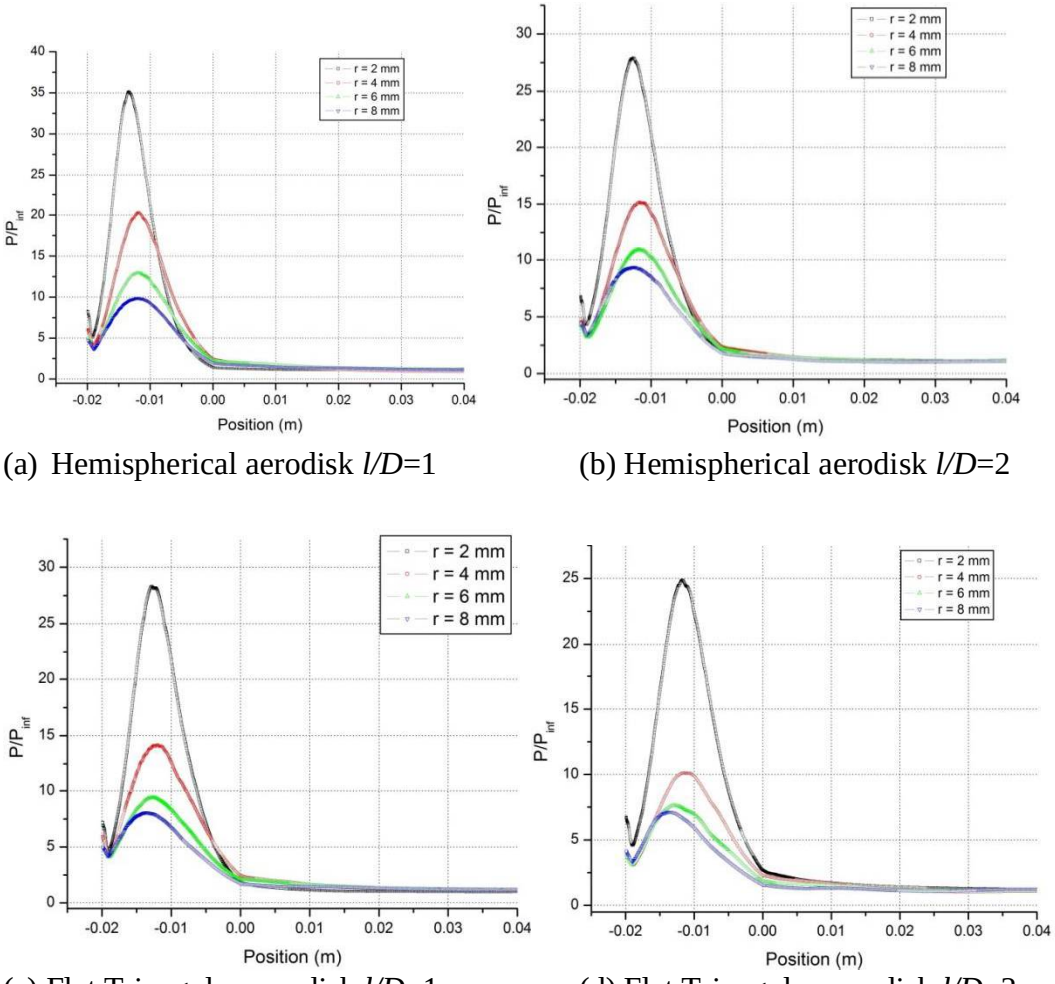

(a) Hemispherical aerodisk *l/D*=1 (b) Hemispherical aerodisk *l/D*=2

(c) Flat Triangular aerodisk *l/D*=1 (d) Flat Triangular aerodisk *l/D*=2

Fig. 5.1: Peak reattachment pressure for single disk aerospike

As can be seen in Fig. 5.2, a significant reduction in drag can be seen with the application of aerospikes at the nose for all cases investigated. For single hemispherical aerodisk spiked configurations, the highest reductions in drag are obtained with 6 *mm* disks which offer reductions of about 60% at *l/D*=1 to 67% at *l/D*=2.5. The reductions become more favorable for the flat aerodisks which give best results for a disk size of 6 *mm*. For this size of the flat aerodisk, the spiked configuration gives a reduction of 57% at *l/D*=1 and of 70% at *l/D* =2.5.

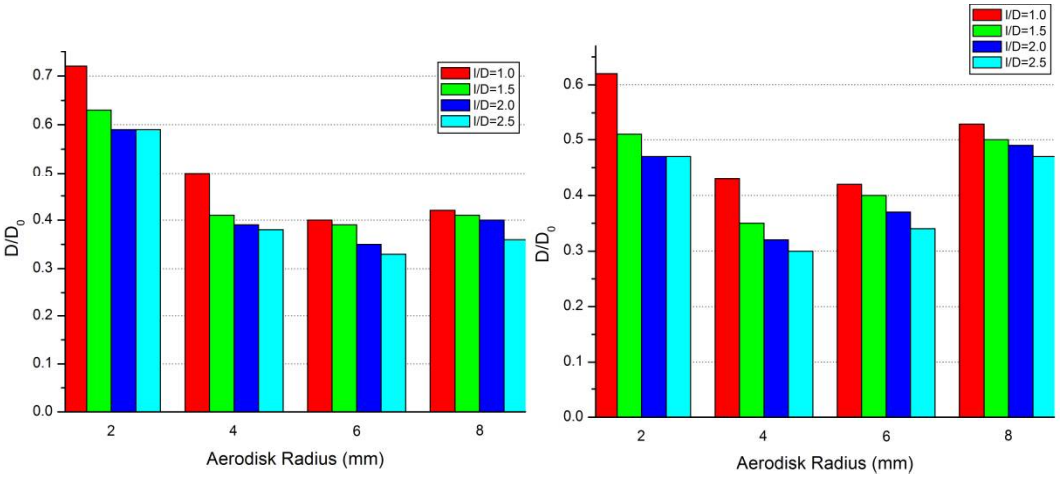

(a) Hemispherical aerodisk (b) Flat aerodisk

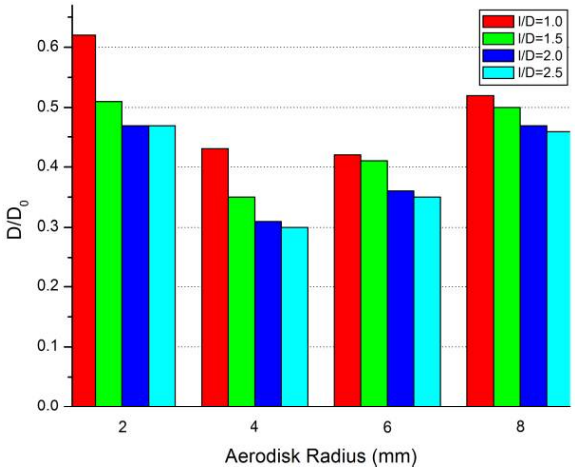

(c) Flat-triangular aerodisk

Fig 5.2: Drag coefficient for single disk aerospike

The single flat triangular aerodisks give the most favorable reductions for a disk size of 4 *mm* with 57% reduction at *l/D*=1 to 70% reduction at *l/D*=2.5.

For a given *l/D* ratio as the radius of the disk is increased from 2 *mm* to 6 *mm*, a decrease in drag is observed for hemispherical aerodisks. For 8 *mm* aerodisk however, the trend is not the same. Although the peak reattachment pressure continues to decrease with increasing radii of the disk, the strong bow shock that forms in front of the aerodisk results in a larger stagnation region where a very high stagnation pressure act, as can be seen in seen in Fig. 5.3. Under these circumstances, a significant portion of the total wave drag is contributed by the aerodisk itself.

For the same radii of the aerodisk, the stagnation pressure acts on a larger region for flat and flat triangular aerodisks as compared to hemispherical aerodisks. Thus, for the flat aerodisk the drag for 6 *mm* is slightly higher than that for 4 *mm* aerodisks. As the disk size increases further, the drag on the aerodisks dominates the total drag on the configuration and an increase in drag is observed for all shapes. This increase is primarily because of increase in the effective stagnation surface area acted upon by high pressure

For hemispherical aerodisk, the curvature of the bow shock is smooth and with increasing radii of the aerodisk, the vortical flow region increases in size laterally, reducing the wave-drag. At a radius of 8 *mm*, the wave drag on the disk itself accounts for a major portion of the overall drag because of a large stagnation area of the front aerodisk as can be seen in Fig. 5.4. This results in an increase in the drag of the whole configuration as the large drag on the aerodisk surpasses the reduction obtained on the main body.

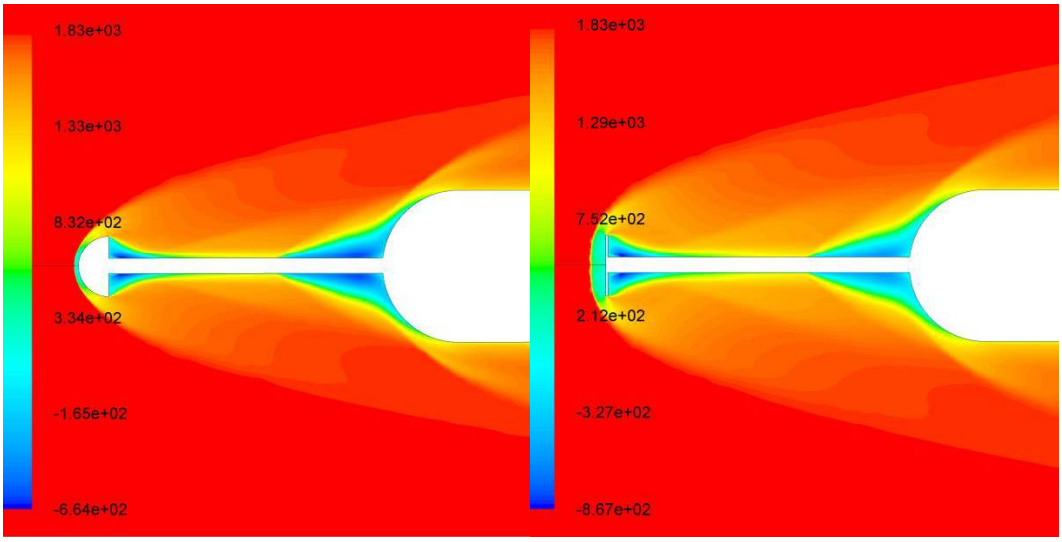

Fig. 5.3: Contours of axial velocity for single disk aerospike with r =4 *mm*

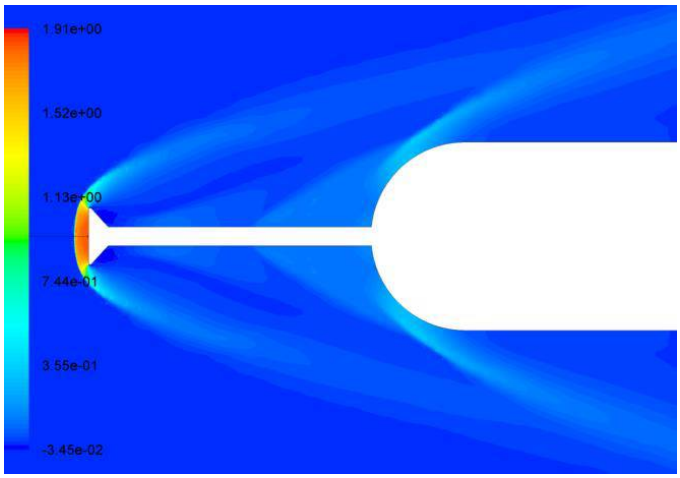

Fig. 5.4: Pressure coefficient for flat aerodisk *l/D=1.5, r =8 mm*

5.2. Heat Flux for Blunt Body with Single Disk Aerospike

For a given *l/D* ratio, as the radius of the disk is increased a decrease in the heat flux can be observed for both flat plate and flat triangular disk. This has also to do with the shape and size of the recirculating zone formed in front of the main body.

As the radius of the disk is increased, the high enthalpy flow is deflected farther away from the main body and the relatively low temperature flow recirculates in front of the main body as can be seen in Fig. 5.5, which shows the contours of

temperature for various single disk aerospikes. At the point of reattachment of the shear layer on the main body, a reattachment shock wave is formed causing an increase in temperature and heat flux. The value of this reattachment heat flux decreases with increasing radius of disk as can be seen in Fig. 5.6. The use of aerodisks results in a significant reduction in total heat transfer rate for all types of aerodisks, as can be observed from Fig 5.6.

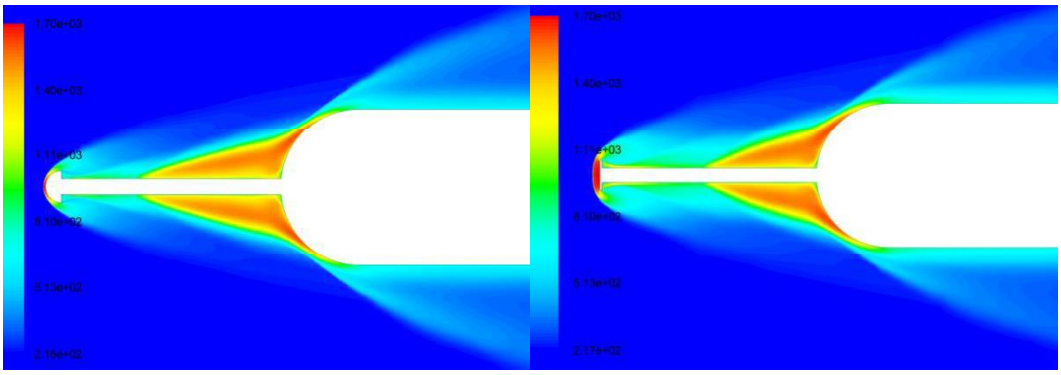

(a)Hemispherical aerodisk *l/D*=2, *r*=4 *mm* (b) Flat aerodisk *l/D*=2, *r*=4 *mm*

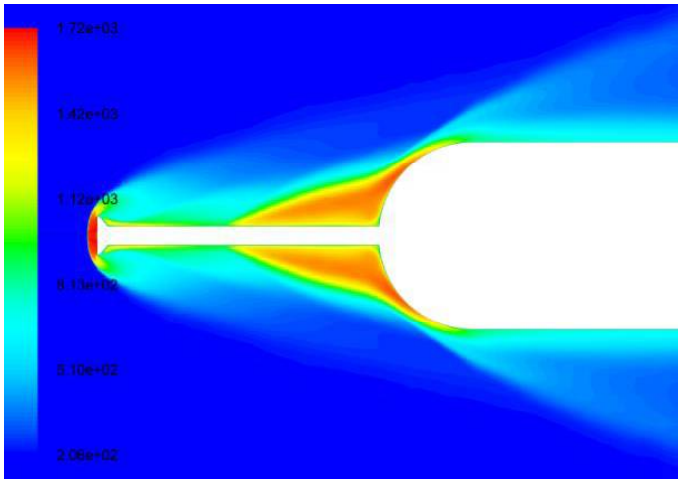

(c) Flat Triangular aerodisk *l/D*=2, *r*=4 *mm*

Fig: 5.5: Temperature contours of single disk aerospikes

For the same radius of aerodisk, as the length of the spike increases, the bow shock is pushed away from the main body and a decrease in heat flux is observed. Although the temperature in the shear layer reattachment layer is severe, most of the kinetic energy is dissipated as heat near the front stagnation region and a

significant amount heat energy transfers to spike disk and length. As can be seen in Fig. 5.7, with increasing length of the aerospike, fluid in the recirculating zone becomes cooler and cooler resulting in reduced overall heat transfer rates to the main body.

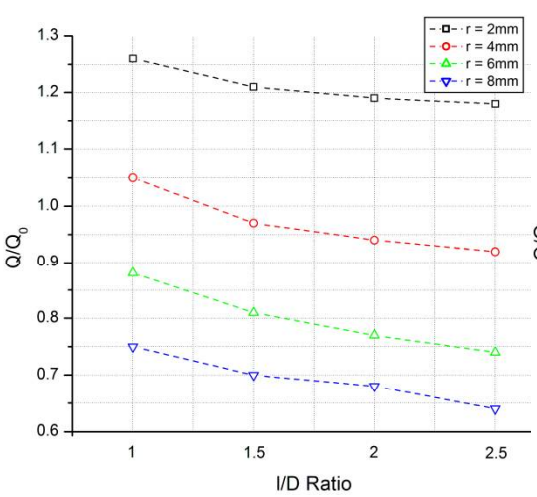

(a) Hemispherical aerodisk

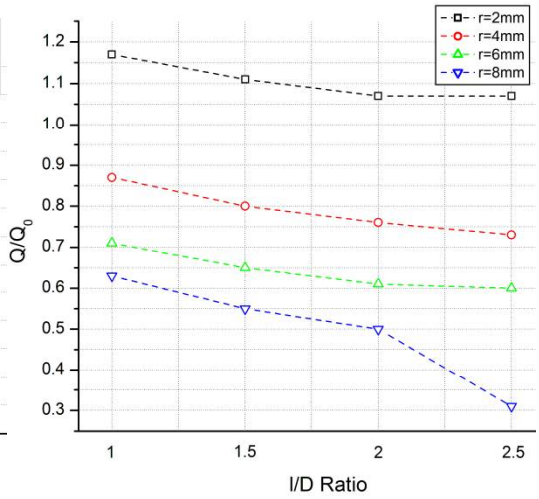

(b) Flat aerodisk

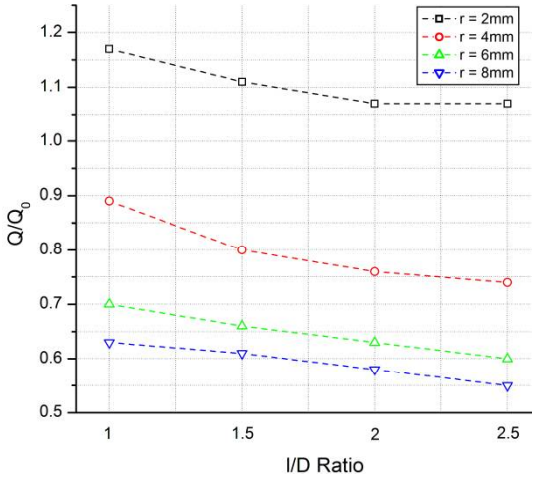

(c) Flat-triangular disk

Fig. 5.6: Integral Heat transfer rates

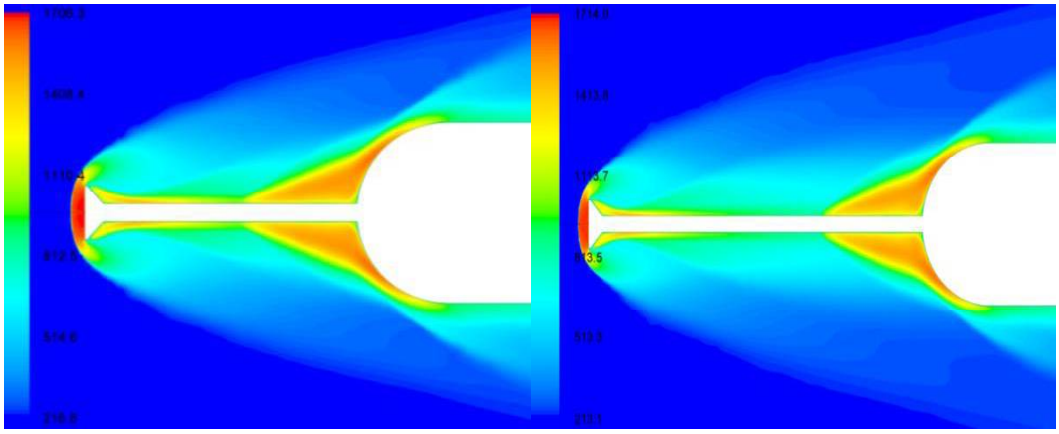

(a) Flat-triangular disk *l/D*=1.5 (b) Flat triangular disk *l/D*=2.5

Fig. 5.7: Temperature contours for flat triangular aerodisk with r_1=*6 mm*

5.3. Flow Field Around Blunt Body With Double Disk Aerospikes

The use of double disk modifies the flowfield significantly by adding extra recirculating region of fluid between the two aerodisks as can be seen in Fig 5.8, which shows the contours of axial velocity for a hemispherical double disk aerospike of *l/D* ratio 2. The blue regions are in the figure are clockwise vortices. The vortices formed in front of the main body and in front of the intermediate aerodisk helps in reducing the drag by creating suction in forward direction. Although a small vortex is formed behind each of the disks, the sizes of these vortices are small and overall effect of vortex system is a reduced drag. For the double disk aerospikes, the intermediate disk, also called as the *rear aerodisk*, is bigger in size as compared to the front aerodisk. The increment is of 2 *mm* in the radius of the aerodisk, for all the geometries. For all *l/D* ratios, the rear aerodisk is positioned at 0.25, 0.5 or 0.75 of the total aerospike length.

The flow between the aerodisks and between the aerodisk and the main body behaves like that for flow over cavities. When the rear disk is placed at 0.25 c, the cavity flow is that for an open cavity and a single dominating vortex is seen between the rear aerodisk and the main body. As the rear aerodisk is moved forward, the extent of the vortical flow increases and becomes more longitudinally aligned.

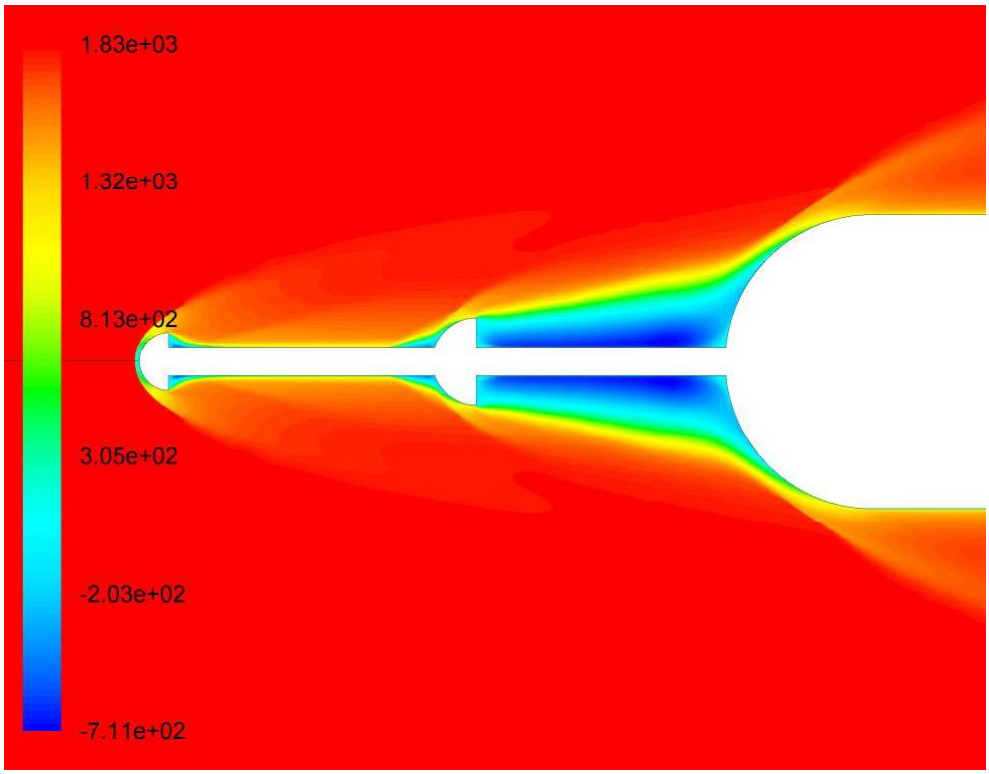

Fig 5.8: Axial Velocity contours for hemispherical double disk aerospike of l/D =2, r_1=6 *mm* r_2=*4 mm*, l_1/l=0.5

With the movement of the rear aerodisk, the size of the vortex in front of the rear aerodisk also increases, resulting greater suction in forward direction. Thus, the movement of the rear aerodisk in forward direction results in decrease of drag of the body. The suction phenomena is amplified for larger radii of aerodisks, as the region of vortical flow ahead of the rear aerodisk is strengthened with increasing disk radii as can be seen in Fig. 5.9. When the rear aerodisk is moved to 0.75*l*, the single vortex in front of the main body splits into two smaller vortices, both rotating in clockwise direction. For longer aerospikes, the presence of twin vortices can be seen for even 0.5*l* positions of rear disk.

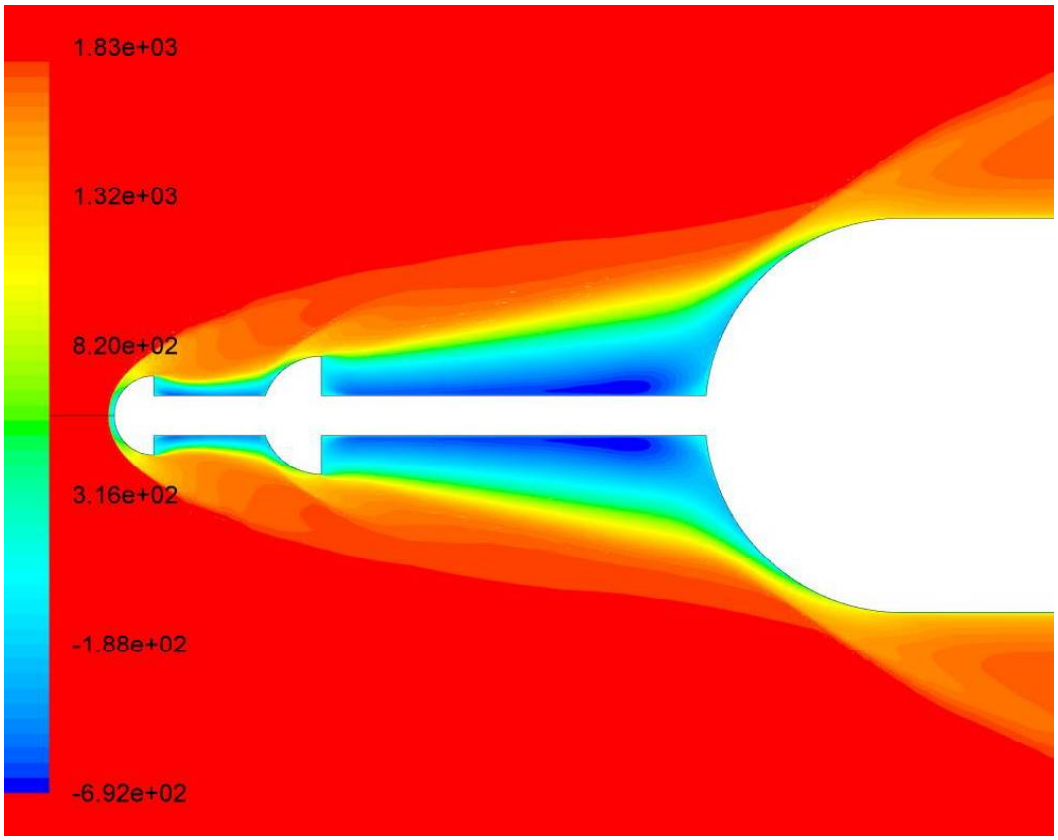

Fig 5.9: Axial Velocity contours for hemispherical double disk aerospike of l/D =2, r_1=6 *mm* r_2=*4 mm*, l_1/l=0.75

5.4. Effect of Aerodisk Shape for Double Disk Aerospikes

The flowfield around blunt body with double aerodisks of flat and flat triangular shape differ significantly from that of hemispherical aerodisks. As can be seen in Fig. 5.10, which shows contours of axial velocity for double flat disk aerospike of l/D=2, l_1/l=0.5, a large single vortex can be seen between the rear disk and the main body. As with hemispherical aerodisks the vortex breaks into two contra rotating vortices as the rear aerodisk moved to 0.75 of the total length of aerospike. Although the normal shock ahead of the front aerodisk is stronger as compared to the hemispherical case due to large frontal area, the presence of relatively large vortex in front of the rear aerodisk results in a reduced drag.

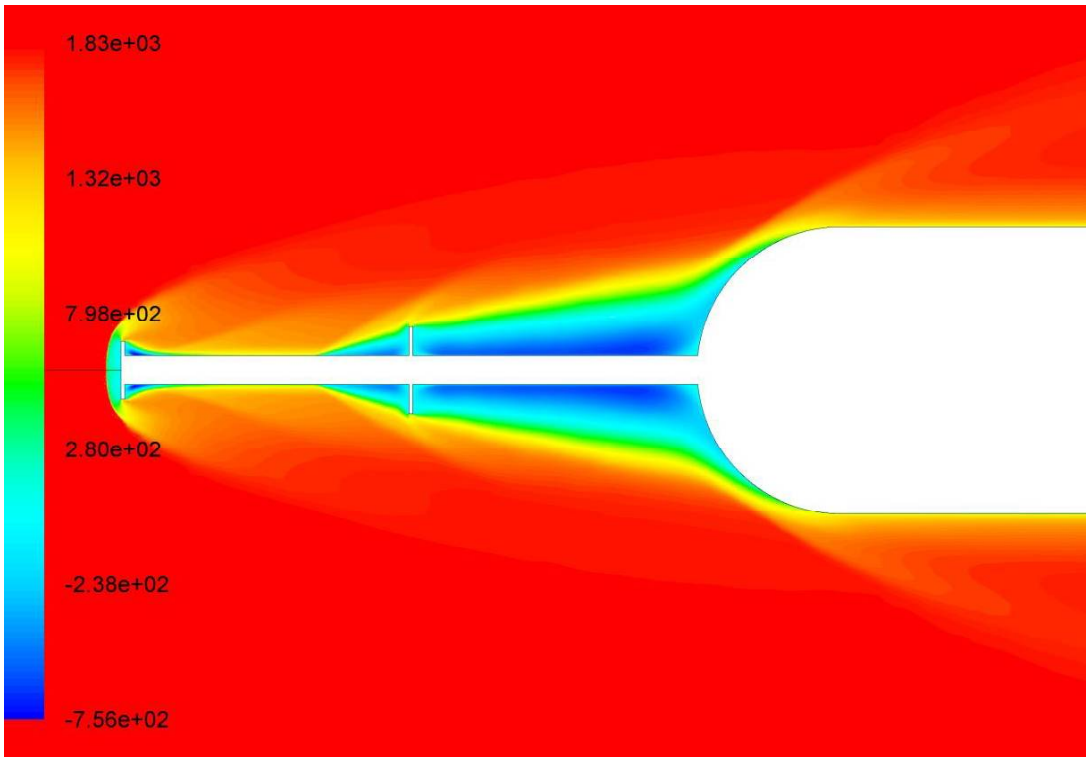

Fig. 5.10: Axial Velocity contours for flat double disk aerospike of l/D =2, r_1=6 *mm* r_2=*4 mm*, l_1/l=0. 50

The flowfield around blunt body with two flat triangular aerodisks is similar to that of those for flat aerodisks. Although the small vertices seen behind the aerodisks for flat aerodisk is not observed for the flat aerodisk. This results in the overlapping of surface pressures for the flat and flat triangular cases as can be seen in Fig. 5.11, which shows the non-dimensional pressure distributions on the surface of typical double disk configuration with hemispherical, triangular and flat triangular aerodisk. Consequently the drag reductions for flat and flat triangular aerodisk configurations are similar.

As can be seen in Fig. 5.11 the surface pressure distribution for double disk aerospikes with r_1=6 and r_2=4 *mm* and l_1/l=0.5 for l/D ratios of 1 and 2. It can clearly be seen that for both shorter and longer aerospikes, the peak attachment pressure for the hemispherical aerodisks is significantly higher than the other two shapes with resultant higher drags for hemispherical aerodisk.

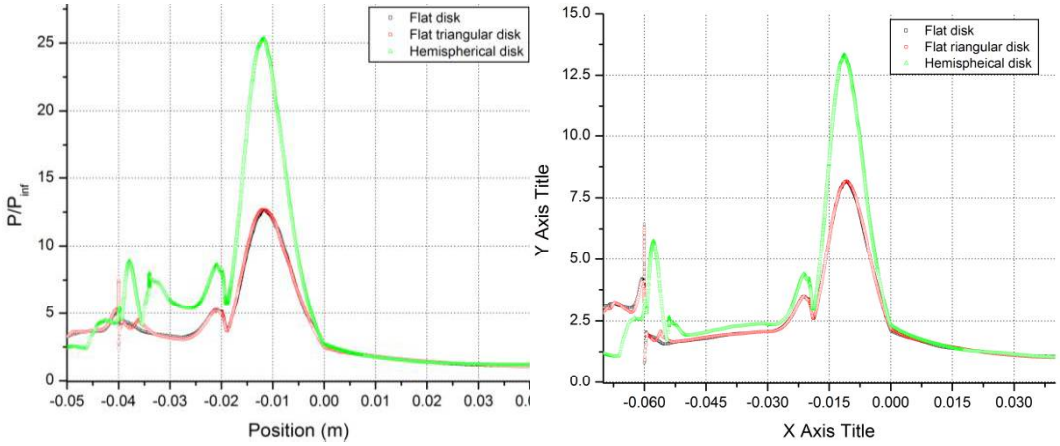

(a) *l/D*=1 (b) *l/D*=2

Fig. 5.11 Surface pressure distribution for double disk aerospikes

5.5. Effect of Double Disk Aerospike on Aerodynamic Drag

As with the single aerodisk aerospikes, the presence of double disks enhances the recirculating flow ahead of the blunt body and hence reduced drags. For two aerodisk spiked blunt bodies, there are two major regions of recirculating flow the helps in the reduction of pressure drag. The pressure rise and skin friction on the rear aerodisk add to the drag, but the overall effect is a reduction in drag as can be seen in Fig. 5.12. The bar charts, shown in Fig. 5.12 presents the aerodynamic drag of hemispherical double disk for *l/D* ratios of 1.0, 1.5, 2.0 and 2.5 for varying radii. For these hemispherical aerodisk spiked blunt body, more than 35% reduction in drag, as compared to the base body, is observed in all cases. The cases shown in Fig. 5.12 (a) have aerodisks of radii 2 *mm* and 4 *mm*, making it a single disk aerospike with disk at some intermediate position. As the overall *l/D* ratio of these hemispherical aerodisk aerospikes is increased, a gradual reduction in the drag of the blunt body is observed, with the longest aerospike investigated giving the lowest drag.

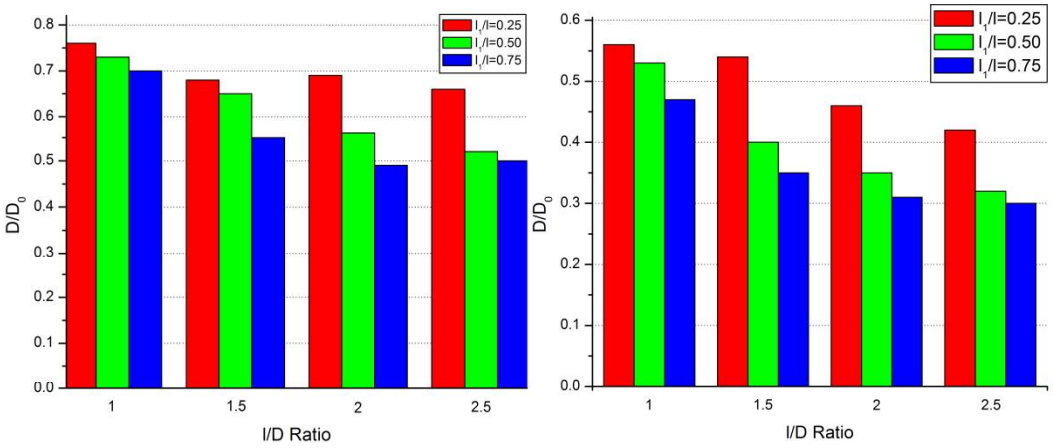

(a) r_1=4 mm r_2=2 mm (b) r_1=6 mm r_2=4 mm

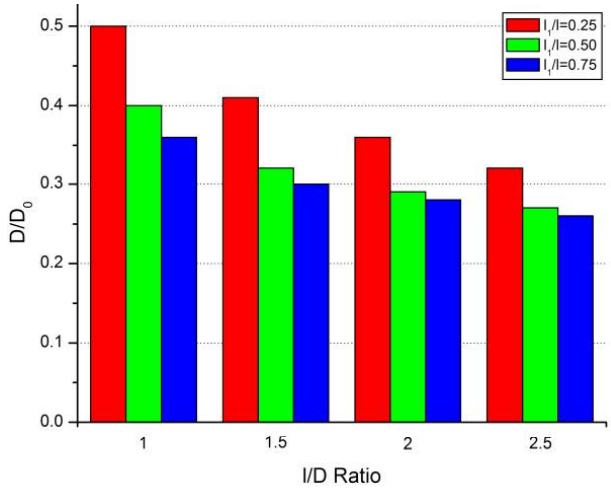

(c) r_1=8 mm r_2=6 mm

Fig. 5.12: Normalized drags for spiked blunt body with two hemispherical aerodisks

For a given length of two-disk aerospike *l*, the second aerodisk is positioned at 0.25 *l*, 05*l* or 0.75 *l* from the stagnation point of the base body. For hemispherical aerodisks as the rear aerodisk is moved forwards for a given length of aerospike, a reduction in drag is observed. This is probably because of the fact that in all these simulations the radii of the rear disk is chosen to be larger than the front aerodisk. Thus, moving the rear disk forward makes the recirculating flow region between

the rear aerodisk and the main body grows larger, which in turn reduces the drag further. In other words, the bigger aerodisk has the dominant role in the drag characteristics of the spiked blunt body. This is more emphasized when we observe the drag of spiked blunt body for increasing radii of aerodisks. With the increasing radius of the aerodisks a substantial reduction in drag is observed. For the hemispherical double disk aerospikes, a reduction in drag of up to 74% is observed for *l/D* ratio of 2.5 and aerodisk radii of r_1=6 *mm* and r_2=4 *mm*. For the largest hemispherical aerodisks investigated, the reduction trend continues for *l/D* ratio of 1.5. The increase in drag observed for single 8 *mm* aerodisk is not seen for the double aerodisk configuration with r_1=8 *mm* and r_2=6 *mm*, as the comparatively smaller front aerodisk weakens the shock wave for the rear larger aerodisk. The trends in reduction of drag for various aerodisk configurations can also be explained in terms of the peak reattachment pressure on the shoulder of the main body. A higher reattachment pressure is generally associated with a higher wave drag. The surface pressure distributions for selected hemispherical single and double-disk aerospikes are shown in Fig. 5.13. As can be seen in Fig. 5.13 (a), (b) and (c), for configurations with rear aerodisk close to the main body have a relatively large reattachment pressure, higher than even the single aerodisk configurations. Consequently, the double disk aerospikes with *l1/l =0.25* offers no improvement in drag reduction over single disk aerospikes. However, for all other configurations the peak reattachment pressure for hemispherical double disk aerospikes is lesser than that for single disk aerospike with same radii of the front disk. The result is a reduced drag for double disk aerospikes as compare to single disk aerospikes. The peak reattachment pressure on the shoulder of the main body reduces by a greater amount as the overall length of the aerospike is increased or as the rear aerodisk is moved forward for the same overall length of the aerospike. The reductions in drag follow the trends followed by the peak reattachment pressure.

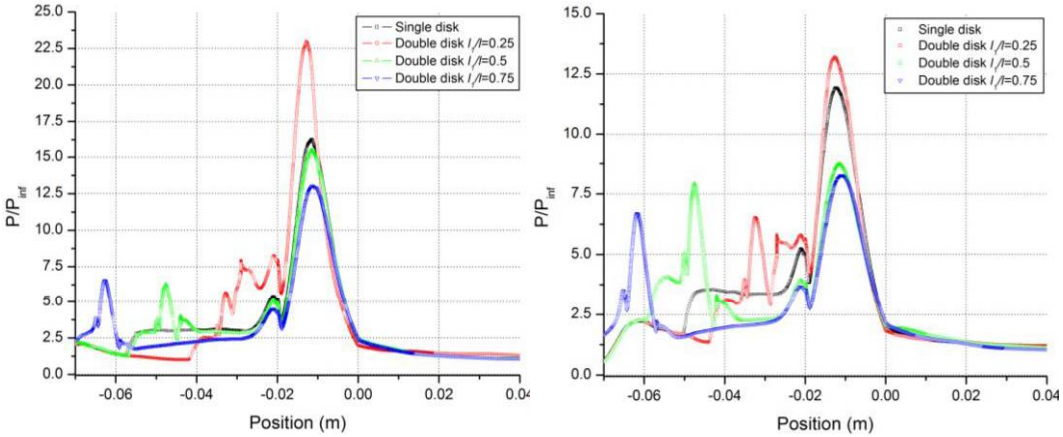

(a) *l/D=1.5, r_1=6 mm* and *r_2=4 mm*, (b) *l/D=1.5, r_1=8 mm* and *r_2=6 mm*

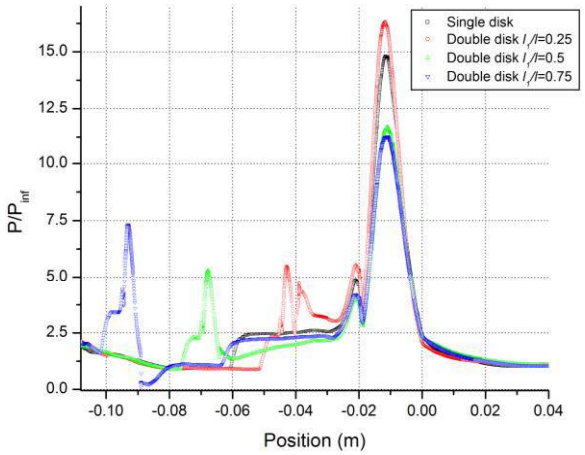

(c) *l/D=2.5, r1=6 mm* and *r2=4 mm*

Fig. 5.13: Surface pressure distribution for hemispherical aerodisk

The peak reattachment pressures for double disk aerospikes of flat plate and flat triangular shaped disks follow a slightly different trend as can be seen in Figs. 5.14 and 15. As with hemispherical aerodisks, for the flat plate and flat triangular aerodisks also the reattachment pressure rise is the maximum for the shortest overall length of aero-spike which is close to the diameter of main body, and becomes lower for larger length of aerospikes. However, the peak reattachment pressure for flat aerodisk is significantly lower than that for hemispherical aerodisks. For an *l/D* ratio of 1.5, the single flat disk with radius 4 *mm*, offers about 30% reduction in peak reattachment pressure single

hemispherical aerodisk and for flat two-disk aerospikes, the reattachment pressures lowers further..

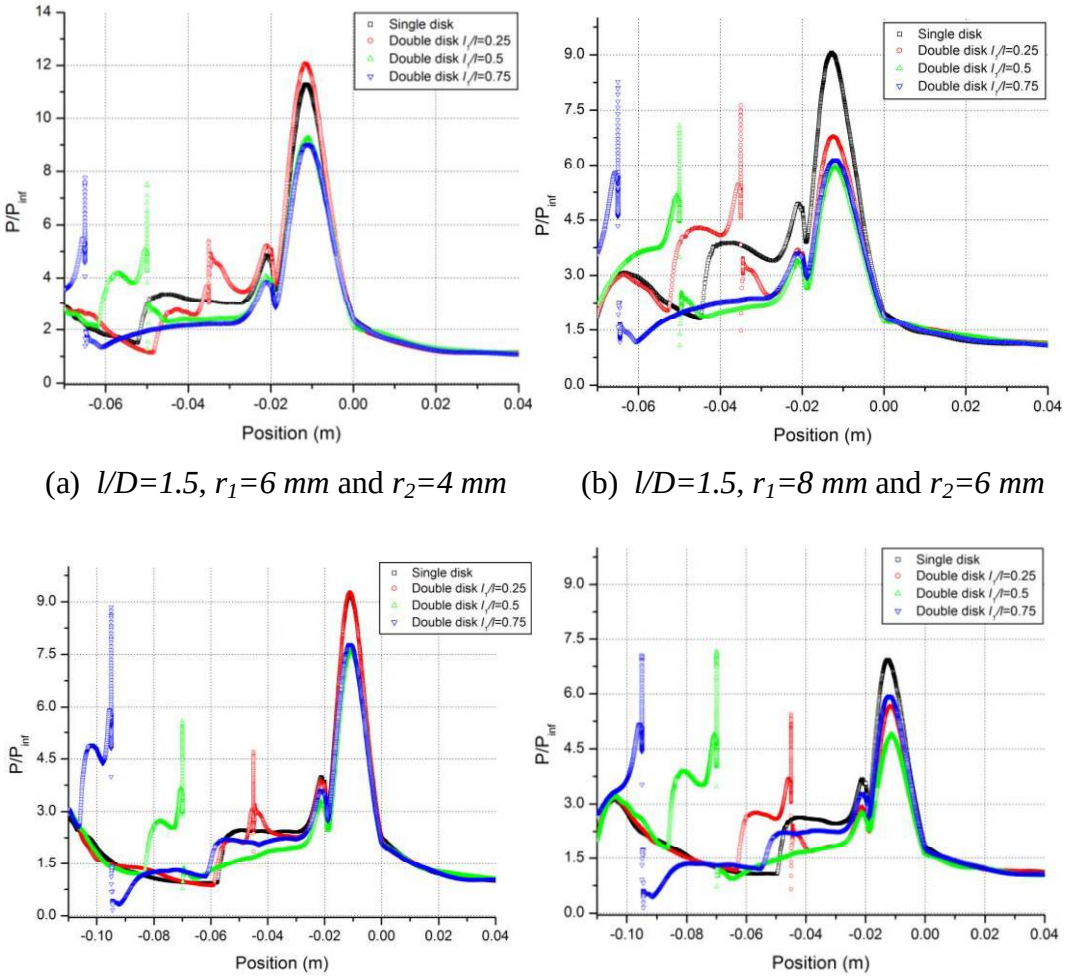

(a) *l/D=1.5*, r_1*=6 mm* and r_2*=4 mm* (b) *l/D=1.5*, r_1*=8 mm* and r_2*=6 mm*

(c) *l/D=2.5*, r_1*=6 mm* and r_2*=4 mm* (d) *l/D=2.5*, r_1*=8 mm* and r_2*=6 mm*

Fig. 5.14: Surface pressure distribution for flat aerodisk

Even for the double flat disk configurations with l_1/l=0.25 the reattachment pressure lower than that for single flat aerodisk The peak reattachment pressure lowers further as the rear aerodisk is moved forward with 25% reduction as compared to single disk aerospike, for the forward most position, for an *l/D* ratio of 1.5 and front disk radius of 4 *mm*. As the radius of the front flat disk in increased, further reduction in peak reattachment pressure and hence the aerodynamic drag is observed.

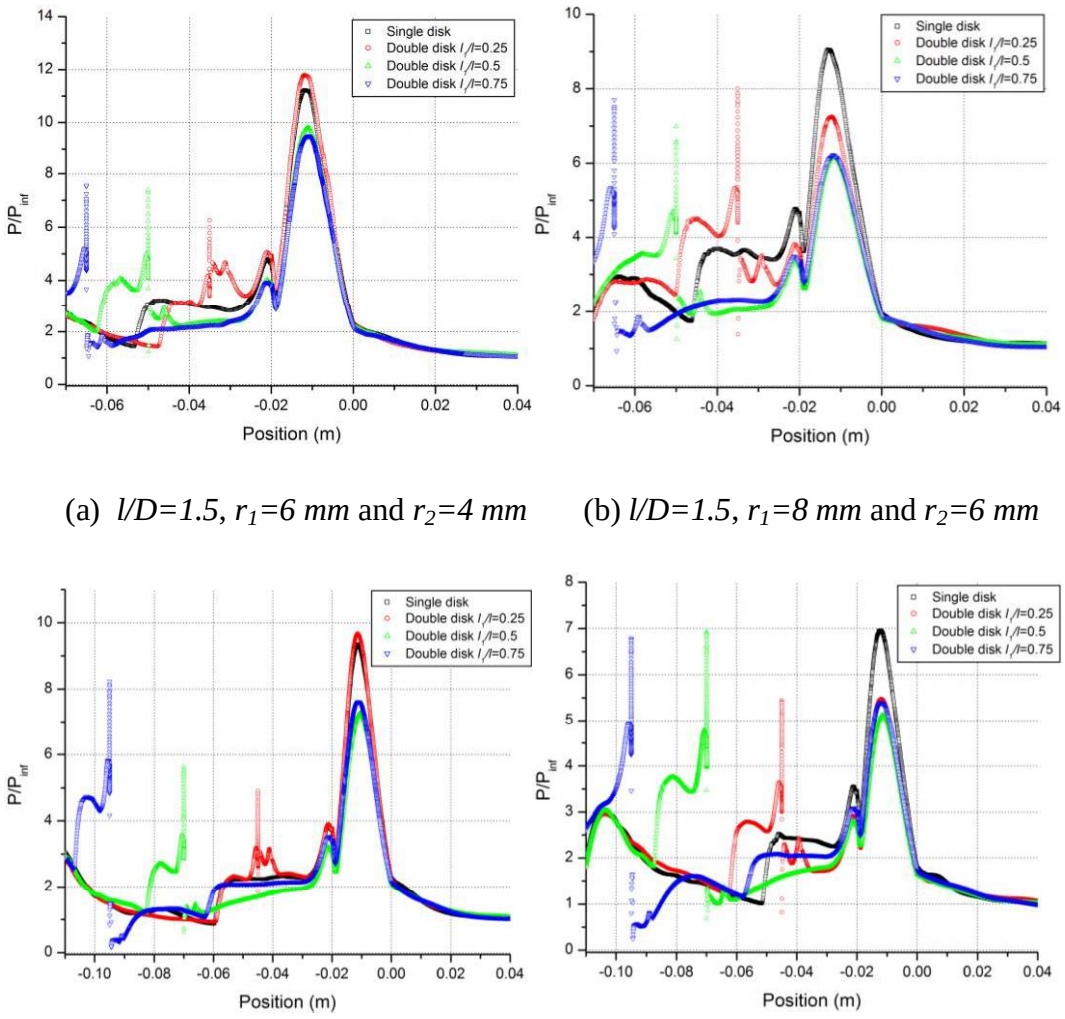

(a) *l/D=1.5*, r_1*=6 mm* and r_2*=4 mm* (b) *l/D=1.5*, r_1*=8 mm* and r_2*=6 mm*

(c) *l/D=2.5*, r_1*=6 mm* and r_2*=4 mm* (d) *l/D=2.5*, r_1*=8 mm* and r_2*=6 mm*

Fig. 5.15: Surface pressure distribution for flat triangular aerodisk

For flat disk configurations with r_1= 8 *mm* and r_2= 6 *mm*, the reattachment pressures are reduced by 22 to 33% for *l/D*=1.5 and by 15 to 33% for *l/D*=1.5, as compared to single flat disk configuration. These peak pressures are respectively about 25% and 50% lower than the corresponding peak pressures for hemispherical aerodisk of same configuration.

The surface pressure distributions for flat triangular aerodisk configurations are very similar to that for flat aerodisk as can be observed from Fig. 5.15, giving similar drag values.

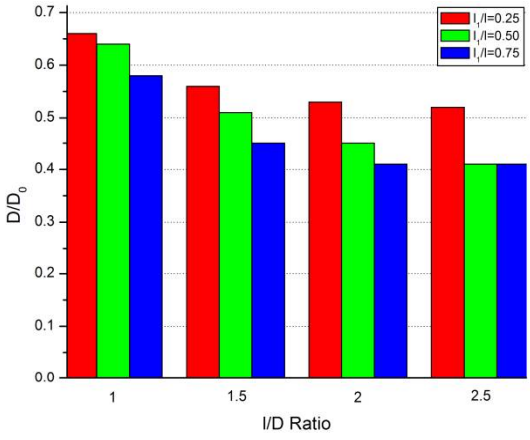

(a) r_1=4 mm and r_2=2 mm

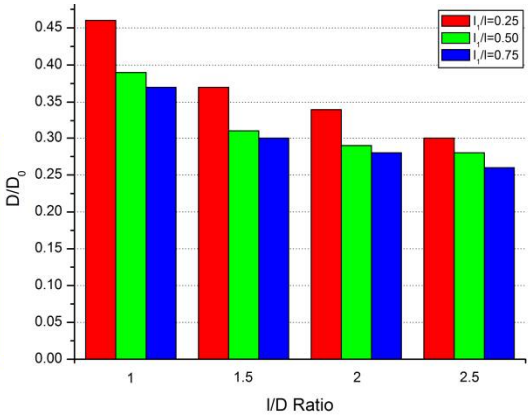

(b) r_1=6 mm and r_2=4 mm

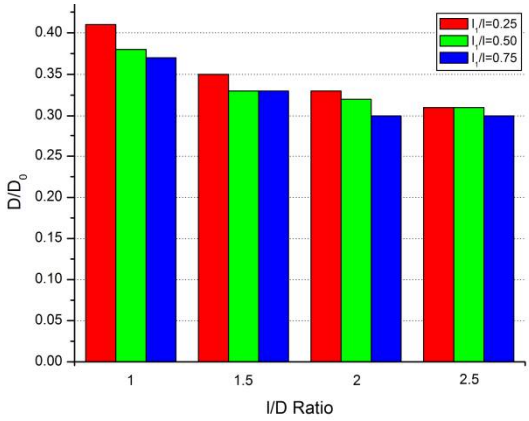

(c) r_1=8 mm and r_2=6 mm

Fig 5.16: Normalized drags for spiked blunt body with double flat aerodisks

The reduced peak reattachment pressure for the double flat disk and flat triangular aerodisk is literally translated to a reduced overall drag as compared to that of hemispherical double disk configurations, as can be seen in the bar charts of Fig. 5.16 and Fig. 5.17 respectively. The bar charts in Fig. 5.16 represent the aerodynamic drag of flat double-disk for *l/D* ratios of 1.0, 1.5, 2.0 and 2.5 for varying radii of the front aerodisk.

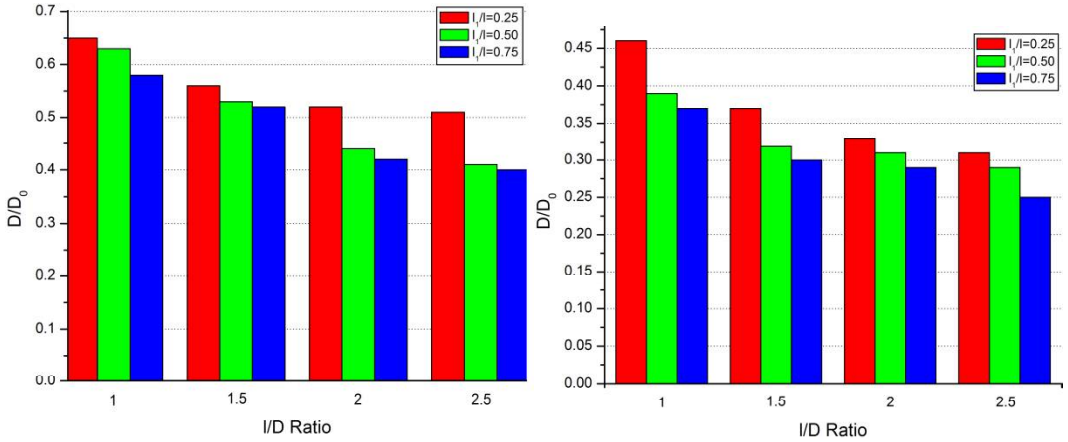

(a) r_1=4 mm and r_2=2 mm (b) r_1=6 mm and r_2=4 mm

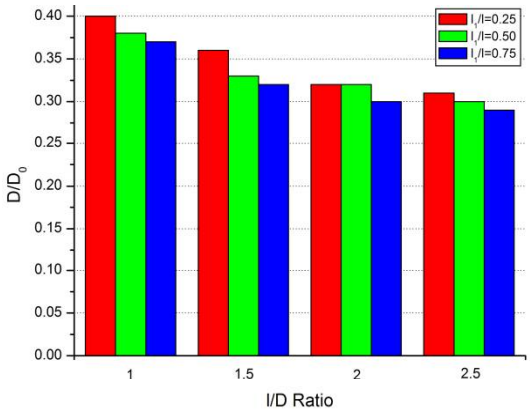

(c) r_1=8 mm and r_2=6 mm

Fig 5.17: Normalized drags for spiked blunt body with double flat triangular aerodisks

As can be seen in bar charts, the drag gradually decreases as rear aerodisk is moved forward, a trend similar in all double disk configurations. The drag reductions in flat aerodisk are considerably higher as compared hemispherical aerodisk with reductions of about 40% to 78% is observed as compared to the base configuration. The drag for double flat aerodisk configurations reduced as the overall length of the aerospike is increased for the same radii of the disks. For the same overall length and the internal positions, as the radii of the disk are

increased, the drag is diminished. But for very large flat aerodisks at *l/D* ratios of 2.5 a slight increase in drag observed due to the fact that the large surface pressures acting on the rear aerodisk compensates the reduced pressures on the main body.

The optimal drag reductions with flat aerodisks are obtained with r_1=6 *mm* and r_2=4 *mm* and *l/D* ratio of 2.5 with rear disk at 0.75l. A reduction of 78% in drag is observed for this configuration.

As with the surface pressure distribution and peak reattachment pressures, the drag reductions for flat triangular aerodisks are almost same as that for the flat aerodisks giving out a minimum of 40% reduction and a maximum of 78% reductions at shortest and longest configurations respectively. The maximum reduction is obtained for the size of r_1=6 *mm* and r_2=*4 mm* with the rear disk at the forward most position as can be seen in fig. 5.17 (b).

5.6. Effect of Double Disk Aerospikes on Heat Transfer Rates

5.6.1. Heat Transfer Rates for Hemispherical Double Disk Aerospikes

The surface heat flux distribution for two disk spiked configurations follows a trend similar to the pressure distribution. A considerable amount of kinetic energy is dissipated as heat at the aerodisks as can be seen in Fig. 5.18. Figure 5.18 shows the surface heat flux distributions for hemispherical aerodisks, normalized with the peak heat flux for the base configuration. The local heat fluxes for hemispherical two disk aerospike is generally lower than that for the base configuration. For the configurations with r_1=*4 mm* and r_2=*2 mm*, which virtually means no front aerodisk, the reattachment heat flux is about 81% higher than that of the base configurations, for an *l/D* ratio of 1 and l_1/l=0.25. As the rear aerodisk is moved forward or as the overall *l/D* is increased, the peak heating decreased, but for no cases with r_1=*4 mm* and r_2=*2 mm*, any reduction in peak heating is observed. As can be seen in Fig. 5.18, a reduction of up to 27% seen at *l/D*=1.5, in the case of configuration with r_1=6 *mm* and r_2=4 *mm* is increased by up to 40% at an *l/D* ratio of 2.5.

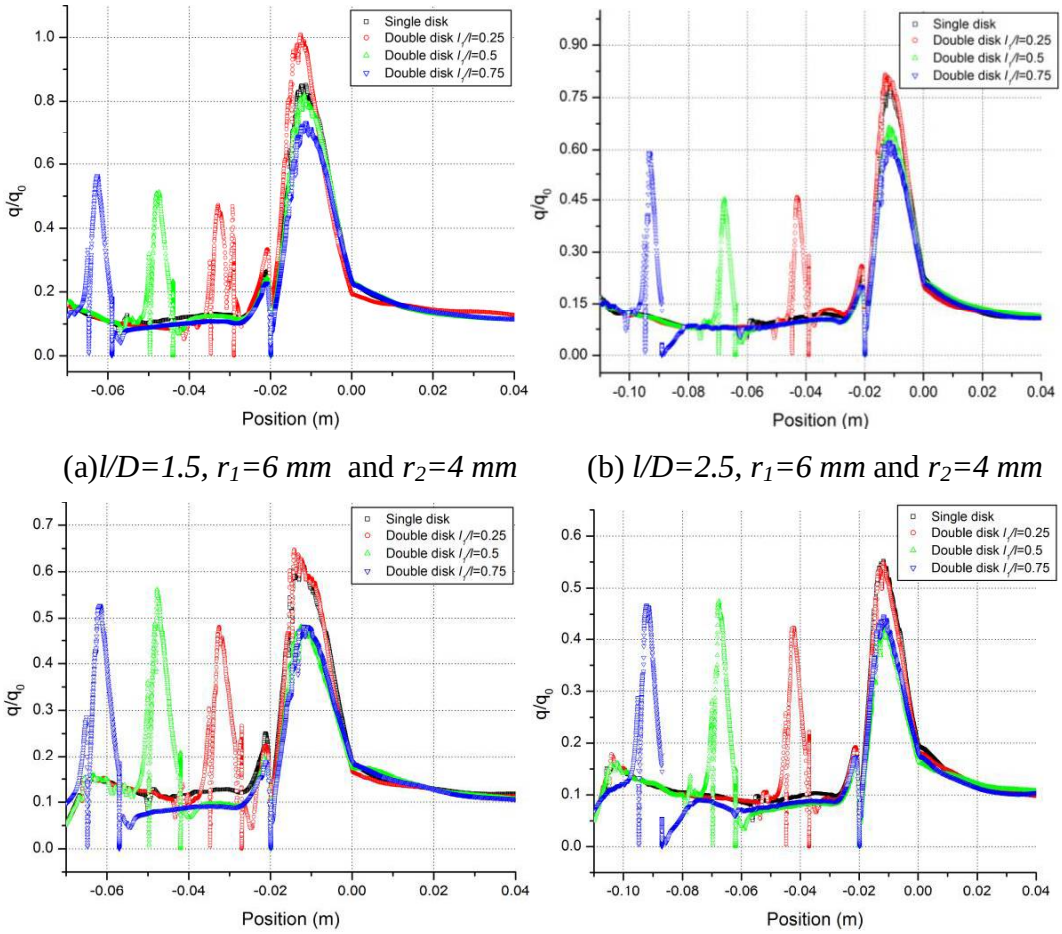

(a)*l/D=1.5, r_1=6 mm* and r_2=4 *mm* (b) *l/D=2.5, r_1=6 mm* and r_2=4 *mm*

(c) *l/D=1.5, r_1=8 mm* and r_2=6 *mm* (d) *l/D=2.5, r_1=8 mm* and r_2=6 *mm*

Fig. 5.18: Surface heat flux distributions for hemispherical double disk

For the configurations with r_1=8 *mm* and r_2=6 *mm*, reductions of about 35% to 52% is observed at an *l/D* of 1.5 and reductions of about 45% to 55% in heat fluxes is observed for an *l/D* of 2.5. The variations at each *l/D* are due to the movement of rear aerodisk. The forward movement of rear aerodisk for a given overall length also improves the peak heat transfer rates. The double disk configurations with the rear disk at 25% of length of aerospike give the highest local heating rates for all lengths and radii of aerodisks. For a smaller *l/D* ratios and rear most position of the rear aerodisk the peak heat fluxes are close to that for the base configuration. As compared to a single aerodisk aerospikes the double disk aerospike configuration gives a lowered peak reattachment heat fluxes, except for the cases with rear disk located at 0.25 of the overall length of

the spike. As can be seen in Fig. 5.18 (c), with same radii of the front aerodisk, the double disk aerospike offers about a 27 % reduction in peak heat fluxes at *l/D* of 1.5 with rear disk at 75% of the total length of spike, whereas the single disk aerospike offers only 10% reduction. The advantage in reduction of peak reattachment heat flux is observed clearly with the used of double disk aerospikes.

The reductions in peak reattachment heat fluxes also impacts the total heat transfer rates to the main body. Although a fair amount of heat is transferred to the aerodisks, the post compression shock wave temperatures result in large heat transfer rate to the main body. Despite the large reattachment heat fluxes, the longer aerospikes show a considerable reductions in total heat transfer rates as can be observed in Fig. 5.19. In Fig. 5.19, the integral or total heat transfer rates to the main body are divided by the total heat transfer rates to the main body in absence of any aerospike or aerodisk.

As can be seen in Fig. 5.19, for a small *l/D* ratios the hemispherical double disk can result in up to 29% increase in total heat transfer rates for r_1*=4 mm* and r_2*=2 mm*. The configurations with r_1*=4 mm* and r_2*=6 mm* are actually single disk aerospikes with the disk placed at some intermediate position on the spike. But with an increase in disk radii, quite favorable reductions in total heat transfer rates were observed as can be seen in Fig. 5.19 (b) and (c). For the configuration with r_1*=6 mm* and r_2*=4 mm*, reduction of about 8% for *l1/l*=0.25 at an *l/D*=2.5 were observed. As the rear aerodisk is moved forward on the spike, further reduction total heat transfer rates can be observed. For configuration with r_1*=6 mm* and r_2*=4 mm*, the reductions in heat transfer rates increased up to 19% at an *l/D* ratio of 2.5 for *l1/l*=0.75, as can be seen in Fig. 5.19 (b). For the configurations with r_1*=6 mm* and r_2*=8 mm*, reductions between 15% and 35% in total heat transfer rates were observed.

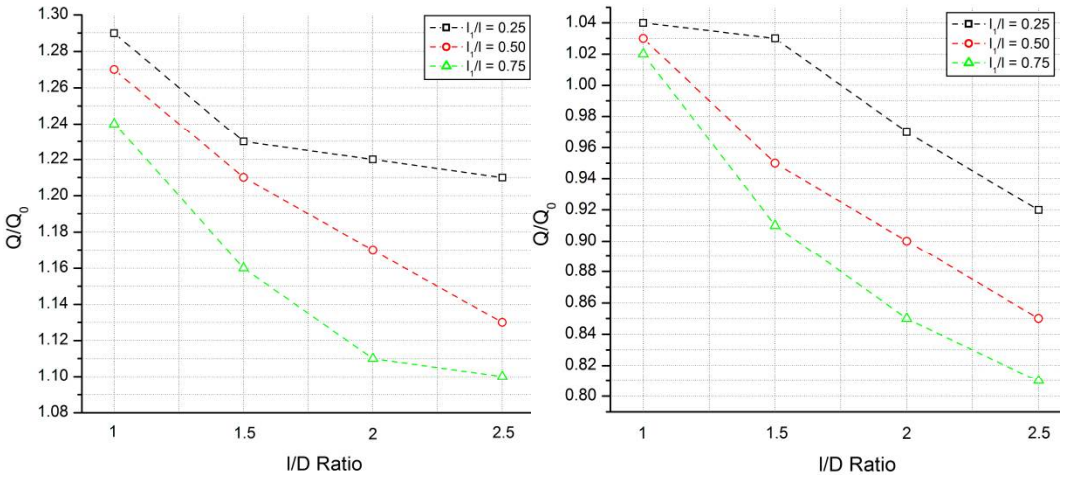

(a) r_1=4 *mm* and r_2=2 *mm* (b) r_1=6 *mm* and r_2=4 *mm*

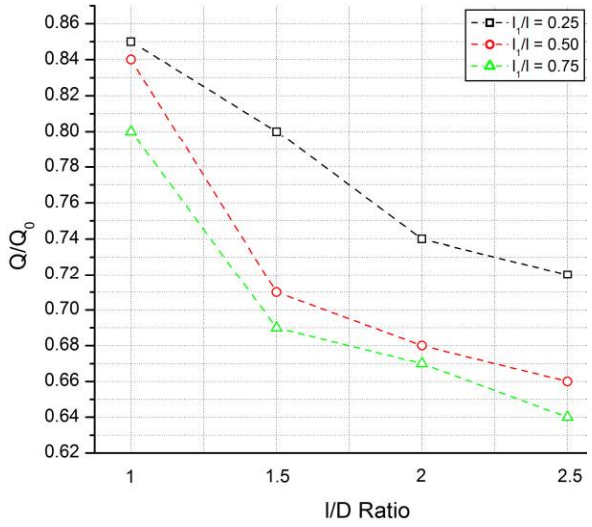

(c) r_1=8 *mm* and r_2=6 *mm*

Fig. 5.19: Total heat transfer rates on main body for hemispherical double disk aerospike for various disk radii.

A clear trend in reduction of total heat transfer rates can be observed, with respect to increase in disk radii or overall *l/D* ratio of aerospike. As the *l/D* ratio of the double hemispherical disk aerospike is increased as gradual reduction in total heat

transfer rates to the main body is observed. The reductions are further augmented by the forward position or the rear dominating aerodisk, thereby the configurations with largest *l/D* ratio and forward most position of the rear disk giving the largest reduction in total heat transfer rates.

Also for a given *l/D* ratio and the intermediate position of the rear disk the size of the disk controls the reduction in total heat transfer rates. Amongst the investigated cases the configurations with larger disk radii giving out the larger reduction in aerodynamic heating. The variations in local heat fluxes and total heat transfer rates depend highly the interactions between the shock waves and shear layers emanating from the front aerodisk with those from the rear aerodisk. Fig. 5.20 shows the temperature contours for hemispherical double disk aerospike configurations with disk radii r_1= *6 mm* and r_2=4 *mm*.

As can be seen from Fig. 5.20(a), for a small *l/D* ratio, with l_1/l=0.25, the shear layer detaches well ahead of the rear aerodisk and the angle of shear layer is such that it strikes directly on the shoulder of the main body, without dissipating much of heat to the rear disk. This results in larger heat fluxes to the main body and hence a large heat transfer rate. As the rear aerodisk is moved forward, the point of detachment of the shear layer also moves forward on the spike. The detached shock layer hits the shoulder of the rear aerodisk dissipating a considerable amount of heat to the rear aerodisk. This results in a reduced reattachment heat fluxes on the main body and a consequently lowered total heat transfer rates.

As the *l/D* ratio is increased, for a given l_1/l ratio, so does the position of the rear disk from the base body. This pushes the detachment point of the shear layer forward resulting in a reduction heat fluxes to the main body as can be seen in Fig. 5.20(c).

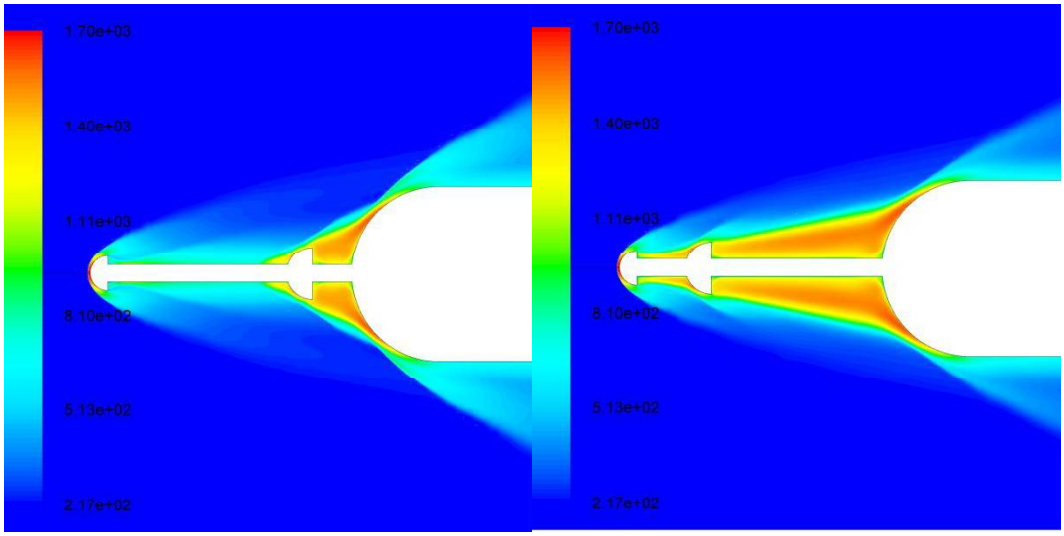

(a) l/D=1.5, l_1/l=0.25 (b)l/D=1.5, l_1/l=0.75

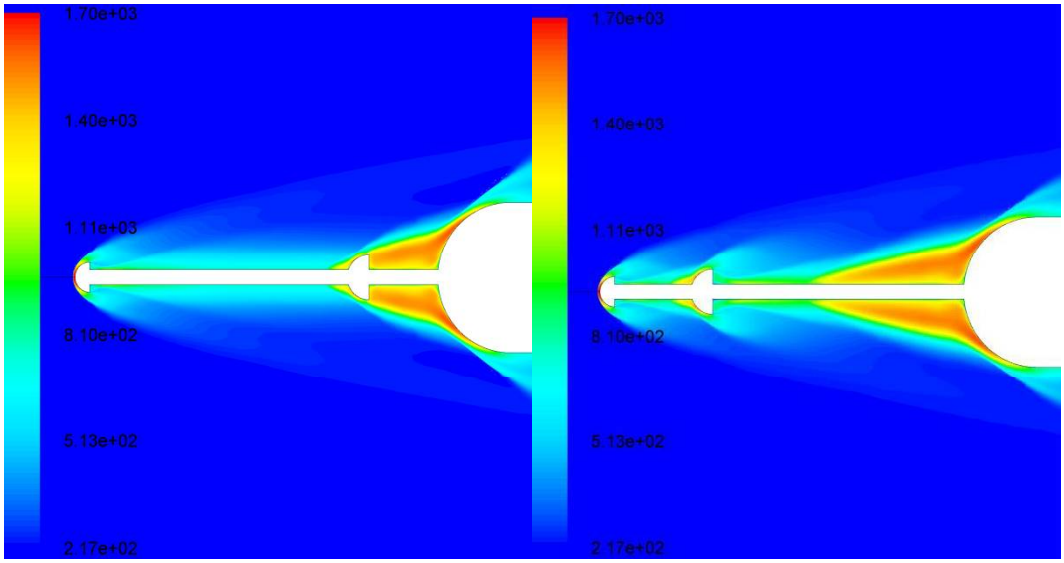

(a) l/D=2.5, l_1/l=0.25 (d)l/D=2.5, l_1/l=0.75

Fig. 5.20: Temperature contours for hemispherical aerodisk with disk radii r_1=6 *mm*, r_2=*4 mm*

For aerospikes with l/D=2.5 however, the rear aerodisk is relatively at a large distance from the base and the detached shear layer reattaches on the spike aft of the rear disk dissipating some heat to the spike. The shear layer detaches again from the spike stem and hits the main body with slightly larger heat fluxes. So the

reduction in heat fluxes with movement of rear aerodisk for longer aerospikes is not as significant as for shorter aerospikes. Nevertheless for r_1=6 *mm* and r_2=4 *mm*, the configuration with *l/D* =2.5 and l_1/l gives the highest reduction in heat fluxes. As the radii of hemispherical aerodisks is increased to a combination of r_1=8 *mm* and r_2=6 *mm*, the shear layer is pushed further away from the main body as can be seen in Fig. 5.21. Because of a large rear disk radius, the detached shear layer hits the rear disk dissipating a considerable amount of heat even for configurations with l_1/l =0.25 as observed in Fig. 5.21 (a).

With the movement of rear disk, the detachment point moves forward on the spike. For an *l/D* =1.5, and l_1/l =0.75, the shear layer detached from the front aerodisk does not reattach on any point on the spike stem, dissipating a large amount of heat to the rear aerodisk. This gives a large reduction in heat fluxes to the main body. As the length of aerospike is increased, the location of shear layer detachment moves forward on the spike for smaller values of l_1/l as can be seen in Fig. 5.21 (c).

For very long aerospikes with rear aerodisk moved to a very forward position, the shear layer reattaches just aft of the rear disk to detach i*mm*ediately before attaching again on the shoulder of the main body, as can be seen in Fig. 5.21 (d). This slightly reduces the magnitude of additional heat flux reduction. Thus, for double hemispherical aerodisk with r_1=8 *mm* and r_2=6 *mm*, added reduction in heat fluxes ceases with forward movement of rear aerodisk beyond *l1/l*=0.5. For this set of disk radii, the configuration with *l/D*=2.5 and *l1/l*=0.5 gives the maximum reduction in heat fluxes as in this case the detachment point of shear layer on the spike is the farthest from the main body, ahead of the rear aerodisk.

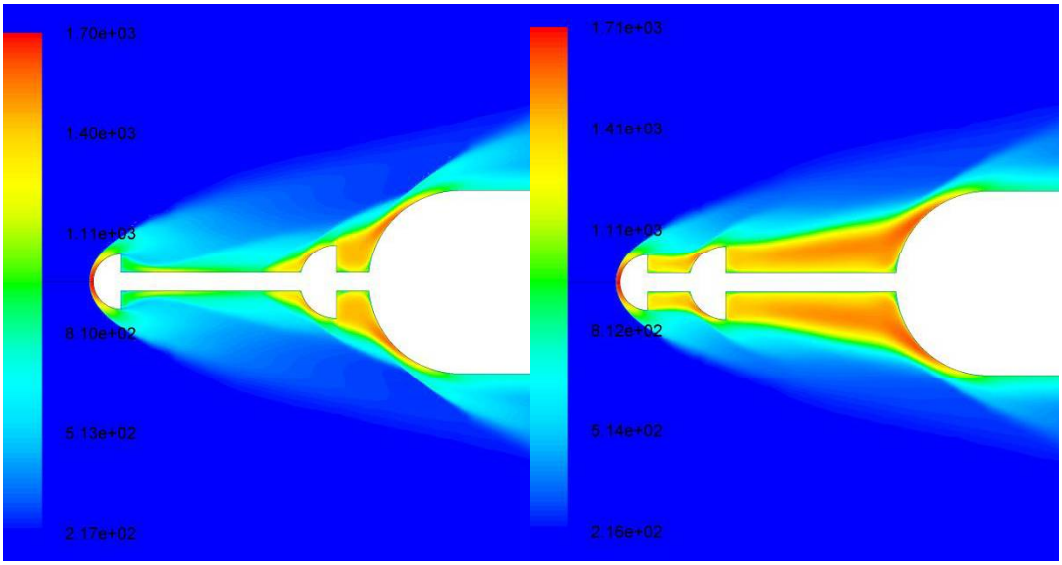

(a) l/D=1.5, l_1/l=0.25 (b) l/D=1.5, l_1/l=0.75

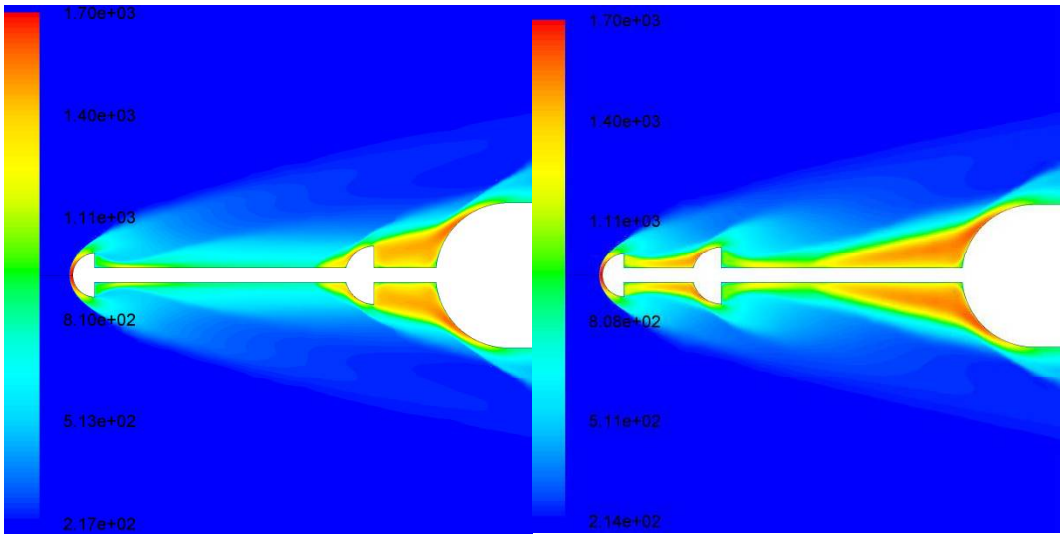

(c) l/D=2.5, l_1/l=0.25 (d) l/D=2.5, l_1/l=0.75

Fig. 5.21: Temperature contours for hemispherical aerodisk with disk radii r_1=8 *mm*, r_2=6 *mm*

5.6.2. Heat Transfer Rates for Flat Double Disk Aerospikes

The local surface heat flux distribution for configurations with double flat disk aerospikes is substantially different from that for configurations with hemispherical disks due to the presence of a sharp rectangular edge on the

aerodisk, as can be seen in Fig. 5.22. As can be seen in Fig. 5.22, which shows the surface heat flux distributions for selected double flat disk configurations, there is sharp increase in local heat transfer rates at the sharp edges of the intermediate aerodisk. This peak heating on the sharp edges are up to 45% higher than the stagnation point heat transfer rate for the base configuration. The detrimental heat fluxes to rear aerodisk increase as the rear aerodisk is moved forward on the aerospike.

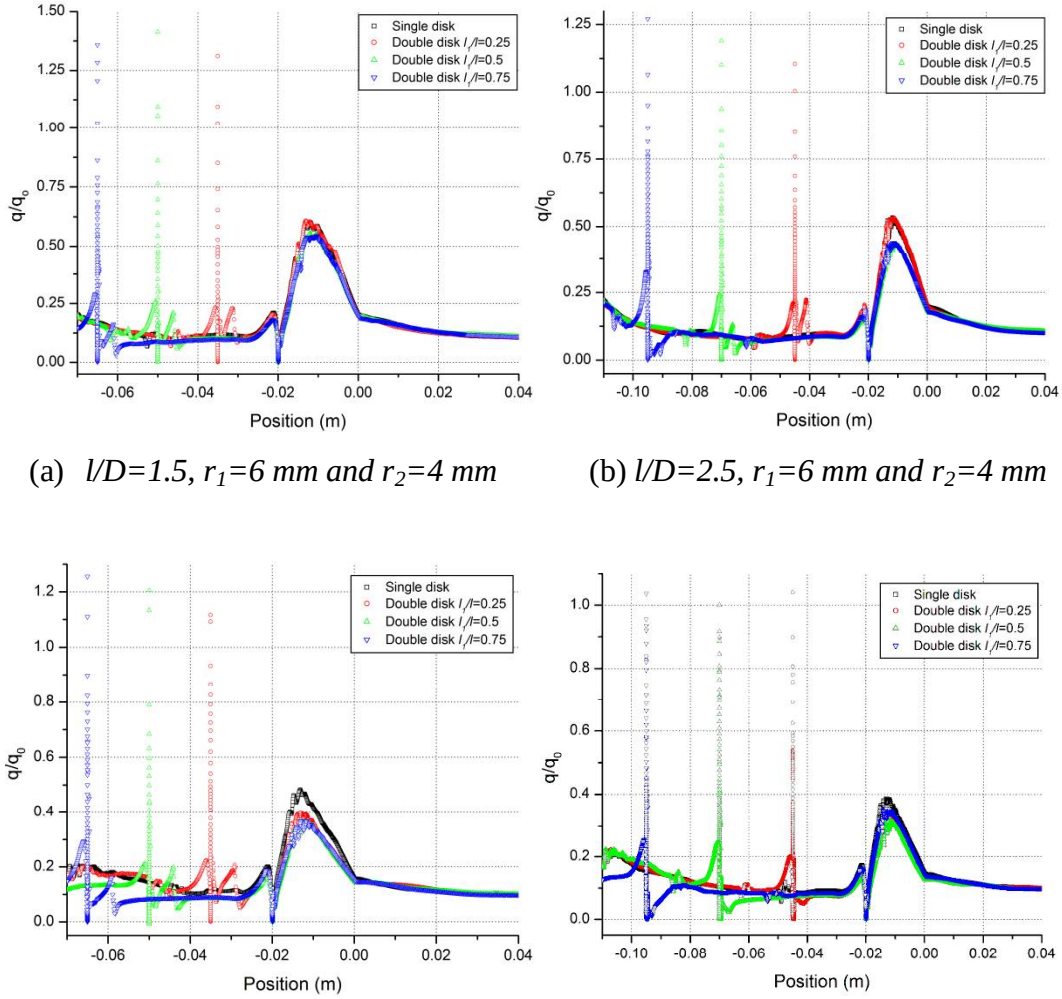

(a) *l/D=1.5, r_1=6 mm and r_2=4 mm* (b) *l/D=2.5, r_1=6 mm and r_2=4 mm*

(c) *l/D=1.5, r_1=8 mm and r_2=6* (d) *l/D=2.5, r_1=8 mm and r_2=6 mm*

Fig. 5.22: Surface heat flux distributions for double flat disk

As the *l/D* ratio of the aerospike is increased, a slight reduction in the local peak heating at the sharp edge is observed. The heating however, remains higher than that of the stagnation point heat transfer rate for the base configuration. The heating at the sharp edges also diminishes as the radius of the aerodisk is increased. For flat disk configurations with *l/D*=2.5 and r_1=8 *mm*, r_2=6 *mm*, the peak heating at sharp edges of the rear disk becomes comparable to the stagnation heat transfer rate of the base configuration. The peak reattachment heat fluxes on the main body for the spiked configurations with two flat aerodisk are however, considerable lower than those for hemispherical aerodisks.

As with the hemispherical aerodisks, the flat two disk configurations with r_1= *4 mm* and r_2=2 *mm* is equivalent to a single disk aerospike with the disk at an intermediate position. These configurations of flat aerodisk are associated with large reattachment heat fluxes to the main body. The peak reattachment heat flux for the shortest aerospike of r_1= *4 mm* and r_2=2 *mm* is about 45% higher than that of the base configuration. As the disk is moved forward or as the *l/D* ratio of the aerospike is increased, a slight reduction in peak reattachment heat flux is observed. For all *l/D* ratios the configurations with l_1/l 0.25 have reattachment heat flux higher than that of base configuration. For the configuration with l_1/l = 0.75, reductions of about 5% and 7% is observed at *l/D* ratios of 2 and 2.5 respectively. As the disk radii is increased to r_1=6 *mm* and r_2=*4 mm*, a substantial reduction in peak reattachment heat fluxes is observed, as can be seen in Fig. 5.22 (a) and (b). For flat aerodisk spiked configurations with r_1=6 *mm* and r_2=*4 mm*, reductions of about 30% in reattachment heat flux for *l/D* of 1 and *l1/l* = 0.25 is observed. As the *l/D* ratio of the spike is increased or as the rear aerodisk is moved at forward position on the aerospike, a gradual decrease in the peak reattachment heat flux is observed. Amongst the investigated cases with r_1=6 *mm* and r_2=*4 mm*, the one with *l/D*=2.5 and l_1/l =0.75 offered a maximum reduction of about 55% in the peak reattachment heat fluxes.

For double flat configurations, as the disk radii is increased to r_1=8 *mm* and r_2 = *6 mm*, further reductions in peak reattachment heat fluxes ca be observed. For this disk size, a reduction of 54% is observed at *l/D*=1 and l_1/l =0.25. As the *l/D* is increased for l_1/l =0.25, the reductions further improve to offer a reductions 64%. As the rear disk is moved forward to l_1/l =0.5, the reductions in peak reattachment heat fluxes goes up to 68% as compared to the peak heating of the base configuration. Any further forward movement of the rear disk with r_1=8 *mm* and r_2 = *6 mm* to l_1/l =0.75, offers no further reduction in heat fluxes. In fact the reductions are diminished slightly at l_1/l =0.75 as compared to l_1/l =0.75 at almost all *l/D* ratios. The reduction in peak reattachment heat fluxes on main body is restricted to 64% at *l/D*=2.5.

The reductions in peak reattachment heat fluxes observed for the flat aerodisk configurations are direct consequence of the shear layer interactions. For the configurations with r_1=4 *mm* and r_2=2 *mm*, the intermediate aerodisk does not interfere with the shear layer formation and detachment for small l_1/l values and hence these configurations have large heat fluxes to the main body. For longer aerospikes or large l_1/l values, a sight interaction is seen which reduces the heat fluxes to the main body slightly. As the disk size is increased, favorable interactions can be observed. Figure 5.23 shows the contours of temperatures for selected cases of double flat disk aerospikes with r_1=4 *mm* and r_2=2 *mm*.

For smaller length of aerospike the shear layer is detached well ahead of the rear aerodisk and gets deflected from the rear disk dissipating a large amount of heat to it. The shear layer is thus pushed far away from the main body even for a backward position of the rear disk i.e. at l_1/l =0.25, yielding large reduction heat fluxes to the main body. As the rearward disk is moved forward, the detachment point of shear layer also moves forward giving lower heat fluxes to the main body. As the rear disk is moved to l_1/l =0.75 position for *l/D* =1.5, the shear layer detached from the front aerodisk do not attach on the spike stem at all and hits the main body as can be seen in Fig. 5.23(b).

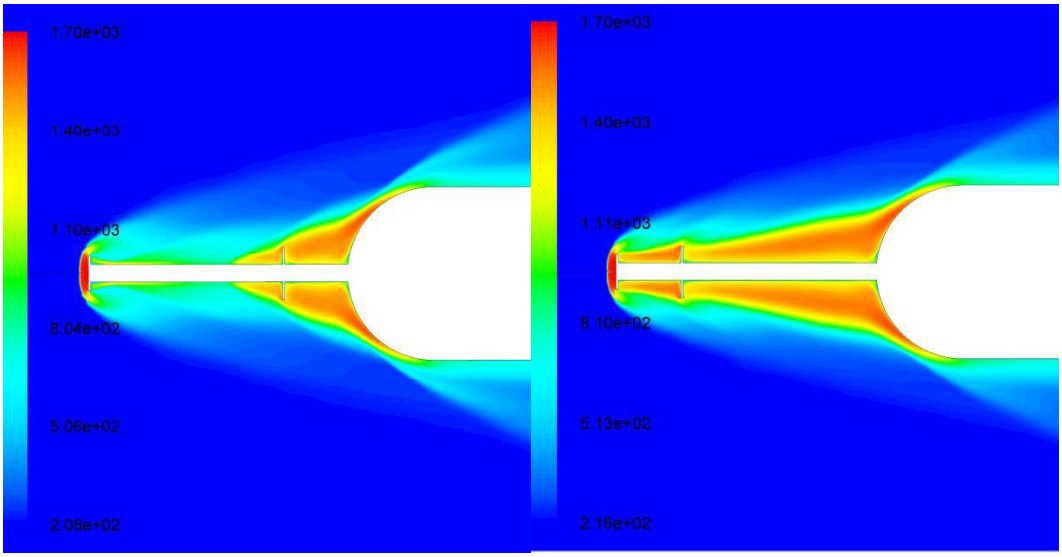

(a) l/D=1.5, l_1/l =0.25 (b) l/D=1.5, l_1/l =0.75

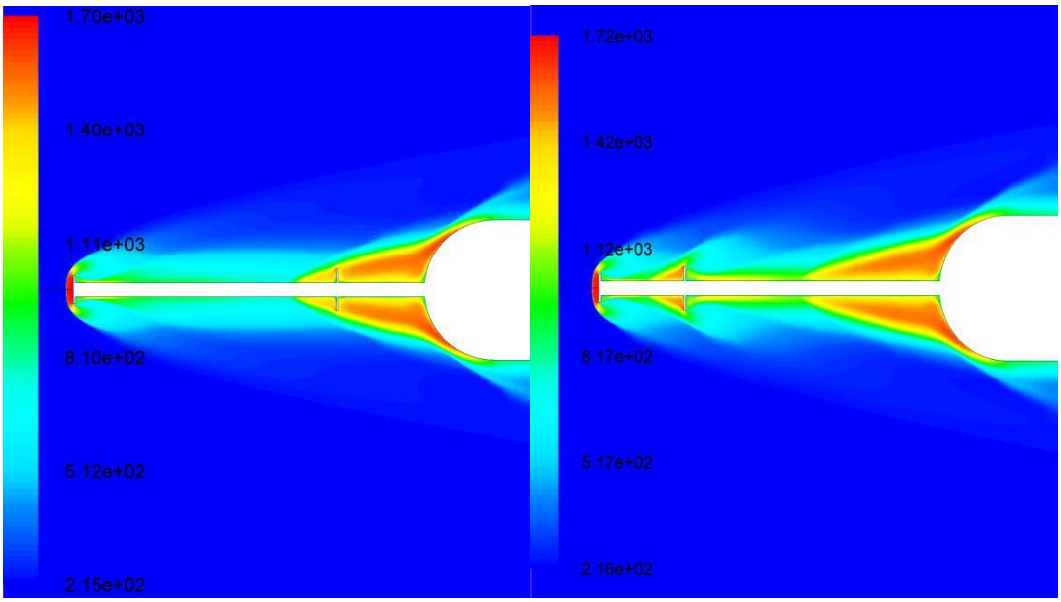

(c) l/D=2.5, l_1/l =0.25 (d) l/D=2.5, l_1/l =0.75

Fig. 5.23: Temperature contours for double flat disk aerospike with disk radii r_1=6 *mm* and r_2 = *4 mm*

For longer aerospikes, the shear layer detaches from the spike ahead of the rear disk for smaller values of l_1/l and the detachment point moves forward with an increase in l_1/l values. But for very long aerospikes of l/D=2.5 with l_1/l =0.75 the

shear layer detaches from locations aft of the rear disk giving no additional advantage in heat flux reduction to the main body as can be seen in Fig. 5.23 (d).

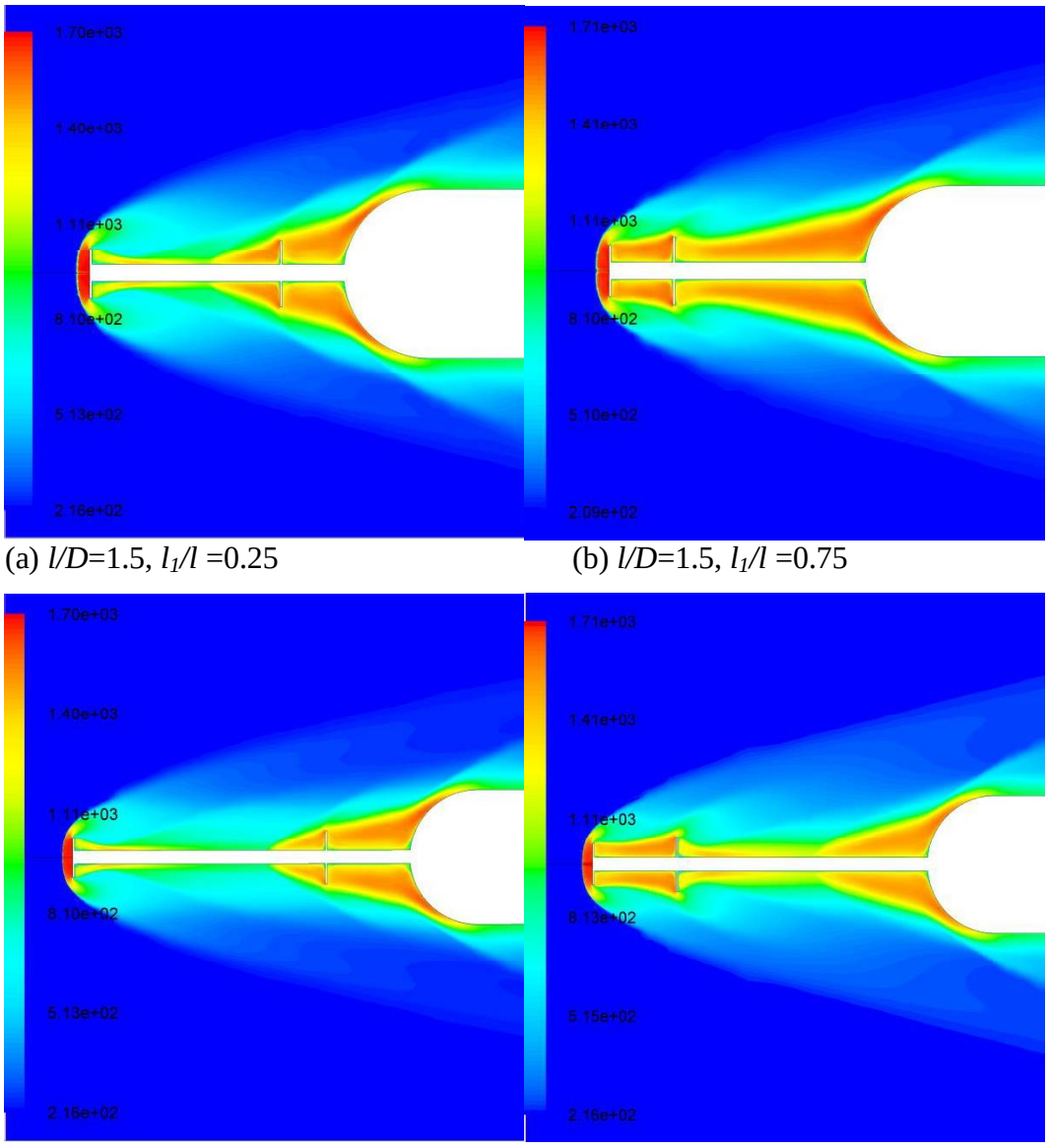

(a) l/D=1.5, l_1/l =0.25 (b) l/D=1.5, l_1/l =0.75

(c) l/D=2.5, l_1/l =0.25 (d) l/D=2.5, l_1/l =0.75

Fig. 5.24: Temperature contours for double flat disk aerospike with r_1=8 *mm* and r_2 =6 *mm*

For the largest disk sizes, i.e. r_1=8 *mm* and r_2 =6 *mm*, the shear layer is pushed further away from the main body as can be seen in Fig. 5.24. For even smaller l_1/l values, the shear layer is deflected by the rear disk taking a large fraction of heat

and thus reduced heating of the main body. For larger values of l_1/l, the shear layer remains detached throughout the length of the spike for all l/D ratios other than 2.5, wherein for l_1/l =0.75 some reattachment can be seen as shown in Fig. 5.24 (d).

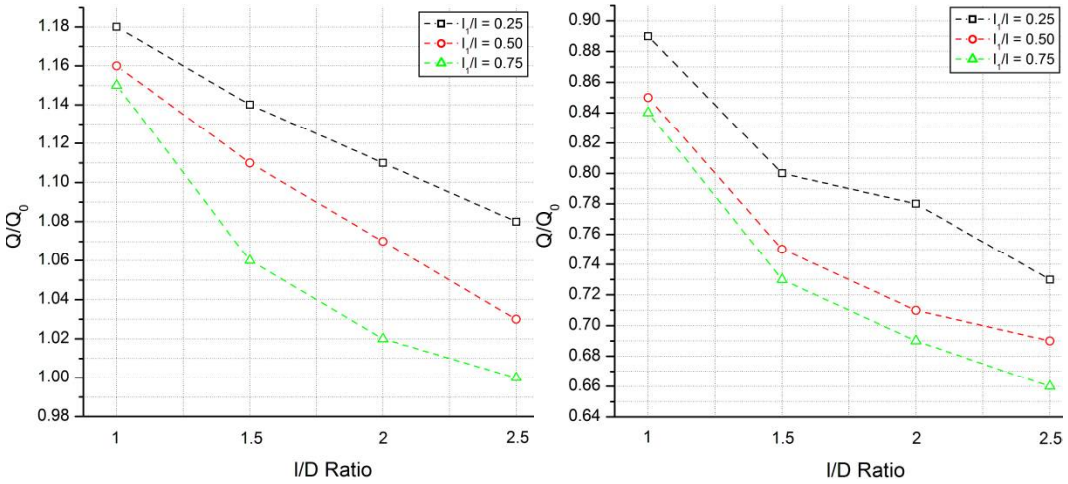

(a) r_1=4 *mm* and r_2=2 *mm* (b) r_1=6 *mm* and r_2=4 *mm*

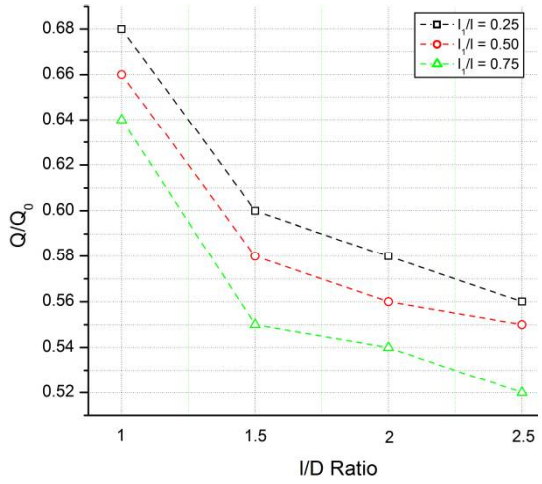

(c) r_1=8 *mm* and r_2=6 *mm*

Fig. 5.25: Total heat transfer rates for double flat disk for various disk radii

Another important aerodynamic heating parameter is the total heat transfer rates, obtained from the surface integral of local heat fluxes. Fig. 5.25 shows the total heat transfer rates of spiked configurations with double flat aerodisks, normalized with the total heat transfer rate for the base configuration. As can be seen in

Fig. 5.25 (a), for the flat disk configuration with r1=*2 mm* and r2=4 *mm*, the total heat transfer rates are up to 18% higher than that of base configuration. But, as the *l/D* ratio of the aerospike is increased or as the rear aerodisk is moved at forward locations the total heat transfer rates to the main body diminishes. These heat transfer rates for r_1=4 *mm* and r_2=2 *mm* flat aerodisk, for no *l/D* and l_1/l values are lower than that for the base configuration.

With an increase in the sizes of the aerodisks, favorable reduction in total heat transfer rates can be observed as well. These reductions are larger as compared to the hemispherical aerodisk of same *l/D* and l_1/l ratios. For disk radii of r_1=6 *mm* and r_2=4 *mm*, the shortest spike with l_1/l =0.25 gives a minimum reduction of 11% in total heat transfer rates. As the *l/D* ratio is increased or as the l_1/l is increased these reductions are further exaggerated with reductions of 27%, 31% and 34% respectively for l_1/l of 0.25, 0.5 and 0.75 at an *l/D* of 2.5. Further increase in the radii of the flat disks further reduces the heat transfer rates. The double flat disk with r_1=8 *mm* and r_2=6 *mm* offers reductions as high as 48% in total heat transfer rates for *l/D*=2.5 and l_1/l =0.75. The double flat aerodisks thus, outperform the hemispherical aerodisks for reduction of heat fluxes and total heat transfer rates to the main body.

5.6.3. Heat Transfer Rates for Flat Triangular Double Disk Aerospikes

The flowfield around spiked blunt body with two flat triangular aerodisks is quite similar to those for spiked blunt body with two flat aerodisks of same radii and other geometric parameters. This can easily be seen in Fig. 5.26, which shows the temperature contours for configurations with both flat aero disk and flat triangular aerodisks superimposed over each other, the top being flat aerodisks and the bottom the flat triangular aerodisks. Due to a high degree of resemblance between the temperature fields for the configurations with flat and flat triangular aerodisks, the resultant peak reattachment heat fluxes and the total heat transfer rates to the main body as also similar. Nevertheless the small differences between the velocity

fields for these two types of aerodisk results in a slightest difference in the heat fluxes for the two and hence the peak reattachment heat fluxes and the total heat transfer rates for the flat triangular aerodisks are presented respectively in Fig. 5.27 and Fig. 5.28.

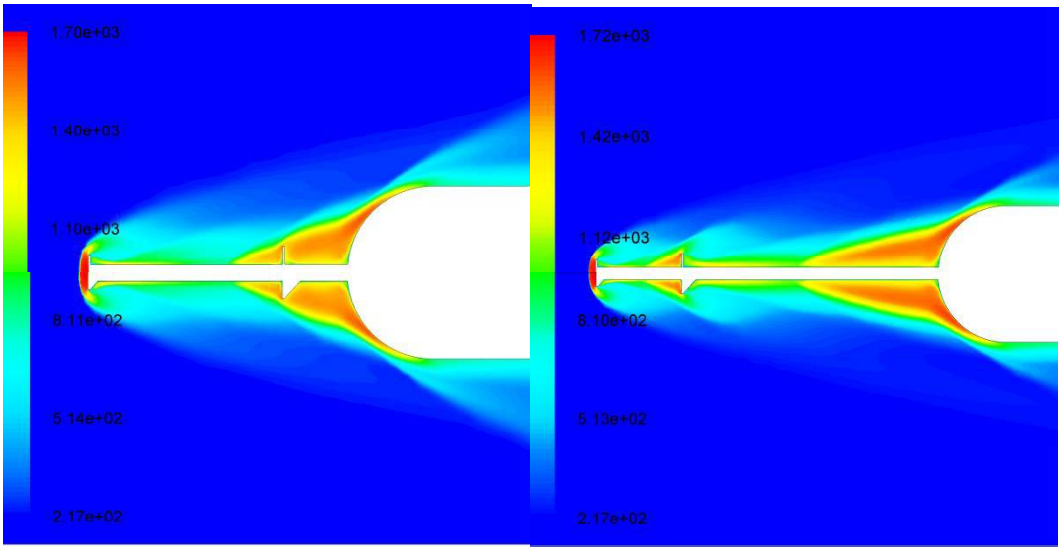

(a)l/D=1.5, l_1/l =0.25 (b)l/D=2.5, l_1/l =0.75

Fig. 5.26: Temperature contours for double disk aerospike with r_1=6 *mm* and r_2=4 *mm*

As far as the peak reattachment heat flux is concerned, the flat aerodisk performs negligibly better than the flat triangular aerodisks with reductions lower by only a percent or two in most cases. The slightest of difference seen in the peak local heat fluxes between the flat and flat triangular aerodisks, diminishes in case of integral heat transfer rates as can be seen in Fig. 5.28. As for configurations with flat aerodisks, the configurations with flat triangular aerodisks also produce a maximum reduction of 48% in total heat transfer rates at l/D=2.5 and l_1/l =0.75 for disk size of r_1=8 *mm* and r_2=6 *mm*.

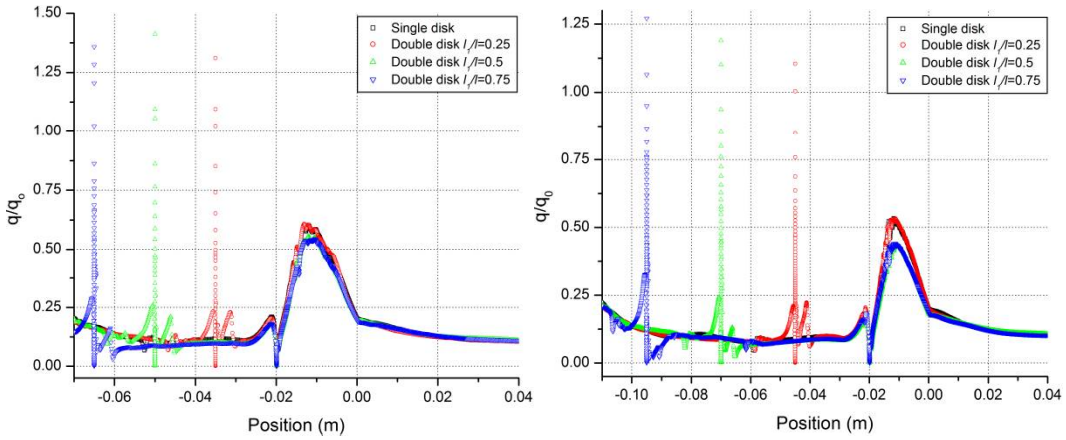

(a)*l/D*=1.5, r_1=6 *mm* and r_2=*4 mm* (b) *l/D*=2.5, r_1=6 *mm* and r_2=*4 mm*

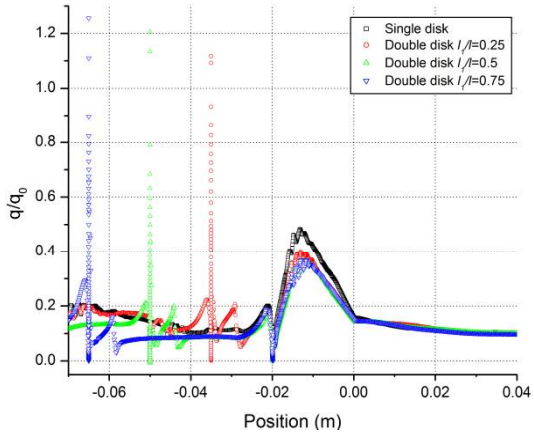

(c) */D*=1.5, r_1=8 *mm* and r_2=*6 mm*

Fig. 5.27: Surface heat flux distributions for double flat disk

5.7. Flowfield around Three Disk Aerospikes

The flowfield around a blunt body with triple disk aerospikes can be analyzed through the study of velocity field around it. Contours of axial velocity for selected cases with triple hemispherical aerodisks are shown in Fig. 5.29. In Fig. 5.29, the regions shown in blue are the regions of reversed flow. The addition of

addition aerodisk thus adds an additional region of recirculation ahead of the blunt body.

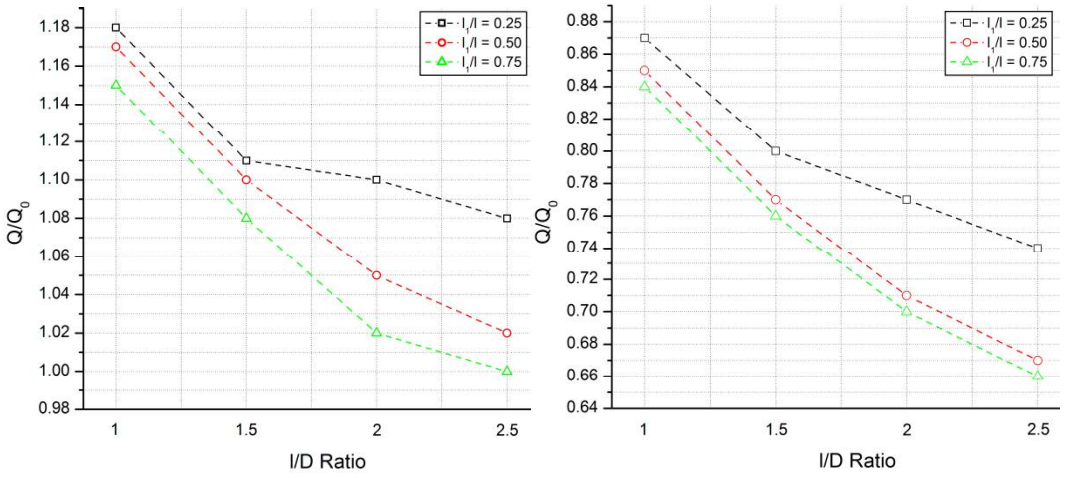

(a) r_1=4 *mm* and r_2=2 *mm* (b) r_1=6 *mm* and r_2=4 *mm*

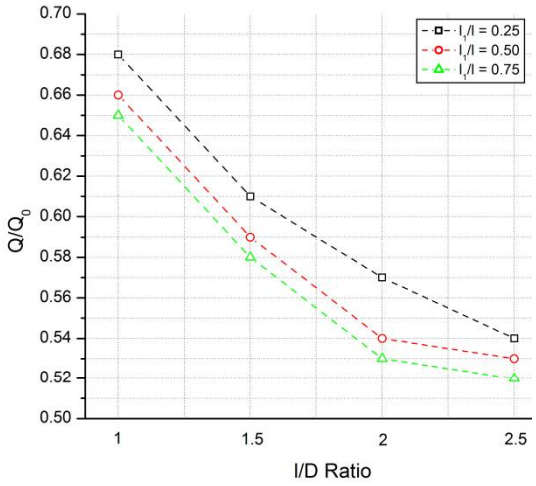

(c) r_1=8 *mm* and r_2=6 *mm*

Fig. 5.28: Total heat transfer rates for double flat triangular disk for various disk radii

The shape, size and the extent of these recirculating flow regions depends upon the overall *l/D* ratio of the aerospike, the internal positions of the intermediate aerodisks and the sizes of the individual aerodisks.

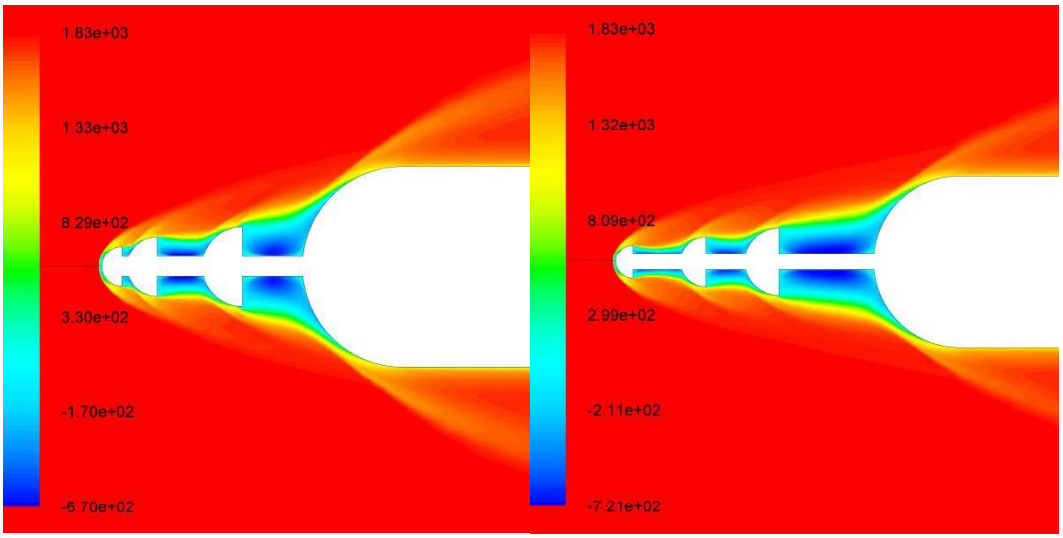

(a) l/D=1, l_1/l =0.5 and l_2/l'=0.75 (b) l/D=1.5, l_1/l =0.5 and l_2/l'=0.5

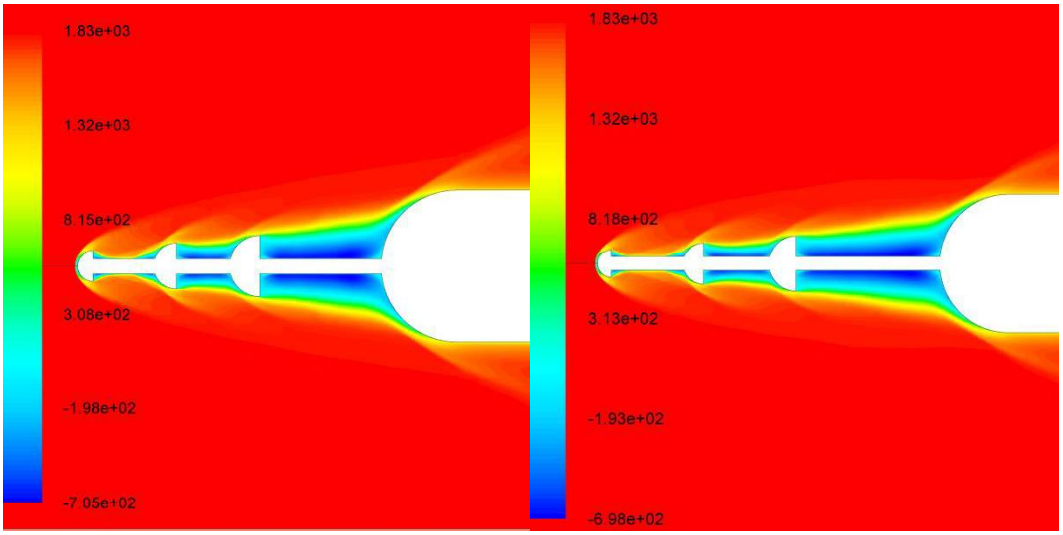

(c) l/D=2, l_1/l =0.5, l_2/l'=0.5 (d) l/D=2.5, l_1/l =0.5, l_2/l'=0.5

Fig. 5.29: Contours of velocity for configurations with triple hemispherical aerodisks

For a very small l/D ratio of the aerospike i.e. 1, the presence of three aerodisks means smaller gaps between the disks and thus single dominant vortex is seen behind each of the aerodisks for all intermediate positions of these disks. Apart

from the dominant vortices small secondary vortices are also formed at the corners formed at the junctions of spike stem and the disks or main body. As the length of the aerospike is increased the shape, size and the orientation of the vortices change depending on the intermediate positioning of the aerodisks. Due to the large radius of the rearmost aerodisk, i.e. r_1= 8 *mm*, only one dominant vortex is formed between the rearmost disk and the main body, for all overall *l/D* values other than 2.5, despite the movement of this disk to l_1/l = 0.5 and 0.75. The vortex however becomes elongated long the spike as the rearmost aerodisk is moved forward on the spike.

For an *l/D* ratio of 2.5 and highest l_1/l of 0.75, this elongated vortex breaks up into two smaller vortices. For smaller *l/D* of 1 and 1.5, single dominating vortices are between each of aerodisks. For *l/D* of 2 and 2.5, and for positions of disks such that l_1/l =0.25 and l_2/l'=0.75, there is a large gap between the rear most disk and the middle disk. For these configurations, the single dominating vortex breaks up and two smaller vortices can be seen. Owing to the small size of the front aerodisk, there are two vortices in the region behind it, for most of the configurations, unless the middle aerodisk is too close to the front aerodisk. As can be seen in Fig. 5.29 (a) and (b), there is a single small vortex behind the front aerodisk for smaller *l/D* ratios of 1.0 and 1.5, and as can be observed in Fig. 5.29 (c) and (d) the two small vortices are present for *l/D* values of 2 and 2.5. Fig. 5.29 also shows a single dominating vortices between the middle and the rear aerodisks and the rear aerodisk and the main body for all *l/D* ratios with l_1/l=0.5.

The flowfield around a triple hemispherical aerodisk with r_1= *6 mm*, r_2=4 *mm* and r_3= 2 *mm* is equivalent to a two aerospike with disk not the front most part of the configuration. The velocity fields are also very similar in both the cases as can be seen in Fig. 5.30, which shows contours of axial velocities, placed one above the other, for a double disk (r_1=6 *mm* and r_2=4 *mm*) and a triple disk (r_1=6 *mm*, r_2=4 *mm* and r_3=2 *mm*)spiked configurations.

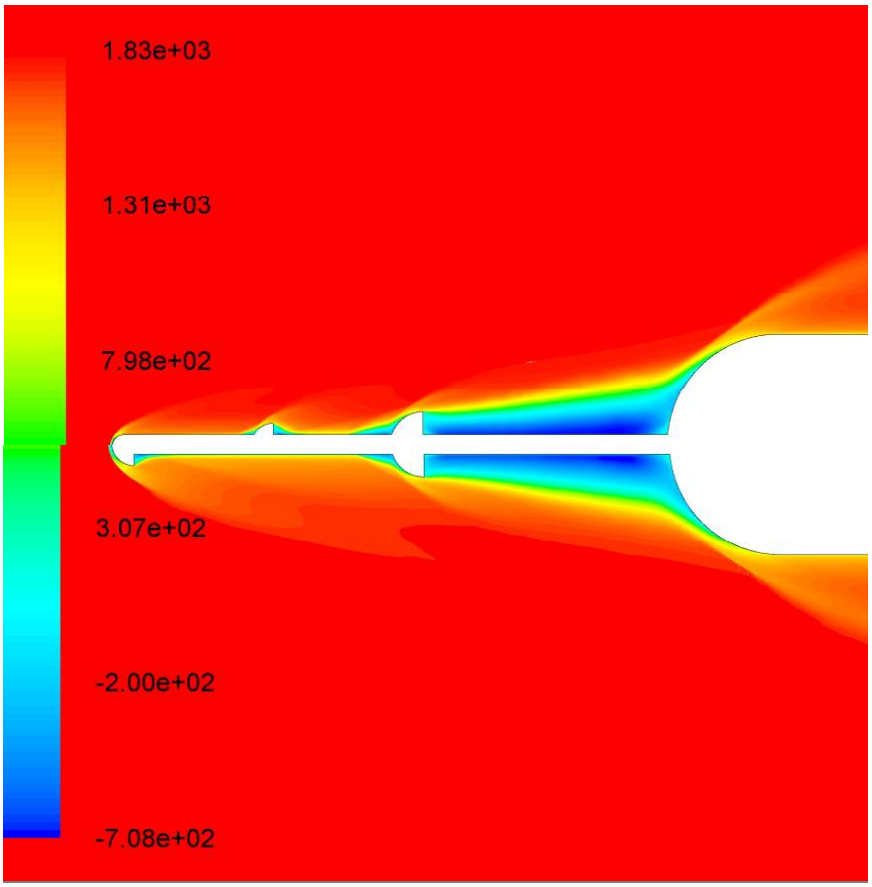

Fig. 5.30: Comparisons of the contours of axial velocity

The velocity filed around spiked blunt body with three flat aerodisk is slightly different from similar configurations with hemispherical aerodisks. This is primarily because of the formation of stronger and larger vortices in front of the flat aerodisks at the junctions of spike stem and the aerodisks as can be seen in Fig. 5.31. In contrast to the hemispherical three disk configurations, a strong and a dominant vortex can be seen between the front aerodisk and the mid aerodisk as can be seen in Fig. 5.31 (a) and (b). This vortex between the front and the mid aerodisks remains intact unless the distance between these two disks becomes very large and single dominant vortex breaks into two smaller vortices as can be seen in Fig. 5.31 (c) and (d).

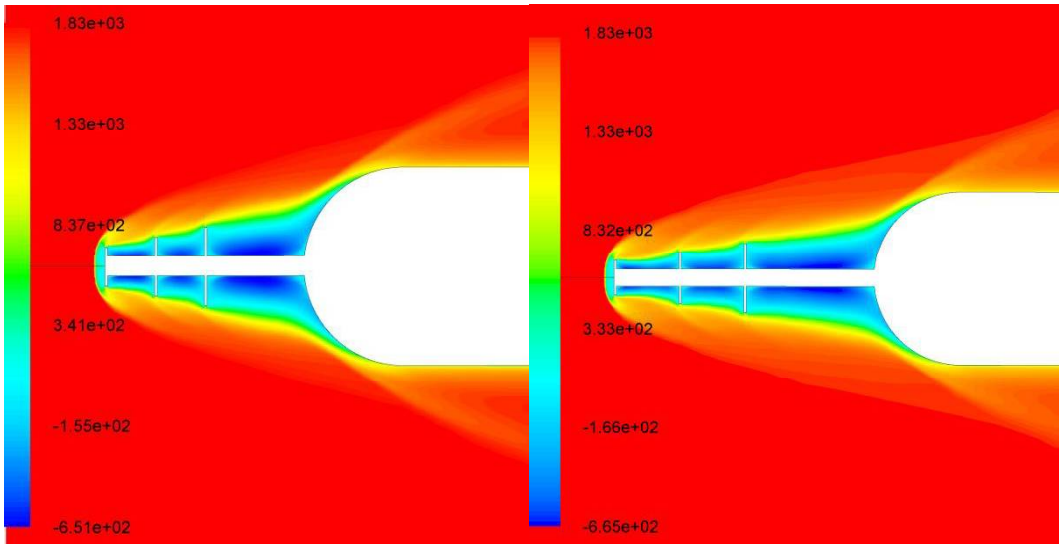

(a) l/D=1, l_1/l=0.5, l_2/l'=0.5 (b) l/D=1.5, l_1/l=0.5, l_2/l'=0.5

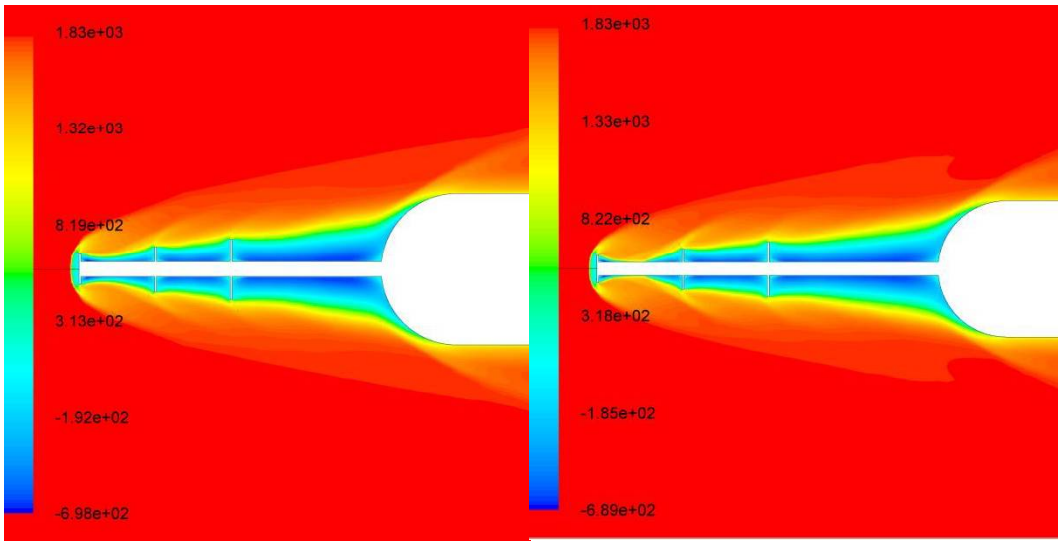

(a) l/D=1, l_1/l=0.5, l_2/l'=0.5 (b) l/D=1.5, l_1/l=0.5, l_2/l'=0.5

Fig. 5.31: Contours of axial velocity for configurations with triple flat aerodisks

It is observed that the vortex breaks up for l/D ratio of 2 and 2.5 if the distance l_2/l' is 0.25 or 0.5. Even for large l/D ratios of 2 and 2.5, if the l_2/l' is 0.75, the distance between the mid and the rear aerodisk is relatively small and a single dominant vortex can be seen. Owing to the larger size of the mid aerodisk, a single dominant vortex is seen between these flat disks for much longer

aerospikes. For very long aerospikes with l/D = 2.5, few cases when l_1/l=0.25 with l_2/l'=0.5 or 0.75 and for the cases when l_1/l=0.5 with l_2/l'=0.75, the distance between the mid and the rear aerodisks become large enough to break the vortex between these disks into two smaller ones. For l/D=2.0, the middle vortex breaks into two when l_2/l'=0.75 for l_1/l=0.25 and l_1/l=0.5. This results in an increased pressure on the windward side of rear aerodisk and a reduced pressure on the leeward side of the mid aerodisk

A single dominating vortex is seen between the main body and the rearmost flat aerodisks for most of the configurations studied. The shape and sizes of the dominating and the secondary vortices changes as the length of the aerospike or the distance between the rear disk and the main body is increased. As the distance increases, the dominant vortex gets elongated along the spike length and the smaller secondary vortex grows in sizes. Finally as the distance gets sufficiently large when l/D=2.5 and l_1/l=0.75 and the vortex breaks into two smaller vortices.
The Mach numbers in vortical flows between the aerodisks, whether hemispherical or flat, are completely subsonic. These rotating flows between the aerodisks are completely isolated from the main flow which only feeds to the momentum of rotation. For the cases with single dominating vortices between the aerodisks, the dividing streamline is almost a straight line joining the top of the three aerodisks to the shoulder of the main body. For configurations with twin vortices between the aerodisks, the outer supersonic flow penetrates deeper and nearer to the spike stem resulting in higher pressure regions and consequent loss in drag reductions.

The flowfield around configurations with three flat triangular aerodisks is quite similar to those for flat aerodisks for all geometric parameters, as can be seen in Fig. 5.32. Figure 5.32 shows the contours of axial velocities for configurations with three flat aerodisk atop configuration with flat triangular aerodisk.

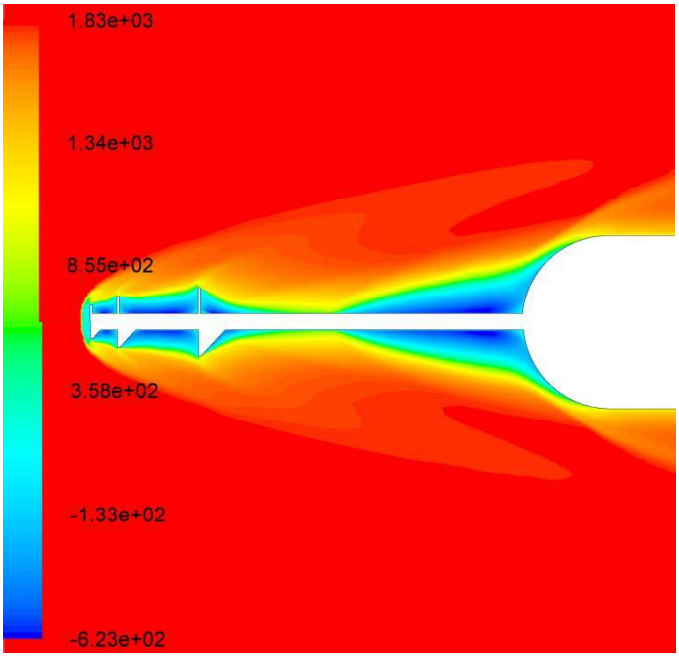

(a) l/D=2.5, l_1/l=0.75, l_2/l'=0.75

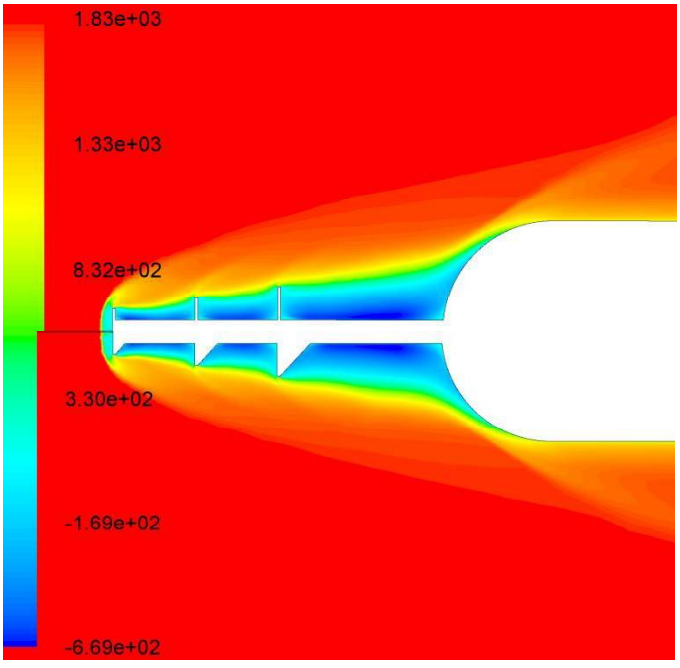

(a)l/D=1.5, l_1/l=0.5, l_2/l'=0.5

Fig. 5.32: Comparisons of contours of axial velocity for triple disk configurations with r_1=8 *mm*, r_2=6 *mm* and r_3=4 *mm*

.

As can be observed from Fig. 5.32(a), for the cases wherein the dominant vortex breaks into two, the vortex formed behind the aerodisks are much smaller for flat triangular aerodisks as compared to flat aerodisks. For smaller *l/D* ratios, the small secondary vortices seen behind the flat aerodisks do not seem to form in case of flat triangular aerodisk as can be seen in Fig. 5.32 (b). Even the *l/D* ratios and values of l_1/l or l_2/l' for which the primary vortex splits into two is slightly higher for flat triangular aerodisks as the slant edge of the triangular disk reduces the effective distance between the aerodisks. Thus, although the majority of flowfield is similar in cases for flat triangular and flat aerodisks, the vortical structure is slightly modified to give better drag reduction for the flat triangular aerodisks. The modification is negligible though, to produce any significant reduction in drag.

5.8. Effect of Three-Disk Aerospikes on Aerodynamic Drag

5.8.1. Drag Reduction for Hemispherical Triple disk Aerospikes

The addition of an extra aerodisk on the aerospike results in two additional regions of recirculating flow, one behind the disk and the other ahead of it. The recirculating zone ahead of the aerodisk assists in reduction of drag whereas the recirculating flow aft of the disk increases drag by creating drag on the aerodisks itself. Although the presence multiple aerodisks reduces the reattachment on the main body, high pressure on aerodisk contributes to the overall drag of the configuration. Thus the drag of spiked blunt body with three aerodisks depends on the *l/D* ratio, position of the mid disk and the sizes of the aerodisks in a coupled manner. The aerodynamic drag obtained for hemispherical aerodisks, normalized by the drag of base configuration without any spike, are shown in Fig. 5.33.

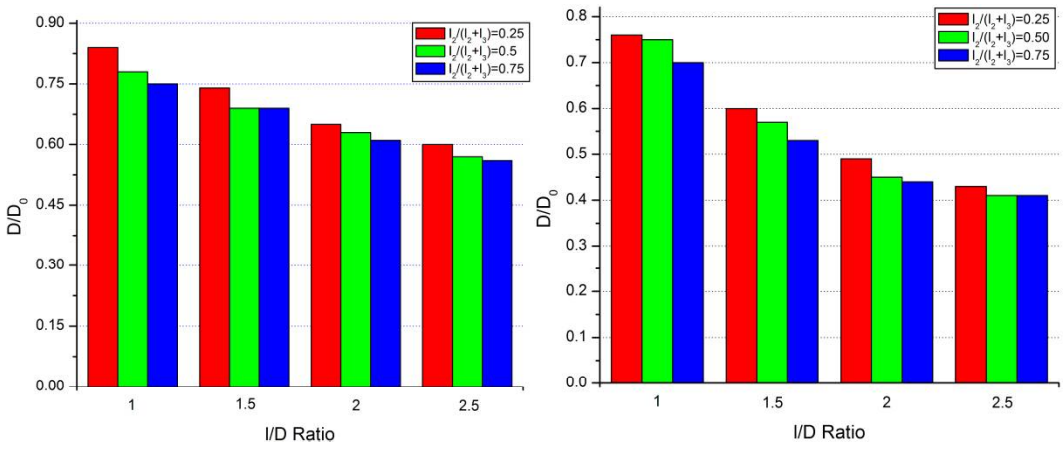

(a) r_1, r_2, $r_{3=}$6,4,2 *mm*, l_1/l=0.25 (b) r_1, r_2, $r_{3=}$6,4,2 *mm*, l_1/l=0.5

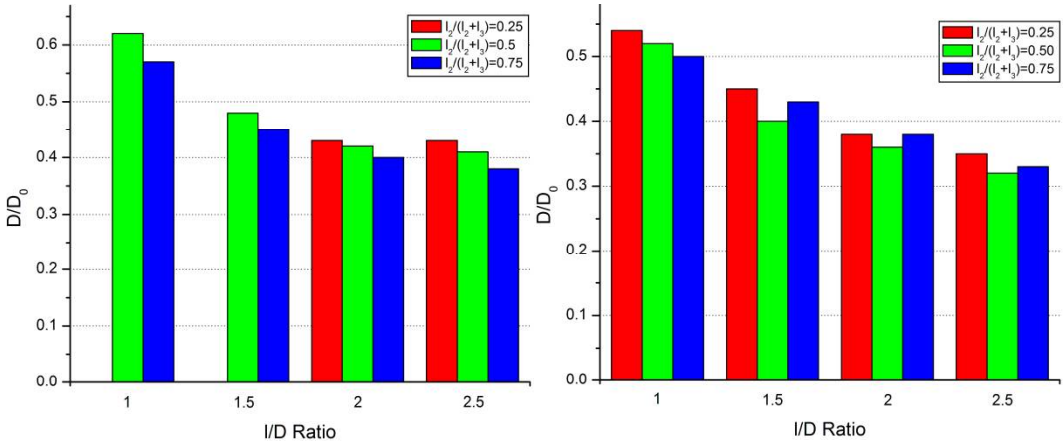

(c) r_1, r_2, $r_{3=}$6,4,2 *mm*, l_1/l=0.75 (d) r_1, r_2, r_3=8,6,4 *mm*, l_1/l=0.25

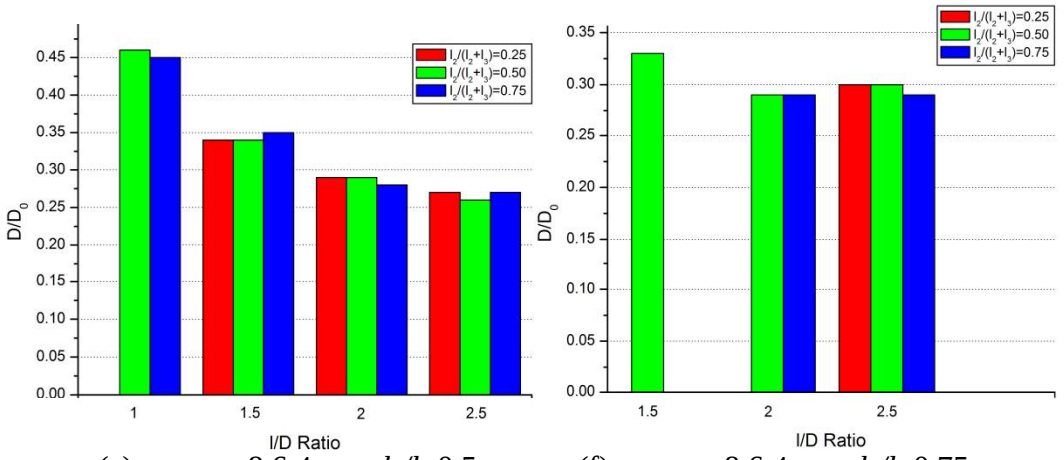

(e)r_1, r_2, r_3=8,6,4 *mm*, l_1/l=0.5 (f)r_1, r_2, r_3=8,6,4 *mm*, l_1/l=0.75

Fig. 5.33: Normalized drag for configurations with three hemispherical aerodisks

As can be seen in Fig. 5.33, as the *l/D* ratio is increased there is a gradual and substantial reduction in aerodynamic. This is because of the fact that as the *l/D* increases, the bow shock is pushed away from the main body, the extent of recirculating flow ahead of the main body increases. This reduces the peak reattachment pressure on the shoulder of the main body and low pressure in stagnation region reducing the drag. For the three disk aerospike, a reduction in drag is also observed as the mid disk is moved forward for a fixed position of the rear disk, i.e. drag reduces as l_2/l' increases for fixed l_1/l. Owing to the fact that the mid disk is bigger in size as compared to the front disk, as the mid disk is moved forward, it comes close to the shock wave, resulting in relatively higher pressure the disk itself, but a reduced pressure behind in the wake and on the rear aerodisk as well as on the main body. The result is thus, reduced reattachment pressure on the shoulder of the main body as can be seen in Fig. 5.34.

Figure 5.34 shows the non-dimensional surface pressure distribution for selected hemispherical three disk configurations of disk radii *2 mm*, 4 *mm* and 6 *mm*. As can be seen in Fig. 5.34 other than the case where $l_1/l=0.25$, the peak reattachment pressure is substantially lower than for the single disk configuration of same front disk radius. The effect of reduced reattachment pressure is to reduce the drag whereas the increased pressure on aerodisks increases the drag only slightly because of small surface are of the aerodisks as compared to the main body. But for the triple aerodisk configuration with $l_1/l=0.75$ and $l/D=2.5$, although the peak reattachment pressure is highly reduced, the large pressure rise on the aerodisks neutralizes the reduction drag as compared to *l/D*=2.0 as can be seen in Fig. 5.33 (c). Nevertheless, reductions in drag of up to 63% is realized for an *l/D* of 2.5 and $l_1/l=0.75$ for triple hemispherical aerodisk configuration with $r_1= 6$ *mm*, r_2=4 *mm* and $r_3=2$ *mm*.

As the disk size is increased to r_1= 8 *mm*, r_2=6 *mm* and r_3=4 *mm*, further reductions in drag could be observed as can be seen in Fig. 5.33 d, e and f. For this size, reductions of up to 55% are realized for even smaller aerospikes of *l/D*.

Increase in *l/D* ratio adds the reductions in drag, with the longest aerospikes with *l/D*=2.5 giving a reduction of about 75% in drag. The decrease in drag with the forward movement of the mid disk is however, not as clear as it was for the three disks of smaller size. This is the consequence of high pressures experienced by the mid and the rear aerodisks at l_2/l'=0.75 as can be seen in Fig. 5.35, which shows the surface pressure distributions for the selected hemispherical three disk aerospike configurations with r_1= 8 *mm*, r_2=6 *mm* and r_3=4 *mm*. For a l_1/l=0.25, as the l_2/l' is increased from 0.25 to 0.5, there is a slight increase in the pressure on the aerodisks, however the reattachment pressure on main body is reduced as. This gives an overall reduction in aerodynamic drag. But as the l_2/l' is further increased to 0.75, there is large jump in pressure on the mid aerodisk with only small reduction reattachment pressure, resulting in marginal increase in drag as compared to configuration with l_2/l' =0.5. For theses configurations, the peak pressure on mid disk is more than 50% of the peak reattachment pressure on the base configuration.

For l_1/l=0.5 and 0.75, the rear aerodisk is at a considerable distance from the main body and owing to its large compared to the other two disks, the drag of the configuration is solely affected by the rear most aerodisk. The effect of the movement of mid disk, does affect the flowfield around the main body as such and the drag remains largely unchanged as can be seen in Fig. 5.33 (e) and (f). This fact is emphasized as we see the surface pressure distribution in Fig. 5.35 (e) and (f), which clearly shows similar pressures on the mid aerodisk for all l_2/l' values. In fact the configuration with l_1/l=0.5 and l_2/l'=0.5 has slightly higher pressure on the mid aerodisk and lower pressures on larger rear disk giving a slightly lower drag as compared to other two l_2/l' values at l_1/l=0.5.

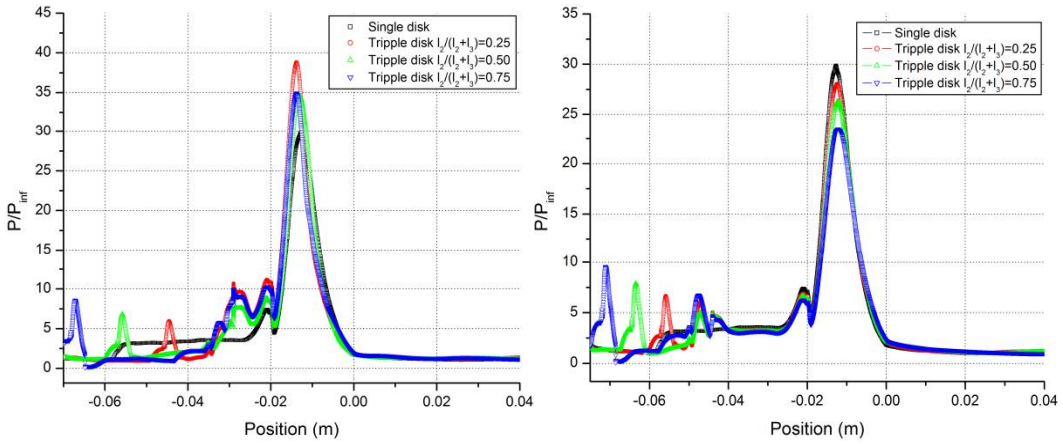

(a)r_1,r_2,r_3=6,4,2 *mm*, *l/D*=1.5, l_1/l=0.25 (b) r_1,r_2,r_3=6,4,2 *mm*, *l/D*=1.5, l_1/l=0.5

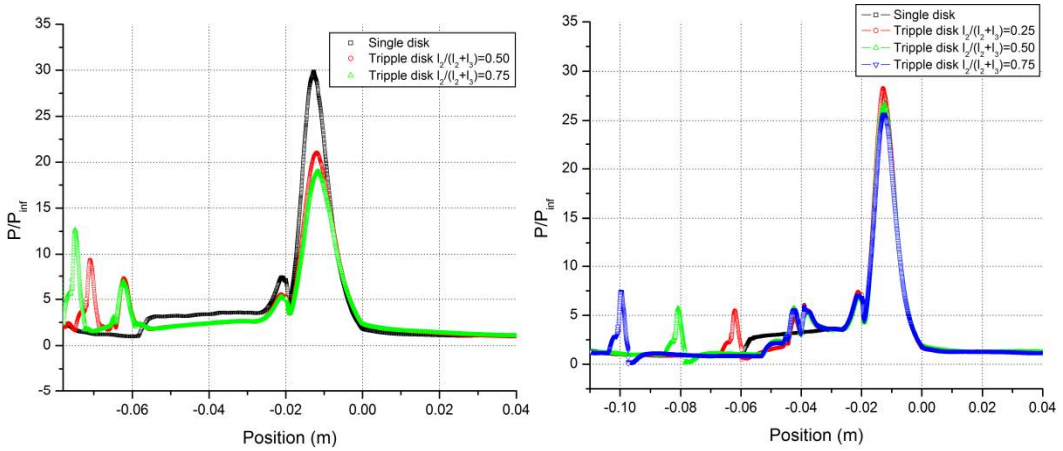

(c) r_1,r_2,r_3=6,4,2 *mm*, *l/D*=1.5, l_1/l=0.75 (d) r_1,r_2,r_3=6,4,2 *mm*, *l/D*=2.5, l_1/l=0.25

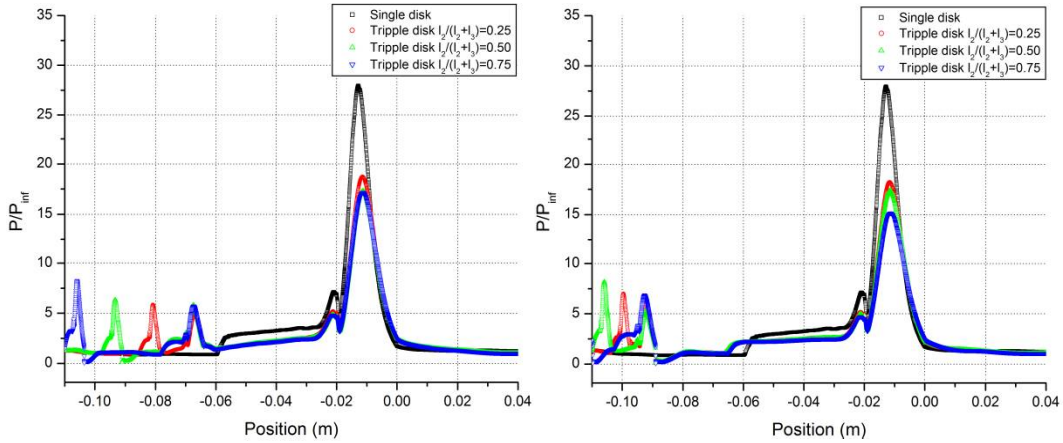

(e) r_1,r_2,r_3=6,4,2 *mm*, *l/D*=2.5, l_1/l=0.5 (f) r_1,r_2,r_3=6,4,2 *mm*, *l/D*=2.5, l_1/l=0.75

Fig. 5.34: Surface pressure distribution for hemispherical aerodisk with r_1=*6 mm*, r_2=*4* and r_3=2 *mm*

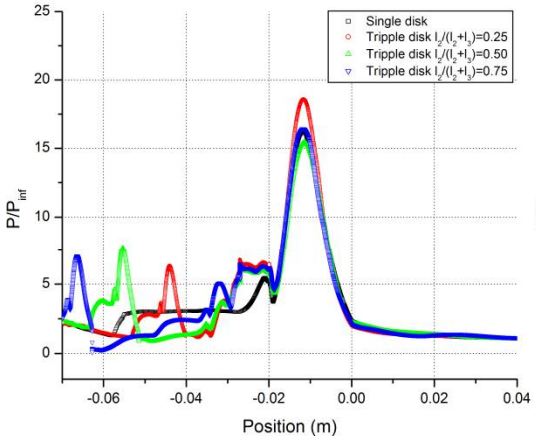

(a) r_1,r_2,r_3=8,6,4 *mm*, *l/D*=1.5, l_1/l=0.25

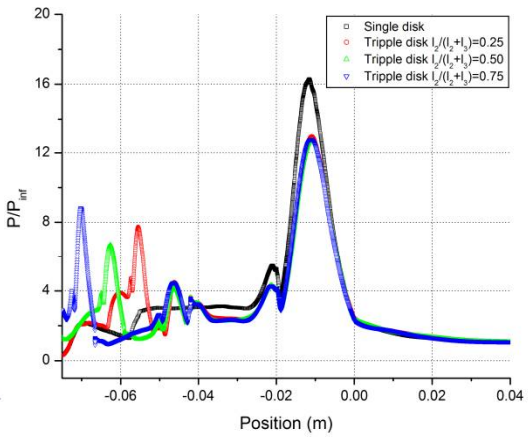

(b) r_1,r_2,r_3=8,6,4 *mm*, *l/D*=1.5, l_1/l=0.5

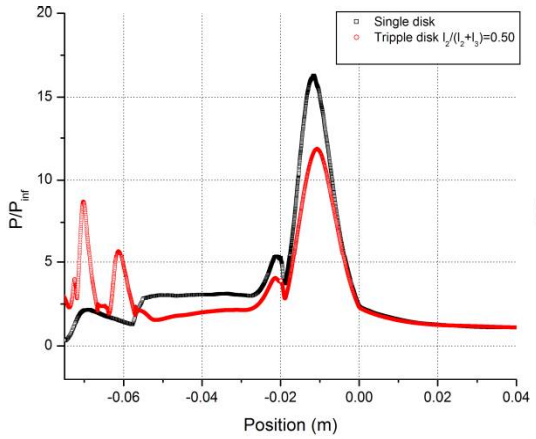

(c) r_1,r_2,r_3=8,6,4 *mm*, *l/D*=1.5, l_1/l=0.75

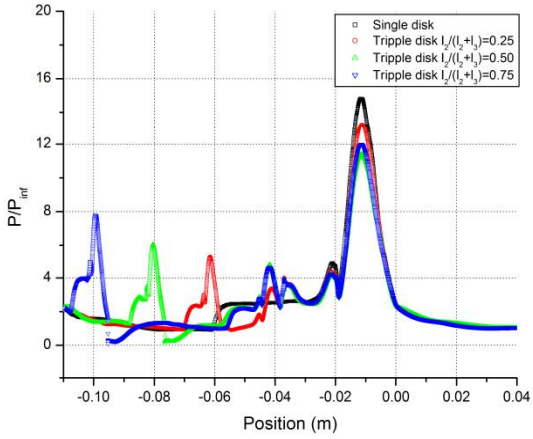

(d) r_1,r_2,r_3=8,6,4 *mm*, *l/D*=2.5, l_1/l=0.25

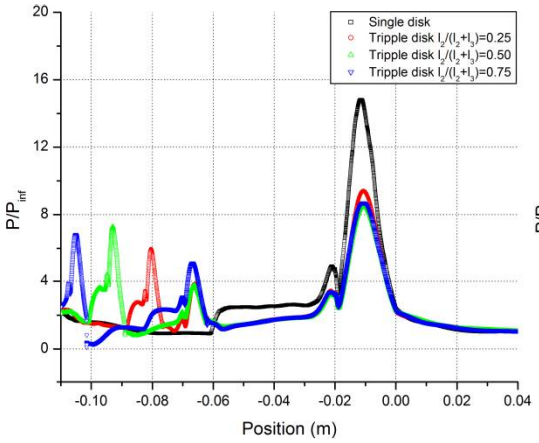

(e) r_1,r_2,r_3=8,6,4 *mm*, *l/D*=2.5, l_1/l=0.5

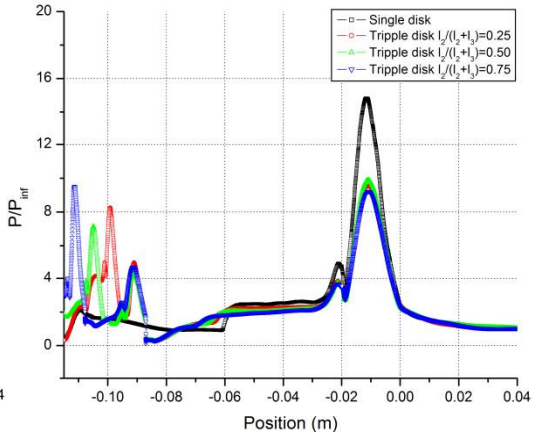

(f) r_1,r_2,r_3=8,6,4 *mm*, *l/D*=2.5, l_1/l=0.75

Fig. 5.35: Surface pressure distribution for hemispherical aerodisk with r_1=*8 mm*, r_2=*6* and r_3=4 *mm*

5.8.2. Drag Reduction for Flat Triple Disk Aerospikes

As with the hemispherical triple disk aerospikes, the flat triple disk aerospikes offer substantial reduction in aerodynamic drag. Owing to the larger recirculating flow regions formed behind the aerodisks, the flat aerodisks exhibits superiority over hemispherical aerodisks in reducing the drag of the configuration. The trend of reduction in drag with an increase in *l/D* ratio and of reduction in drag with forward movement of the rear and the mid aerodisks is faithfully followed by the flat aerodisks as well as can be observed in Fig. 5.36. For disk sizes of r1=6 *mm* r2=4 *mm*, r3=*2 mm*, the flat aerodisks give drag reductions between 28% and 55% for the rear aerodisk placed at l1/l=0.25. The drag reductions are augmented as the rear aerodisk is moved forward to a position of l1/l=0.5, wherein reductions of about 38% at *l/D*=1to 66% at *l/D*=2.5 is achieved. As the rear disk is moved to l1/l=0.75, a slight reduction in drag is further observed for *l/D* ratios of 1 and 1.5. But for larger *l/D* values, the large recirculating zone formed behind the rear aerodisk tend to increase the drag, thus neutralizing the reduction with forward movement of the mid aerodisk. No further reductions in drag for configurations with l1/l=0.75 is observed as *l/D* is increased from 2 to 2.5 or as l2/l' is increased. For the larger flat disk configurations with r1= *8 mm*, r2= *6 mm* and r3=*4 mm*, a substantial amount of drag reduction is achieved at smaller l1/l and l2/l' values itself. As the *l/D* ratio is increased or as the rear aerodisk is moved forward, the flat aerodisks experiences a large pressure on its surface as it can be seen in Fig. 5.37, which shows surface pressure distributions for selected configurations with flat aerodisks. Also as l1/l is increased, the peak pressure on the main body shoulder reduces dramatically but there is an associated rise in pressure of the windward surface of the aerodisk. The increased pressure on the relatively large aerodisk adds to the overall drag. The reductions in peak pressure thus, yields only a very small or negligible reduction in total drag of the configuration as the rear aerodisk is moved forward, especially for larger *l/D* values. At *l/D*=1.5, for l1/l=0.5 or 0.75, the pressure on the main body is much lower than on the disks giving slight reduction in drag as compared to *l/D*=1 or l1/l=0.25.

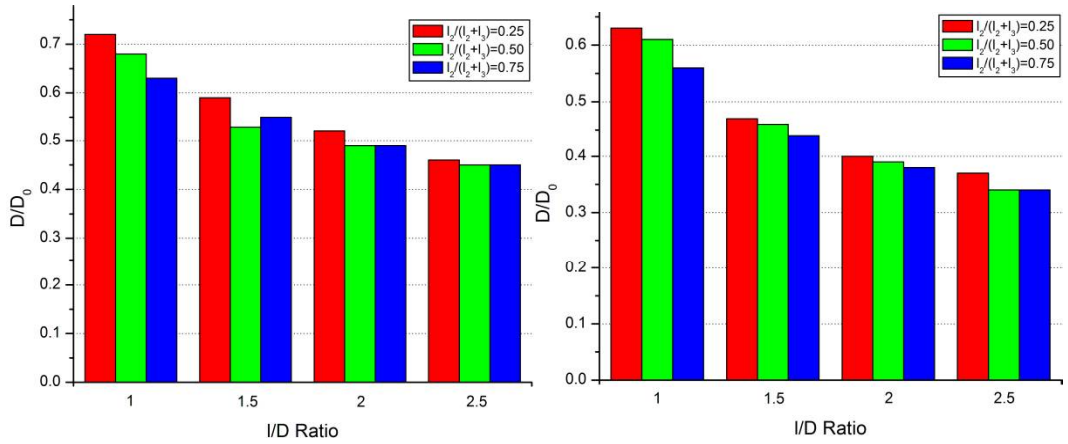

(a) r_1,r_2,r_3=6,4,2 *mm*, l_1/l=0.25 (b) r_1,r_2,r_3=6,4,2 *mm*, l_1/l=0.5

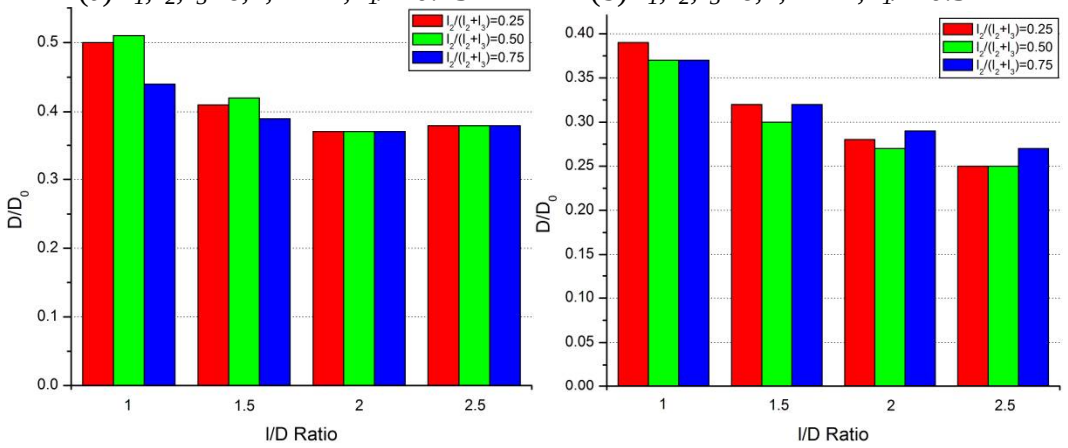

(c) r_1,r_2,r_3=6,4,2 *mm*, l_1/l=0.75 (d) r_1,r_2,r_3=8,6,4 *mm*, l_1/l=0.25

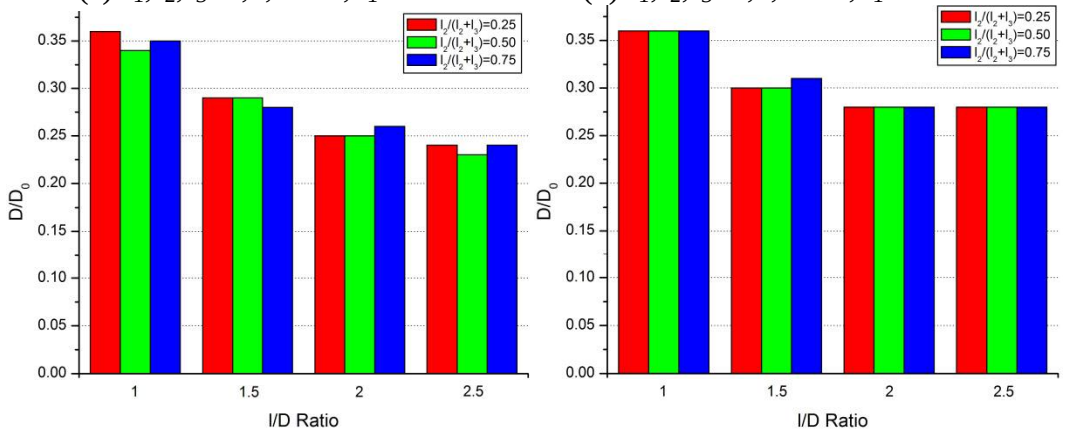

(e) r_1,r_2,r_3=8,6,4 *mm*, l_1/l=0.5 (f) r_1,r_2,r_3=8,6,4 *mm*, l_1/l=0.75

Fig. 5.36: Normalized drag for configurations with three flat aerodisks

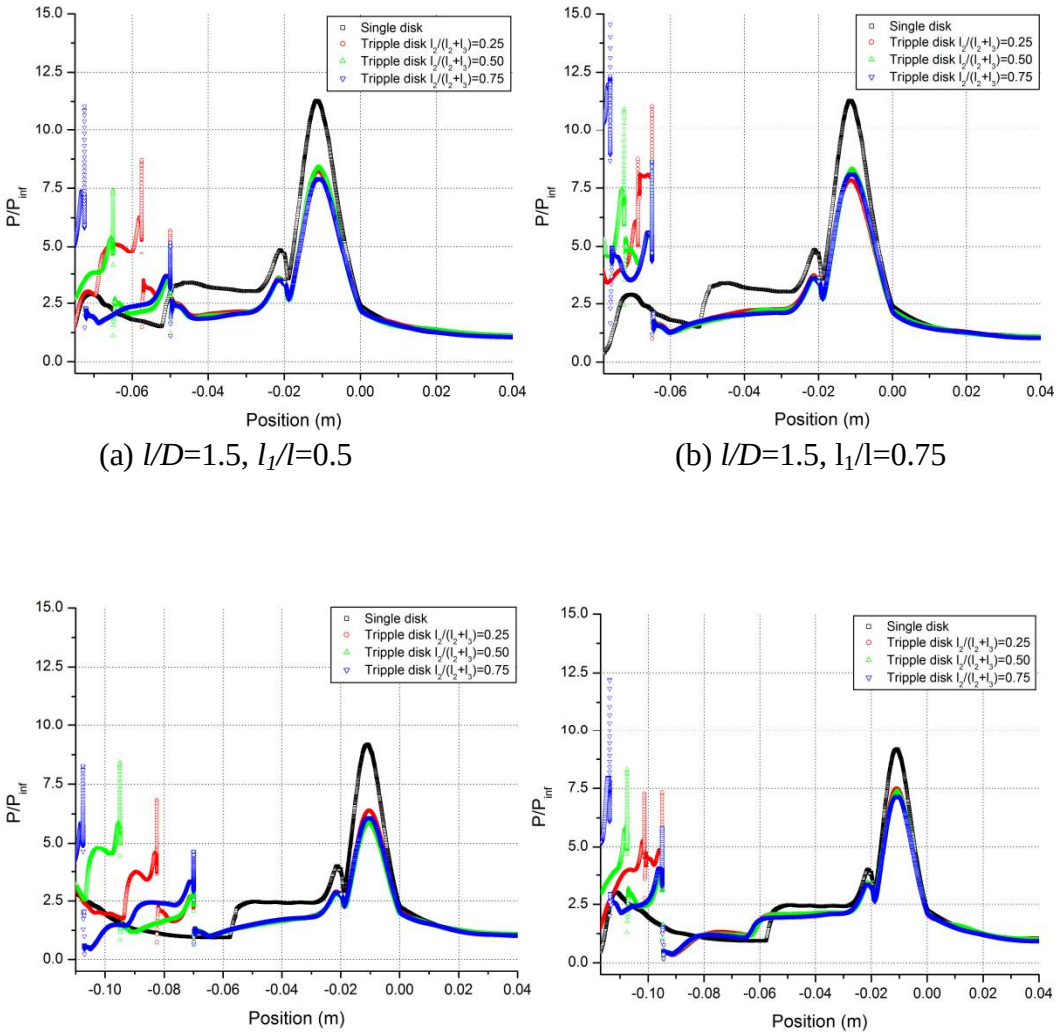

(a) l/D=1.5, l_1/l=0.5 (b) l/D=1.5, l_1/l=0.75

(c) l/D=1.5, l_1/l=0.55 (d) l/D=2.5, l_1/l=0.75

Fig. 5.37: Surface pressure distribution for flat aerodisk with r_1, r_2, r_3=*8,6* & 4 *mm*

When the rear disk with radius 8 *mm* is placed at its forward most position i.e. l_1/l=0.75, a large drag experienced by this disk dominates the drag on the main body and an increment in drag as compared to l_1/l=0.5 is seen for all l/D ratios and positions of l_2/l' except a few cases with l/D=1. The large pressures on aerodisks for l_1/l=0.5 and 0.75 for l/D of 2.5 is clearly evident from Fig. 5.37 (c) and (d). Thus for disk sizes of r_1=*4 mm*, r_2=6 and r_3=8 *mm*, the configurations with l_1/l gives the best results for drag reduction in cases with three flat aerodisk offering about 75% and 78% reductions at l/D = 2 and l/D = 2.5 respectively.

These maximum reductions comes for l_2/l' ratio of 0.5 and not for the forward most position of l_2/l'=0.75 as for the later configuration the single dominating vortex between the rear and the mid aerodisks split into two smaller vortices. Of the two, the small vortex in the wake of mid disk adds to the drag of the configuration and the small vortex in front of rear aerodisk results in smaller forward suction than the case with l_2/l'=0.5. The cumulative effect if a slight increase in drag of the spiked configuration. Nevertheless, the flat disk configurations with l_1/l=0.75 gives a reduction of 73% in drag for *l/D* values of 2 and 2.5 irrespective of l_2/l' values.

5.8.3. Drag Reduction for A Flat Triangular Three Disk Aerospikes.

The flowfield around spiked configuration with flat triangular aerodisk is similar to that for flat aerodisks. This also means that the drag experienced by configurations with flat triangular aerodisks are quite close to those experienced by configurations with flat aerodisk. They also follow the common trends in that the drag is diminished as *l/D* ratio is increased or as the l_2/l' ratio is increased or as the l_1/l ratio is increased except for very long aerospike. The normalized drags for various spiked configurations with three flat triangular aerodisks are shown in Fig. 5.38. For smaller *l/D* ratios, the flat triangular aerodisks give marginally lower drag as compared to the flat aerodisks by a percent or two. For flat triangular aerodisks of sizes r_1=6 *mm* r_2=4 *mm*, r_3=2 *mm*, the maximum reductions, obtained at *l/D*=2.5, were about 55% for l_1/l= 0.25 and 66% for l_1/l=0.5 and 65% for l_1/l=0.75. Increase in radius to r_1=8 *mm* r_2=6 *mm*, r_3=4 *mm* leads to further reductions in drag. These reductions are exaggerated are low *l/D* values and values of l_1/l=.25. For triple flat triangular aerodisk with r_1=4 *mm* r_2=6 *mm*, r_3=8 *mm*, maximum reduction in drag of about 75% for l_1/l=0.25, 76% for l_1/l=0.5 and 72% for l_1/l=0.75 are obtained all at *l/D* =2.5 with l_2/l'=0.5.

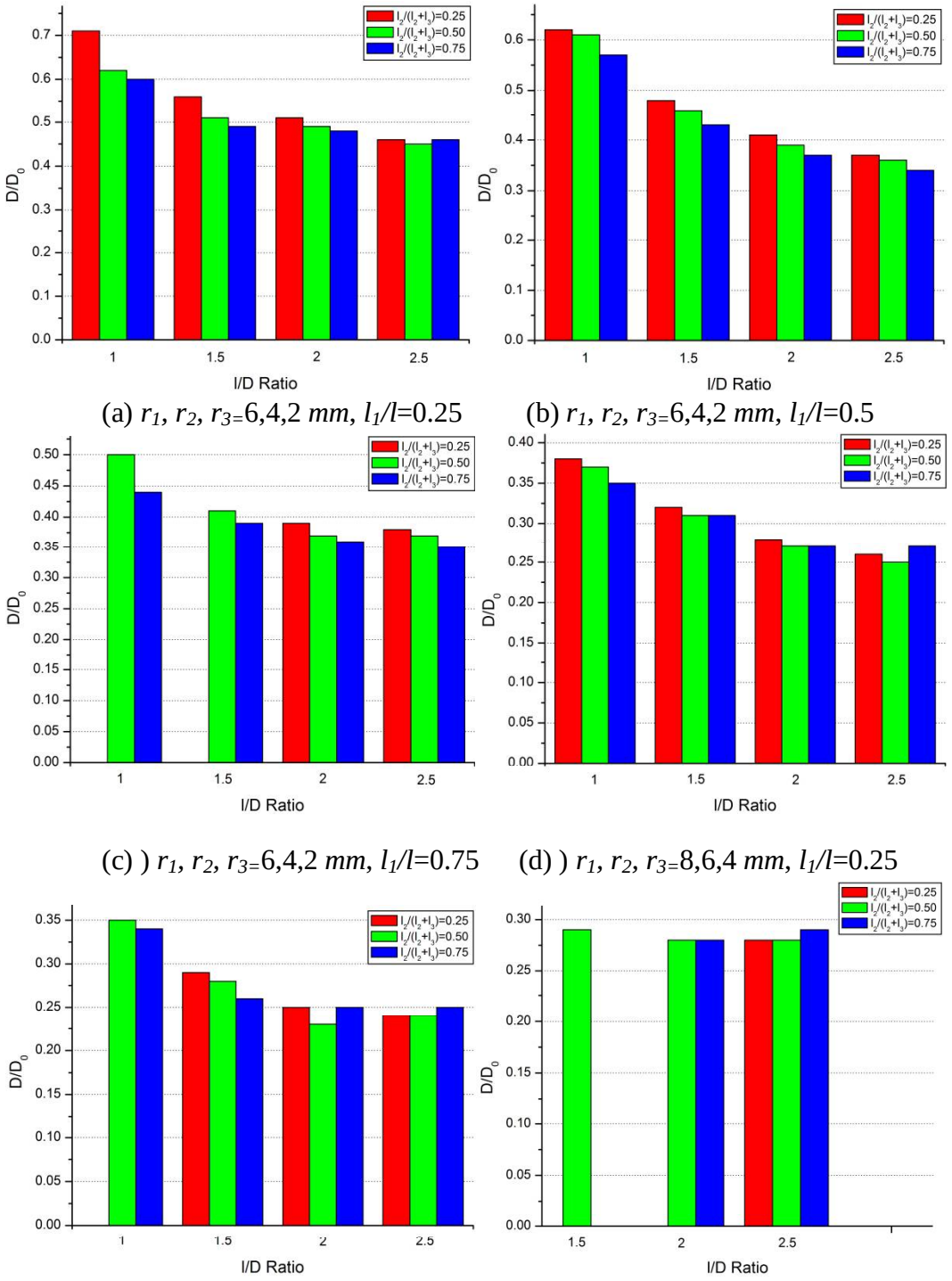

(a) r_1, r_2, r_3=6,4,2 *mm*, l_1/l=0.25

(b) r_1, r_2, r_3=6,4,2 *mm*, l_1/l=0.5

(c)) r_1, r_2, r_3=6,4,2 *mm*, l_1/l=0.75

(d)) r_1, r_2, r_3=8,6,4 *mm*, l_1/l=0.25

(e) r_1, r_2, r_3=8,6,4 *mm*, l_1/l=0.5

(f) r_1, r_2, r_3=8,6,4 *mm*, l_1/l=0.5

Fig. 5.38: Normalized drag for configurations with three flat triangular aerodisks

For longer aerospikes, when the rearmost disk is moved to forward most position an increase in drag is observed because of the high pressure drag on large disk itself. So any increase in *l/D* ratio of the flat triangular aerodisk which further moves the rear disk away from the main body offers no added reduction in drag, as can be seen in Fig 5.38 d.

5.9. Effect of Three Disk Aerospikes on Heat Transfer Rates

The local surface heat fluxes are highly affected by the presence of multiple aerodisks in front of the main body. Figure 5.39 shows the normalized local surface heat fluxes to the spiked blunt body configurations with three hemispherical aerodisks of radii with r_1*=6 mm,* r_2*=4 mm* and r_3=2 *mm*. As with all spiked configurations, there is a severe heating due to attachment of shear layer on the shoulders of the blunt body with three disks as well. As can be seen in Fig. 5.39, there is a detrimental reattachment heating on shoulders of base body with three disk configurations with r_1*=6 mm,* r_2*=4 mm* and r_3=2 *mm* for l_1/l=0.25 and l_1/l=0.5 at *l/D*=1.5. This value is about 30% to 59% higher than the stagnation point heat fluxes of base configuration, for l_1/l=0.25 and about 10% to 37% higher for l_1/l=0.5. For larger *l/D* values, some respite in peak reattachment heat fluxes is seen and even for l_1/l=0.25, the heating on the shoulders is comparable to that of the base configuration. As the rear aerodisk is moved forward favorable reductions in local surface heat fluxes can be observed as can be seen in Fig. 5.39 (e) and (f). At *l/D*=2.5, reductions of 5 to12% for l_1/l=0.5 and of 9% to 21% for l_1/l=0.75 with the hemispherical disks of sizes r_1*=6 mm,* r_2*=4 mm* and r_3=2 *mm*.
As the disk size is increased, more favorable reductions in the peak reattachment heat fluxes can be observed. For hemispherical triple disk configurations with r_1*=8 mm,* r_2*=6 mm* and r_3=4 *mm*, the peak reattachment heat flux lower to that of the base configuration for even the lowest *l/D* values of 1.

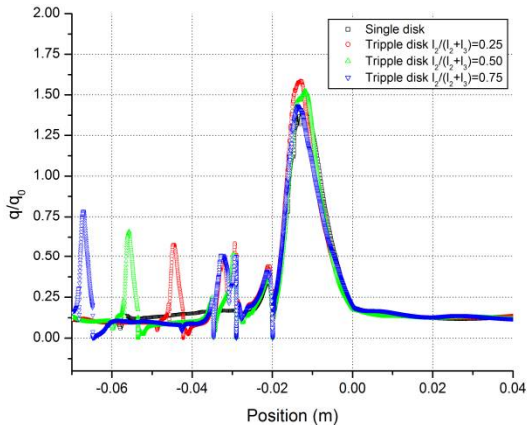

(a) l/D=1.5, l_1/l=0.25

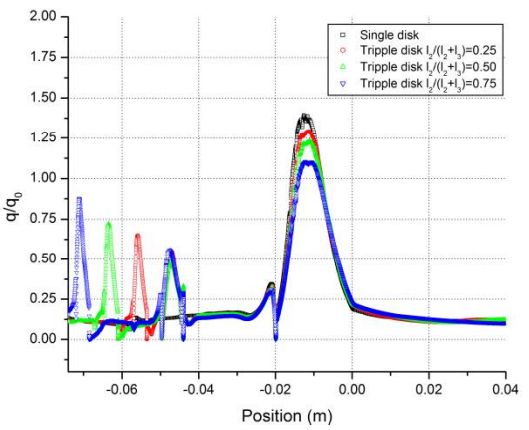

(b) l/D=1.5, l_1/l=0.5

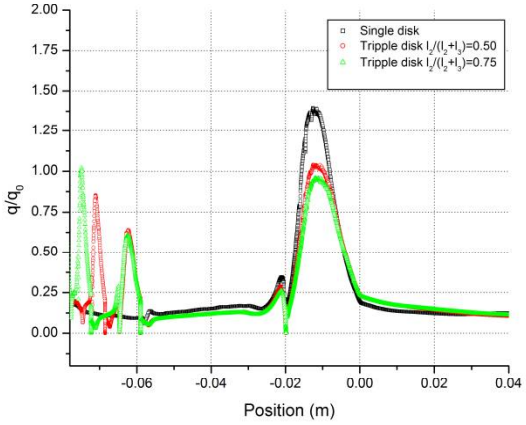

(c) l/D=1.5, l_1/l=0.75

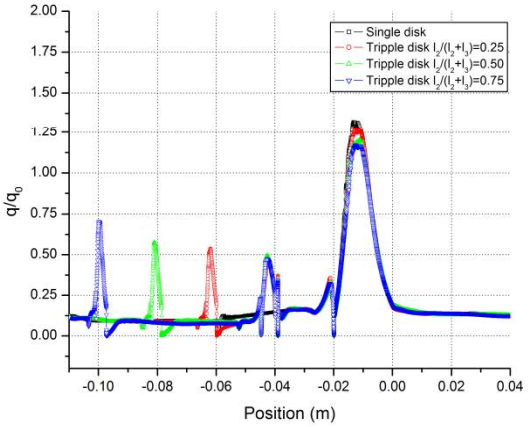

(d) l/D=2.5, l_1/l=0.25

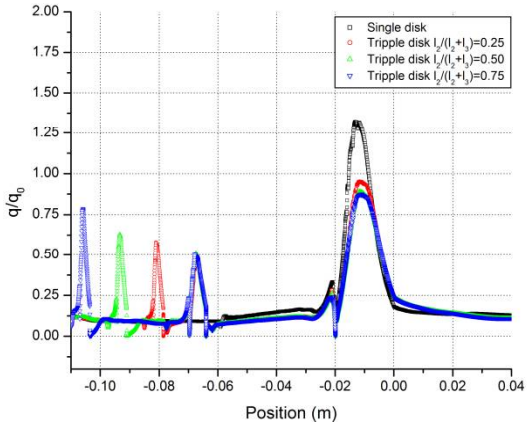

(e) l/D=2.5, l_1/l=0.5

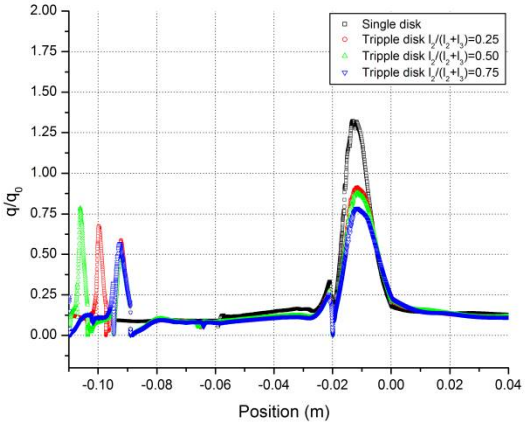

(f) l/D=2.5, l_1/l=0.75

Fig. 5.39: Surface heat flux distribution for flat aerodisk with r_1=6 *mm*, r_2=4 *mm* and r_3=2 *mm*

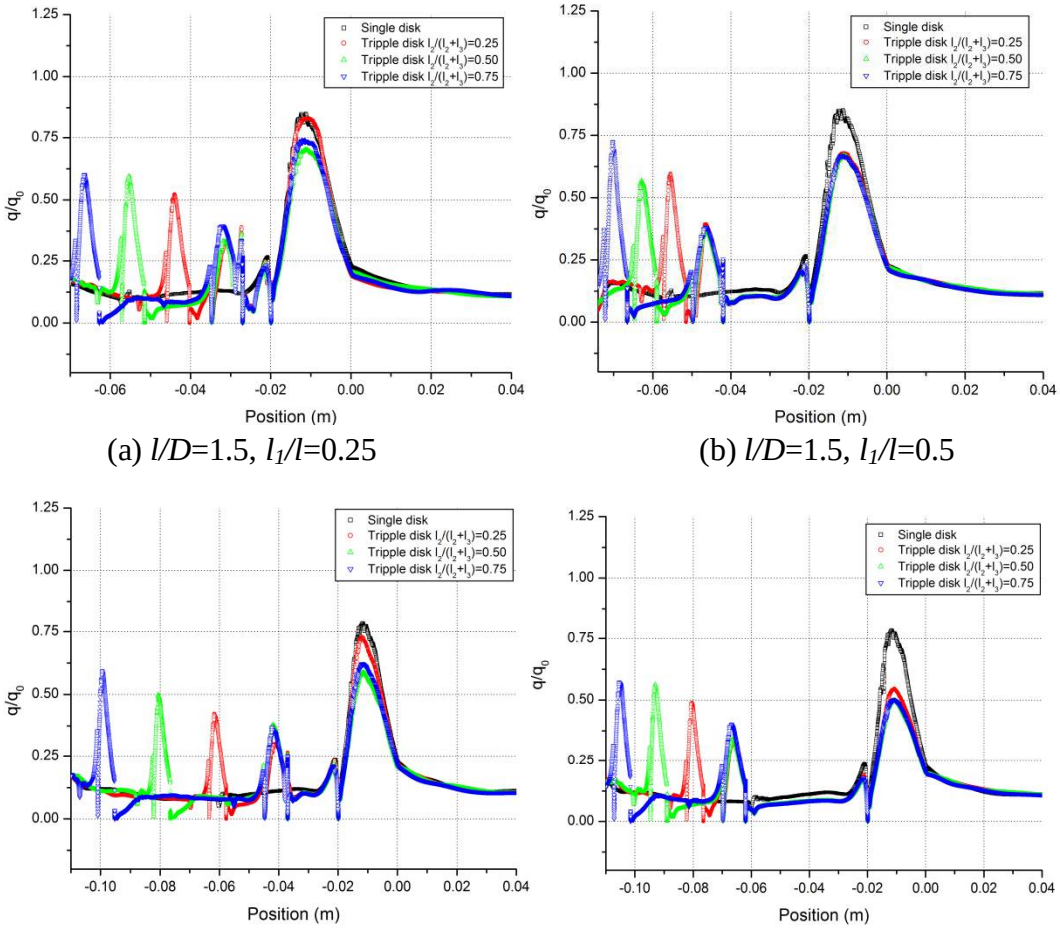

(a) l/D=1.5, l_1/l=0.25 (b) l/D=1.5, l_1/l=0.5

(c) l/D=2.5, l_1/l=0.25 (d)l/D=1.5, l_1/l=0.5

Fig. 5.40: Surface heat flux distribution for hemispherical aerodisk with r_1=*8 mm*, r_2=*6 mm* and r_3=4 *mm*

As the *l/D* of the aerospike is increased or as the rear aerodisk is moved forward more reductions in peak reattachment heat fluxes is observed as can be seen in Fig. 5.40. For hemispherical aerodisk configurations with disk sizes r_1=*8 mm*, r_2=*6 mm* and r_3=4 *mm*, and *l/D* =1.5, reductions in heat fluxes of up to 26%, 33% and 36% were obtained respectively for l_1/l of 0.25, 0.5 and 0.75. For longer aerospikes with *l/D*=2.5, the reductions were enhanced to 38%, 50% and 48% respectively for l_1/l of 0.25, 0.5 and 0.75.

A slightly diminished reduction in local surface heat fluxes at l_1/l =0.75 is because of the shear layer detaching aft of the rear aerodisk for these cases and hitting the main body at steep angles resulting in higher aftershock temperatures

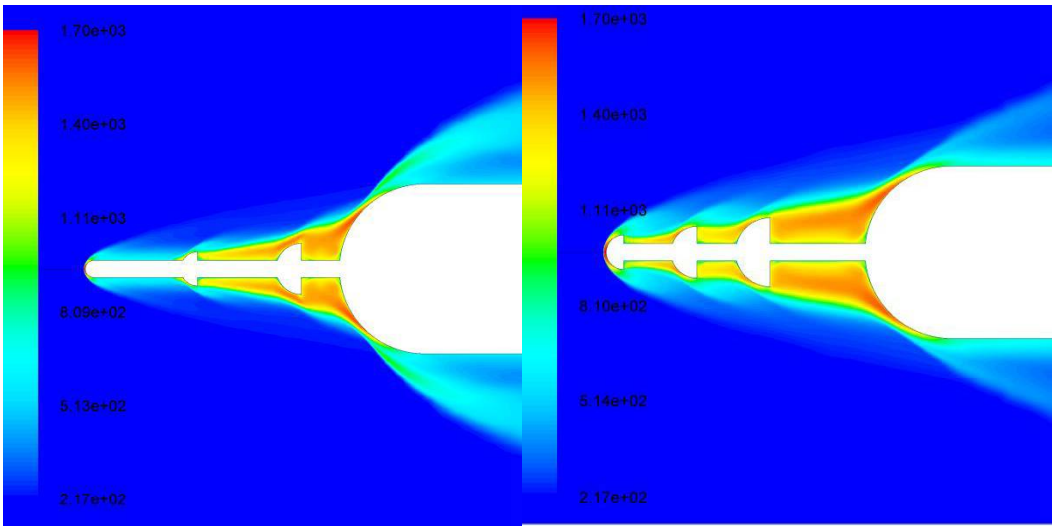

(a)l/D=1.5, l_1/l=0.5, l_2/l'=0.5 (b) l/D=1.5, l_1/l=0.5, l_2/l'=0.5

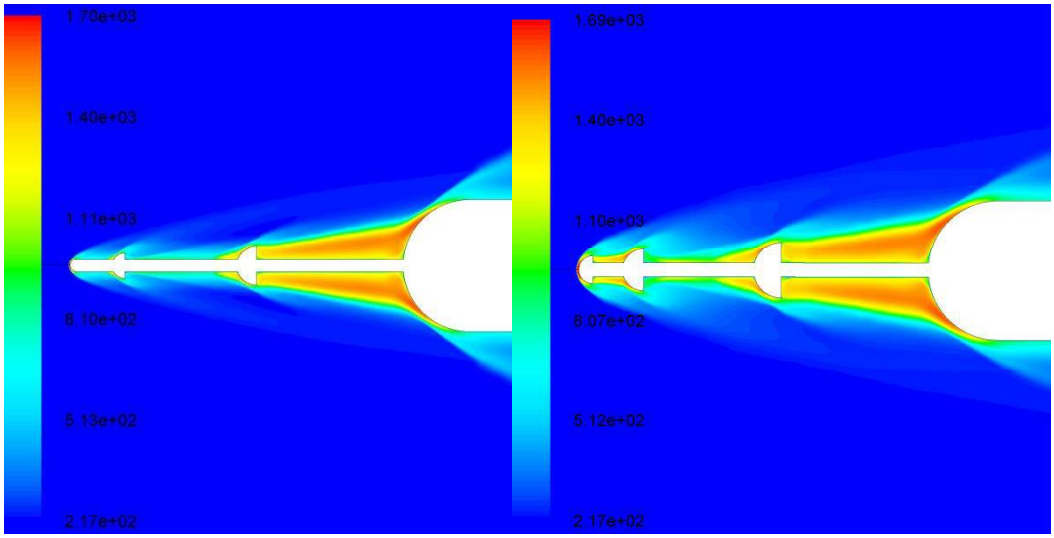

(c) l/D=2.5, l_1/l=0.5, l_2/l'=0.75 (d) l/D=2.5, l_1/l=0.5, l_2/l'=0.75

Fig. 5.41: Contours of temperatures for hemispherical three disk aerospikes with disk sizes (a), (b) r_1=*6 mm*, r_2=*4 mm* and r_3=2 *mm*, and (c), (d) r_1=*8 mm*, r_2=*6 mm* and r_3=4 *mm*

The increase in local surface heat fluxes for smaller *l/D* values in Fig. 5.39 (a), (b) and (c) can be attributed to the fact that for the smaller *l/D* configurations the shear layer detaches from the spike well ahead of the mid aerodisk, hitting the rear aerodisk, dissipating a small fraction of the heat to it, before hitting the rear aerodisk and finally impinging on the shoulders of the main body. For these cases, the shear layer is inclined to the main body at higher angle before the reattachment, causing a large after shock temperature and velocity gradient on the shoulders of the main body as can be seen in Fig. 5.41 (a) and (b).

The large temperature and velocity gradient induced causes a large heat fluxes aft of the reattachment shock wave. For longer aerospikes, the shear layer detaches just ahead of the mid aerodisk, strikes it, dissipating a large amount of heat. Thereafter the shear layer attaches on the spike stem before detaching again to the hit the rear aerodisk, dissipating further amount of heat to the rear aerodisk. Finally a very weak shear layer inclined at very low angles to the aerospike attaches on the main body, as can be seen in Fig. 5.41 (c) and (d), dissipating a considerably lower heat fluxes.

For the same *l/D* values, shear layer for the configurations with larger radii disks are substantially deflected by mid and rear disks and become less inclined to the spike axis. This results in relatively lower post shock temperature and hence a reduced local heating.

Similar to the hemispherical aerodisk, the triple flat aerodisks also offers significant reductions in heat fluxes for larger of *l/D* as can be seen in Fig. 5.42 and 5.43. Figure 5.42 shows the surface heat flux distributions for selected cases with r_1*=6 mm*, r_2=4 and r_3=2 *mm* while Fig. 5.43 shows the same for similar configurations with r_1*=8 mm*, r_2=6 and r_3=4 *mm*. For shorter flat triple aerodisks with r_1*=6 mm*, r_2=4 and r_3=2 *mm*, the peak reattachment heat fluxes is severe for *l/D*=1, with about 55% to 35% increase as compared to the base configuration.

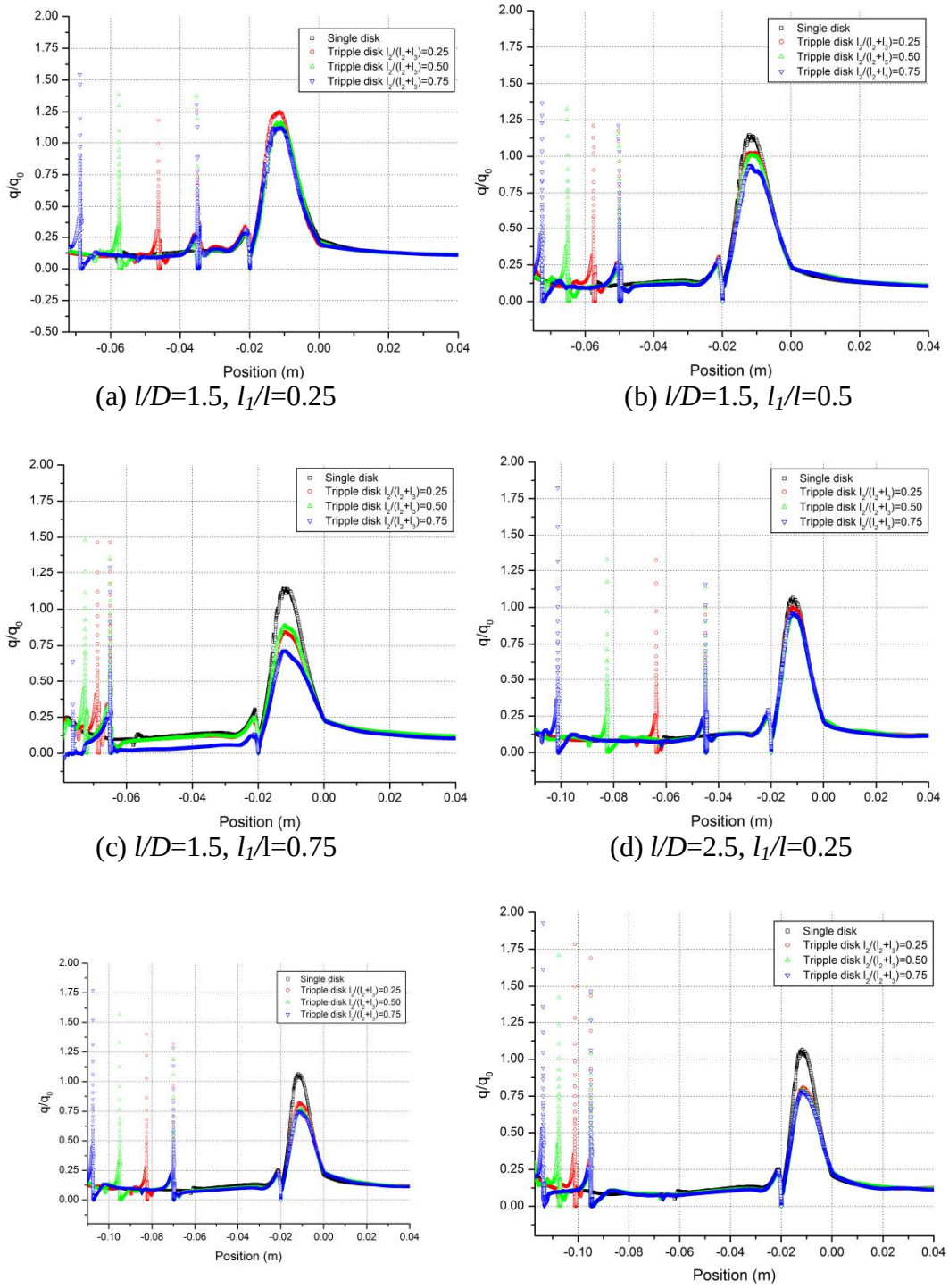

(a) l/D=1.5, l_1/l=0.25 (b) l/D=1.5, l_1/l=0.5

(c) l/D=1.5, l_1/l=0.75 (d) l/D=2.5, l_1/l=0.25

(e) l/D=2.5, l_1/l=0.5 (f) l/D=2.5, l_1/l=0.75

Fig. 5.42: Surface heat flux distribution for flat aerodisk with r_1=6 *mm*, *r2=4* and r_3=2 *mm*

As the length of the aerospike is increased, the peak reattachment heat fluxes fall gradually to values 25% to 12% higher than the base value for l/D=1.5 at l_1/l =0.25. These values further diminish as the l_1/l is increased to 0.5 or 0.75. As can be seen in Fig. 5.42, at l/D=1.5, a reduction of up to 22% can be achieved for l_1/l =0.75 with l_2/l'=0.75 as well. For the highest l/D investigated, i.e. 2.5, the flat aerodisks give about 21% reduction in peak heat fluxes to the main body, which is much higher, a reduction as compared to that of hemispherical aerodisks. Although a significant reduction in heat fluxes can be seen for flat disks, a severe heating at the sharp edges of the mid aerodisks can be seen. The heating is due to the small surface area of the edge on which the shear layer impinges. This heating is about 1.5 times the peak heating of the base configuration and increases as the l/D ratio is increased or as the mid aerodisk is moved ahead towards the bow shock. The heating on the sharp edges for l/D=2.5 and l_1/l =0.75 can go up to 1.9 times the peak heating of the base configuration. These detrimental heating rates at sharp edges continue even if the radii of the disks are increased to larger sizes. The heating in all cases however, remains below 200% of the peak heating of the base configuration.

As the disk radii is increased to r_1=*8 mm*, r_2=6 and r_3=4 *mm*, more favorable heat reductions could be observed. With such large disks, a substantial reduction heat flux was obtained at lower l/D values itself as can be seen in Fig. 5.43. Even for an l/D ratio of 1, reductions of about 40% to 48% were observed for various values of l_1/l and l_2/l'. These reductions were enhanced to about 54% to 58% for l/D value of 2.5 and l_1/l ratio of 0.5 or 0.75, as can be seen in Fig. 5.43 (e) and (f).

The surface heat flux distribution for flat triangular aerodisk configurations is pretty similar to the heat flux distribution for the flat aerodisk configurations and thus the figures are not repeated here. Due to a slanting backward face of the disks, the peak heating of the individual aerodisks is slightly lower for the flat triangular aerodisks as compared to the flat aerodisks.

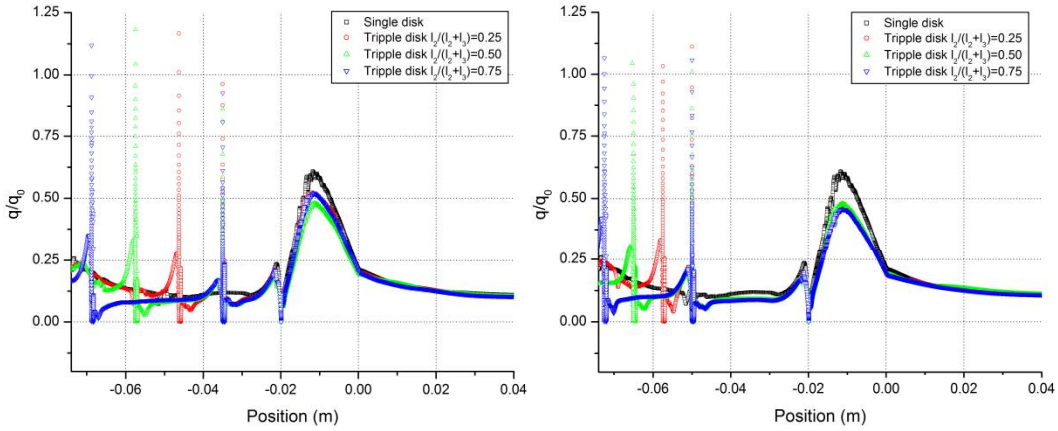

(a) l/D=1.5, l_1/l=0.25 (b) l/D=1.5, l_1/l=0.5

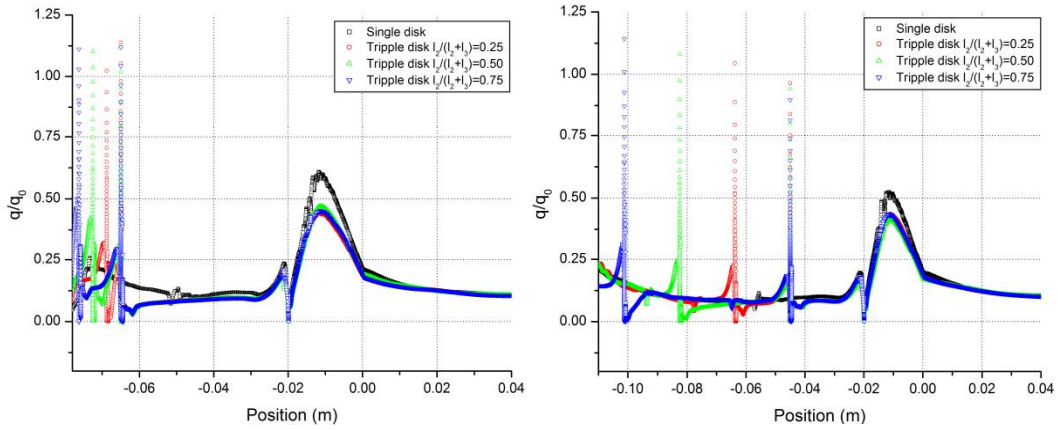

(c) l/D=1.5, l_1/l=0.75 (d) l/D=2.5, l_1/l=0.25

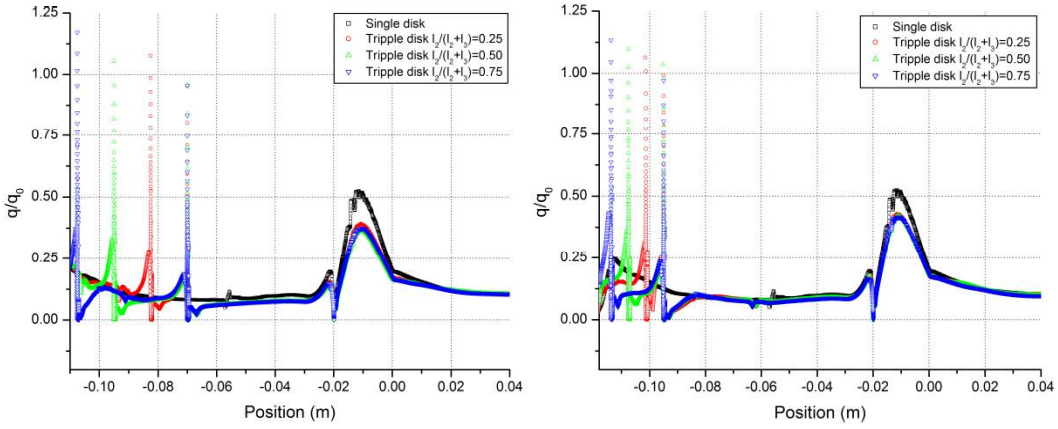

(e) l/D=2.5, l_1/l=0.5 (f) l/D=2.5, l_1/l=0.75

Fig. 5.43: Surface heat flux distribution for flat aerodisk with r_1=*8 mm*, *r2=6* and r_3=4 *mm*

Nevertheless, the triple disk aerospike configurations with flat triangular aerodisks produce almost exact reductions in peak reattachment heat fluxes for all geometric arrangements of the aerodisks. In cases where the results differ, for example the case with *l/D*=1.5, the differences are less a couple of percentages.

The surface integral of the local heat flux distribution over the main body accounts for the total heat transfer rates to it. This is an important measure of the aerodynamic heating of a hypersonic vehicle. Figure 5.44 shows the total heat transfer rates to main body of the spiked configurations with three hemispherical aerodisks, normalized with the total heat transfer rates to the base configuration without any spike. As can be seen in Fig. 5.44 (a), (b) and (c), for disk size of r_1=6 *mm*, r_2=4 *mm* and r_3=2 *mm*, there is an increase in the total transfer rates to the main body as compared to the base configuration. The total heat transfer rates however, reduces as the *l/D* of the spike is increased or as the rear aerodisk is moved forward or as the mid disk is moved forward a given *l/D* ratio. For *l/D* ratio of 1, the heating rate as high as 33% more than that of base body heat transfer rate is observed at l_1/l=0.25 and l_2/l'=0.25.

With disk size of r1=*6 mm*, r2=4 *mm* and r3=*2 mm*, the only case wherein some reduction total heat transfer rates is observed is the configuration with l1/l=0.75 and l2/l'=0.75, giving a small reduction of 7% in total heat transfer rates as compared to the base configurations. The larger sized hemispherical aerodisks with disk size of r1=*8 mm*, r2=6 *mm* and r3=*4 mm* offers much favored reductions in total heat transfer rates to the main body. Even for an *l/D*= 1, the heating rates are comparable to that for the base configurations and not higher than that configuration.

With an increase in the *l/D* ratio, a reduction of about 20% can be achieved at a lower l_1/l value of 0.25 as can be seen in Fig. 5.44 (d). For this l_1/l of 0.25, as the *l/D* ratio is increased from 2 to 2.5 for an l_2/l' of 0.25, the total heating rate remains unchanged at about 13% lower than the base body heating.

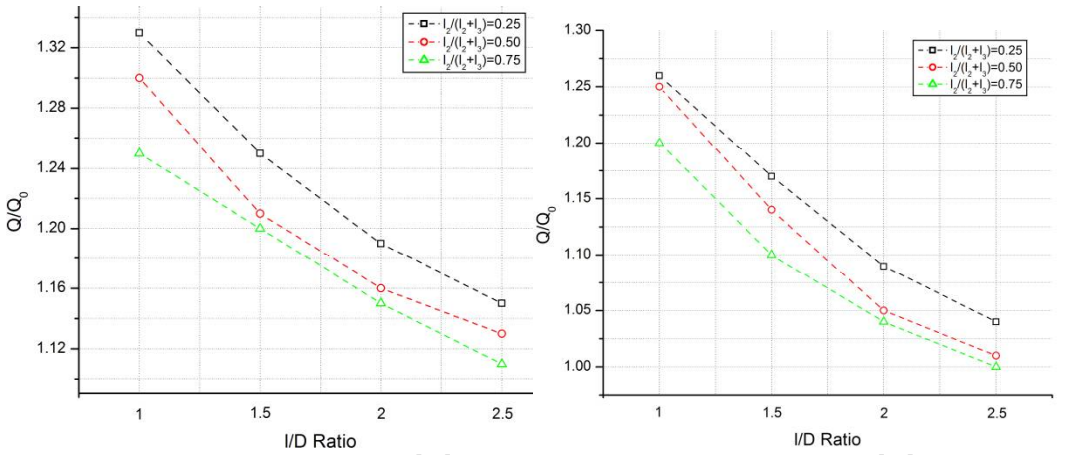

(a)) r_1, r_2, r_3=6,4,*2 mm*, l_1/l=0.25 (b) r_1, r_2, r_3=6,4,*2 mm*, l_1/l=0.5

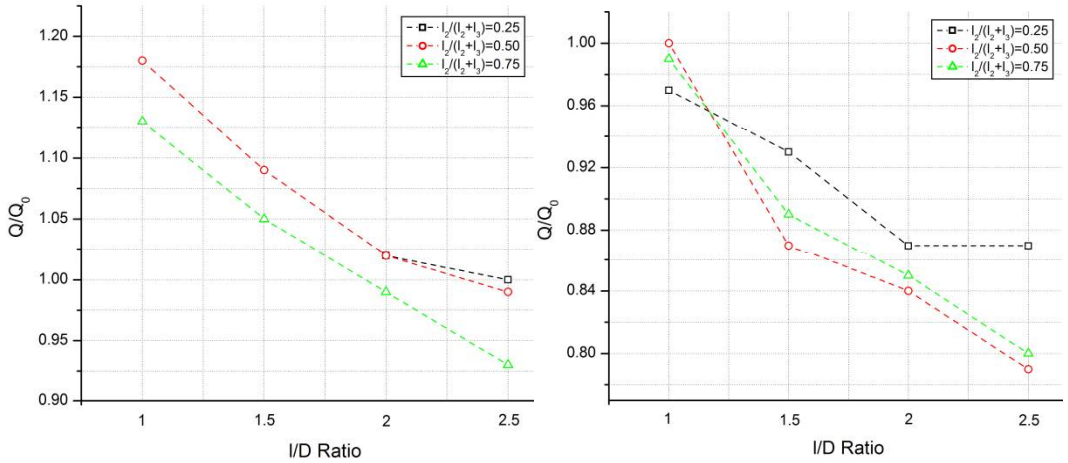

(c) r_1, r_2, r_3=6,4,*2 mm*, l_1/l=0.75 (d) r_1, r_2, r_3=8,6,*4 mm*, l_1/l=0.25

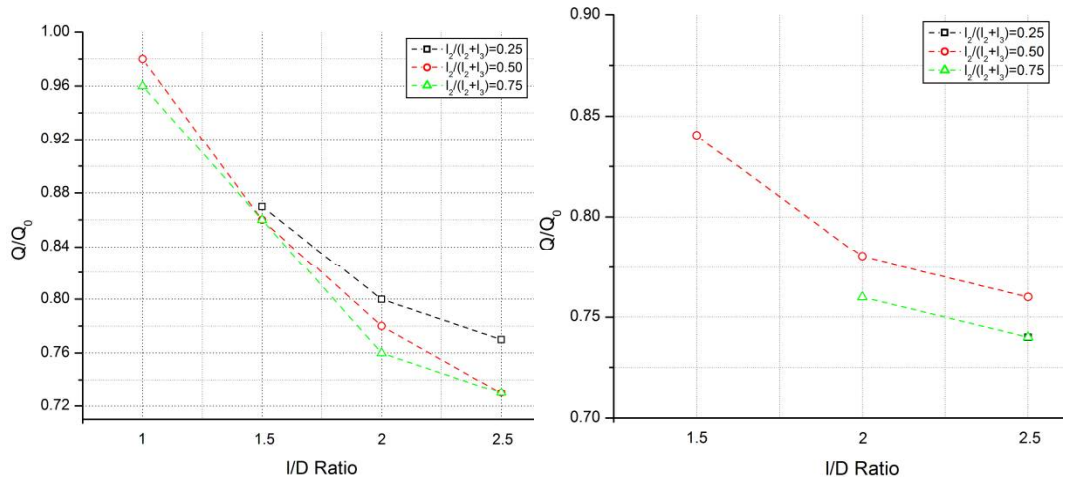

(e) r_1, r_2, r_3=8,6,*4 mm*, l_1/l=0.5 (f) r_1, r_2, r_3=8,6,*4 mm*, *l1/l*=0.75

Fig. 5.44: Total heat transfer rates for various hemispherical triple aerodisk

Such a behavior is primarily observed because of the largest aerodisk dominating the heat transfer rates to the main body. For this configuration, the shear layer detached ahead of the mid aerodisk and strikes the rear aerodisk which dissipates a large amount of heat. A the rear disk is very large and very close to the main body, an increase in *l/D* by 0.5 which shifts the rear aerodisk by 0.5*0.25*0.25D forward does not alter the configuration of shear layer much and hence a similar total heat transfer rates. For larger values of l_1/l and with longer aerospikes the triple hemispherical aerodisks can give up to 27% reduction in total transfer rates as can be seen in Fig. 5.44 (e) and (f).

The total heat transfer rates to spiked configurations with three flat aerodisks is slightly better than those with three hemispherical aerodisks as can be seen in Fig. 5.45. Flat aerodisk configurations with even smaller disk sizes of r_1*=6 mm*, r_2=4 *mm* and r_3*=2 mm mm* give small reductions of about 4% to 8% total heat transfer rates at high *l/D* values of 2 and 2.5. For r_1*=6 mm*, r_2=4 *mm* and r_3*=2 mm* flat aerodisks with l_1/l=0.75, any increase in *l/D* from 2 to 2.5 does not reduce the heat transfer rates any further. For these longer aerospikes the shear layer detaches from aft of the rear aerodisk increasing the heat fluxes to the main body and the effectiveness of high *l/D* values is lost.

With the flat aerodisk configurations of larger disk sizes of r_1*=8 mm*, r_2=6 *mm* and r_3*=4 mm*, a substantial reduction in total heat transfer rates is obtained at all *l/D* ratios and internal positions of the rear and the mid aerodisk. For *l/D* ratio of 1, these larger flat aerodisks give reductions of 19%-25% in heat transfer rates for various positions of the intermediate aerodisks. The reductions in total heat transfer rates improve as the l_1/l ratio is increased or as the l_2/l' ratio is increased.

As the *l/D* ratio these r_1*=8 mm*, r_2=6 *mm* and r_3*=4 mm* flat aerodisks is increased, gradual reductions in total heat transfer rates are observed till *l/D* ratio of 2. At this *l/D* ratio, reductions of about 29-33% at l_1/l =0.25, 35-36% at l_1/l =0.5 and 35-39% at l_1/l =0.75 is observed.

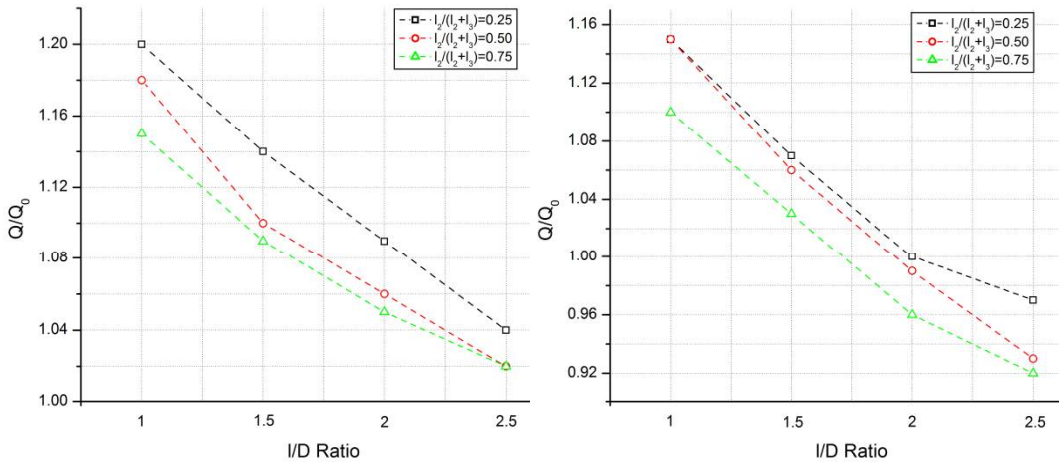

(a) r_1, r_2, r_3=6,4,*2 mm*, l_1/l=0.25 (b) r_1, r_2, r_3=6,4,*2 mm*, l_1/l=0.5

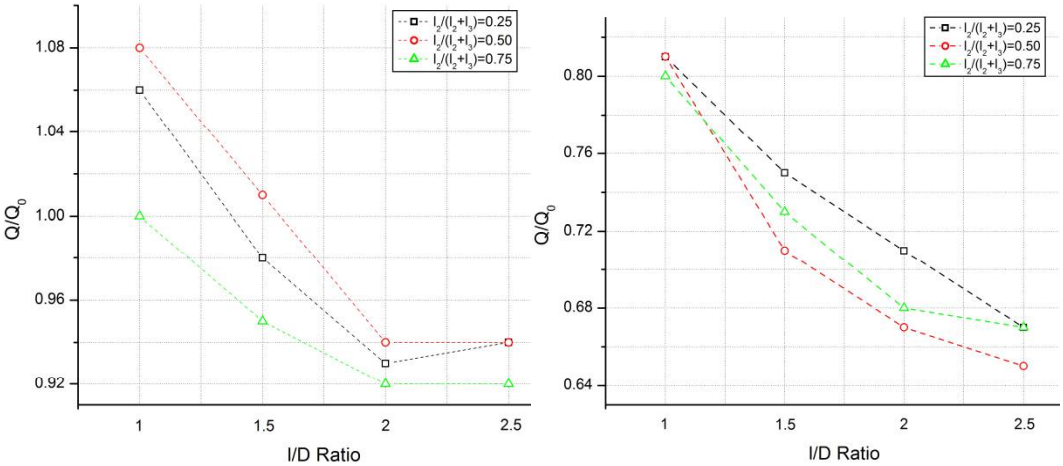

(c) r_1, r_2, r_3=6,4,*2 mm*, l_1/l=0.75 (d) r_1, r_2, r_3=8,6,*4 mm*, l_1/l=0.25

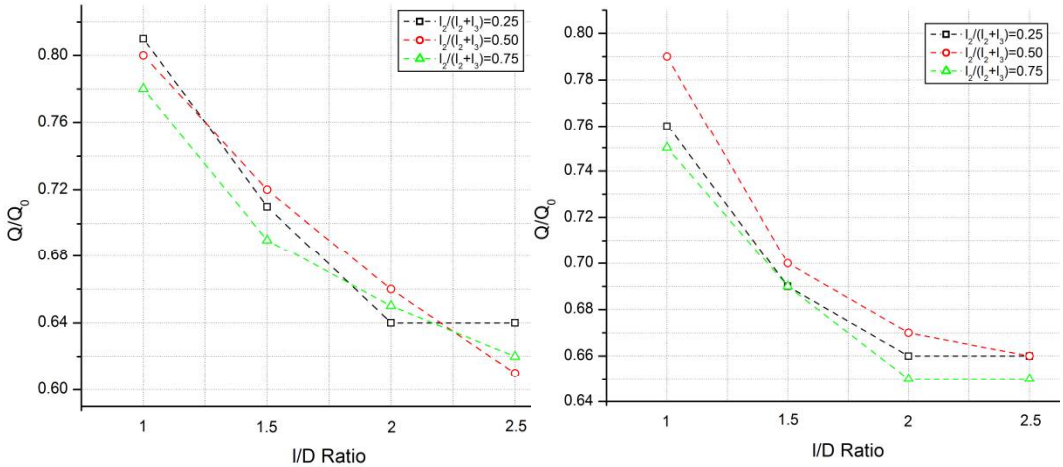

(e) r_1, r_2, r_3=8,6,*4 mm*, l_1/l=0.5 (f) r_1, r_2, r_3=8,6,*4 mm*, l_1/l=0.75

Fig. 5.45: Total heat transfer rates for various hemispherical triple aerodisk configurations

As the *l/D* ratio is increased to 2.5, only a slight reduction in total heat transfer rates is seen for a few cases. For the cases with l_1/l =0.75, no additional reduction in total heat transfer rates is seen when *l/D* ratio is increased to 2.5 from 2 as once the shear layer detachment point moves to a point aft of the rear disk, any movement of upstream aerodisk does not alter the heat fluxes to the main body. Nevertheless the triple flat aerodisk give a maximum reduction of 39% in total heat transfer rates which if far superior to that provided by the triple hemispherical aerodisks with just 27% maximum reduction.

The flat triangular aerodisks provides reductions in total heat transfer rates that are similar to those provided by flat disks. For shorter aerospikes with *l/D*=1, the flat triangular gives a slightly lesser increase in total heat transfer rates as compared to flat aerodisks of same size and configurations. But as the *l/D* ratio is increased, the differences in reductions provided by the two shapes become negligible. The highest reduction in total heat transfer rates provided by the flat triangular aerodisk is also about 38% for *l/D*=2, l_1/l=0.5 and l_2/l'= 0.5.

5.10. Comparisons between Single, Double and Three Disk Aerospikes

The effectiveness of aerospikes and aerodisks in reducing aerodynamic drag at supersonic and hypersonic speeds is already established. Its effect on aerodynamic heating is however, is not very clear and depends a lot on the behavior of the boundary layer. The addition of multiple disks on the aerospike seems to reduce the aerodynamic drag further as can be seen in Fig. 50, which shows the drags for a few selected spiked configurations with hemispherical and flat aerodisks.

As can be seen in Fig. 5.46a, for hemispherical aerodisks the single disk configuration with disk radius of 4 *mm* gives about 59% reduction in drag at *l/D*=1.5. The hemispherical double disk configurations with same radii of front aerodisk give drag reductions of 60% and 65% at l_1/l=0.5 and l_1/l=0.75 respectively for *l/D*=1.5.

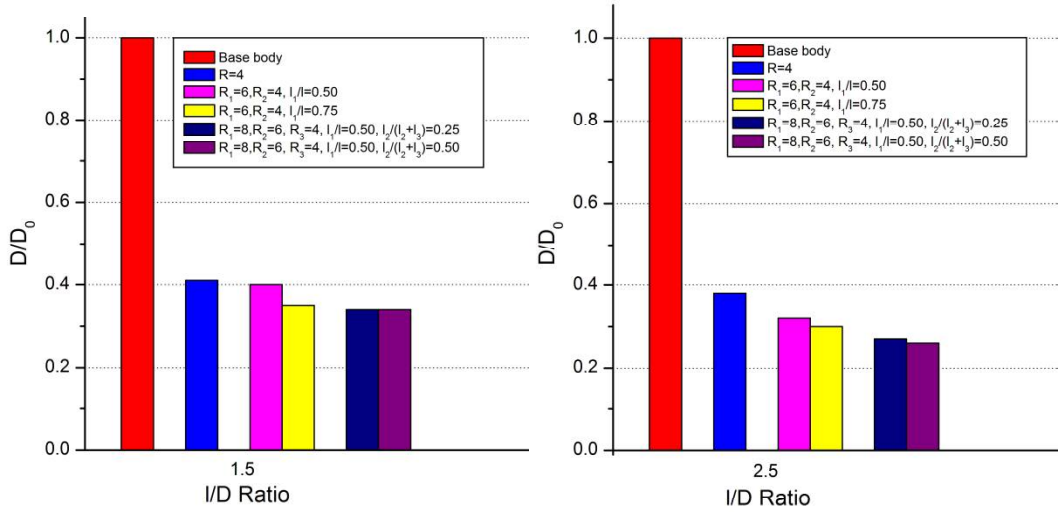

(a) Hemispherical Aerodisks, *l/D*=1.5 (b) Hemispherical Aerodisks, *l/D*=2.5

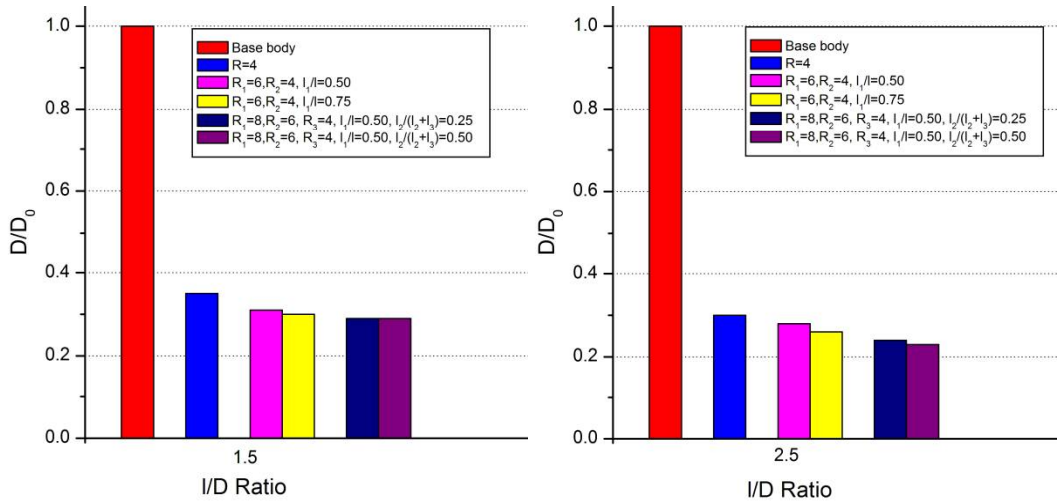

(a) Flat aerodisks, *l/D*=1.5 (b) Flat aerodisks, *l/D*=2.5

Fig. 5.46: Comparison of drag for selected single and multiple disk spiked configurations

The three disk configurations with same front disk size give 66 to 67% reductions in drag for *l/D* ratio of 1.5. Thus for smaller *l/D* ratios, the multiple disk hemispherical gives a marginal advantage over single disk aerospike for drag

reduction. For longer aerospikes the situation improves slightly as can be seen in Fig. 50b. At *l/D* ratio of 2.5, the 4 *mm* single hemispherical aerodisk offers about 62% reduction in drag while the two disk aerospikes offer 68% and 70% reductions at l_1/l=0.5 and 0.75 respectively. The three disk configurations offer a still higher reduction between 73% and 74% in aerodynamic drag.

For flat aerodisks also the effect of multiple aerodisk on drag reductions are similar. The single flat aerodisk of size 4 *mm* gives a reduction of 65% in drag at *l/D*=1.5 while the two flat disk aerospikes with same size of the front aerodisk and *l/D* ratio give better reductions of about 69% to 70%. For three flat aerodisks, these reductions scale up marginally to 72%. At a higher *l/D* ratio of 2.5, the maximum reductions given by flat aerodisk of radius 4 *mm* is 70% for single aerodisk, 74% for double aerodisk and 77% for treble aerodisks as can be seen in Fig. 5.46 d.

It is clear from the above results that although the use of multiple aerodisk improves the drag reduction for a spiked blunt body at hypersonic speeds, the improvements are however, small. Nevertheless the drag for spiked configurations with three disks is less than that for configurations with two disks, for all other parameters being the same. Similarly the drag for spiked configurations with two disks is less than that for configurations with single disk. The reductions in the drag for spiked configurations with multiple aerodisks are due to reduced stagnation pressure and peak reattachment pressure on the shoulders of the main body as can be seen in Fig. 5.47. As can be seen in fig.5.47, the peak reattachment pressure on shoulder of the main body is significantly lower for spiked bodies as compared to the stagnation pressure for the base configurations. These peak reattachment pressures fall gradually as the number of aerodisks is increased from zero to three for both hemispherical and flat disk shapes. As compared to the single disk aerospikes, at *l/D*=2.5, the peak reattachment pressure is reduced by approximately 25% for two disk configurations and by 50% for the three aerodisk spiked configurations.

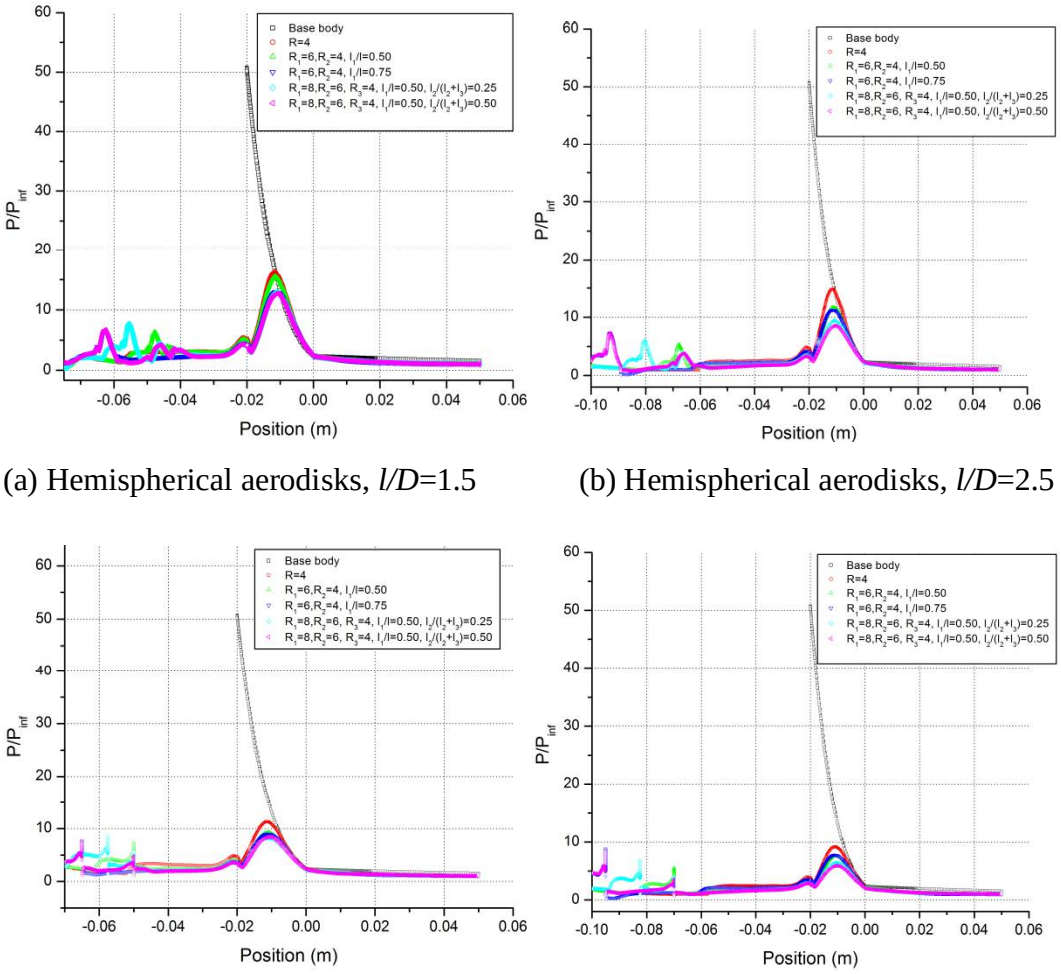

(a) Hemispherical aerodisks, *l/D*=1.5 (b) Hemispherical aerodisks, *l/D*=2.5

(c) Flat aerodisks, *l/D*=1.5 (d) Flat aerodisks, *l/D*=2.5

Fig. 5.47: Comparison of surface pressure distribution for selected single and multiple disk spiked configurations with front disk size of *4 mm*

These reductions in peak reattachment pressures are however, not translated completely into drag reductions as there are only small added reductions in drag as the number of disk is increased from one to two and three. These diminished reductions are due to the fact that as the number of aerodisks increases, the wetted surface area increases, which in turn increase the viscous drag. This increase in viscous traction diminishes slightly, the advantages gained by reduced reattachment pressures for the multiple aerodisk spiked body. Also, as the size of the disks increases, the peak pressures on the aerodisks increases. As a large

amount of kinetic energy is converted to pressure energy and dissipated as heat at the aerodisks, the kinetic energy of the fluid wetting the main body is less, which results in lowered reattachment pressure on the main body. But the increased pressures on the relatively larger aerodisks means a slight increase in the overall drag of the configuration. Nevertheless the multiple disk aerospikes are superior to single disk aerospike in drag reduction at hypersonic speed of 6.2.

The local surface heat fluxes are greatly modified by the presence of multiple aerodisks. Despite large local heat fluxes at the front and the intermediate aerodisk, the reattachment heat flux at the point of reattachment of the shear layer on the shoulder of the main body, is relatively very high. For very small radii of the front aerodisk i.e. r_1=2 *mm* the peak reattachment heat flux is higher than that for the base configuration. But for the larger aerodisk spiked configurations, the peak reattachment heat fluxes are lower than that of the base configurations as can be seen from Fig. 5.48, which shows the normalized local surface heat fluxes for selected spiked configurations with front disk radii of 4 *mm*. These reductions in heat fluxes however, should be interpreted completely within the ambit of assumptions made especially of the freestream turbulence levels. Nevertheless, for hemispherical aerodisks with front disk radius of 4 *mm*, the reduction of 15% in peak heat fluxes at *l/D*=1.5 improves to 27% with two aerodisks and improves further to 33% with three hemispherical aerodisks. At a higher *l/D* ratio of 2.5, the reduction of 21% with single hemispherical disk with radius 4 *mm* improves to 33% with two aerodisks and to 50% with three hemispherical aerodisks with the same radius of the front aerodisk. The flat aerodisks are much superior in reducing the reattachment heat flux to the main body. A single flat aerodisk of radius 4 *mm* gives a reduction of 39% at an *l/D* ratio of 1.5. At the same *l/D* ratio and radius of the front aerodisk, the spiked configurations with two flat aerodisks give reductions of about 48% which further improves to 54% for three aerodisks. As can be seen in Fig. 5.48 d, for an *l/D* ratio of 2.5 a single flat aerodisk of radius 4 *mm* gives a reduction of 47% in peak reattachment heat fluxes which increases to 54% for two disks and goes up to 63% for the three flat disk configurations.

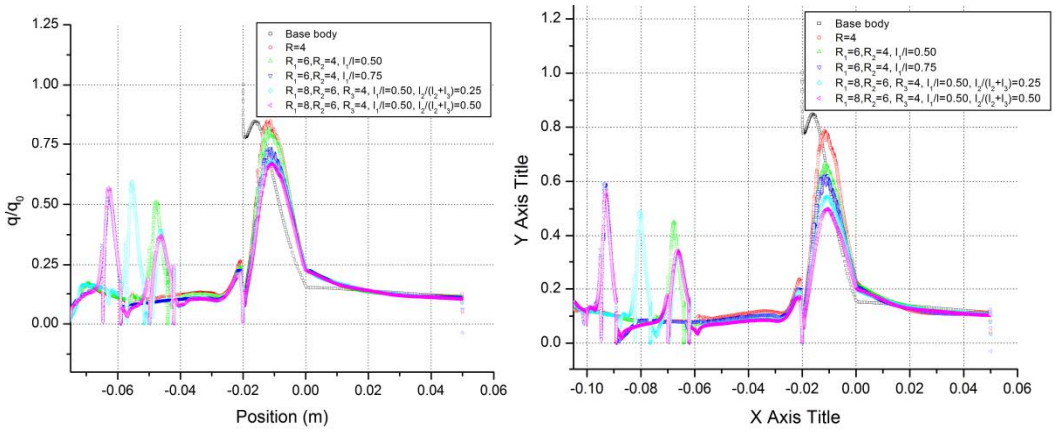

(a) Hemispherical aerodisks, *l/D*=1.5 (b) Hemispherical aerodisks, *l/D*=2.5

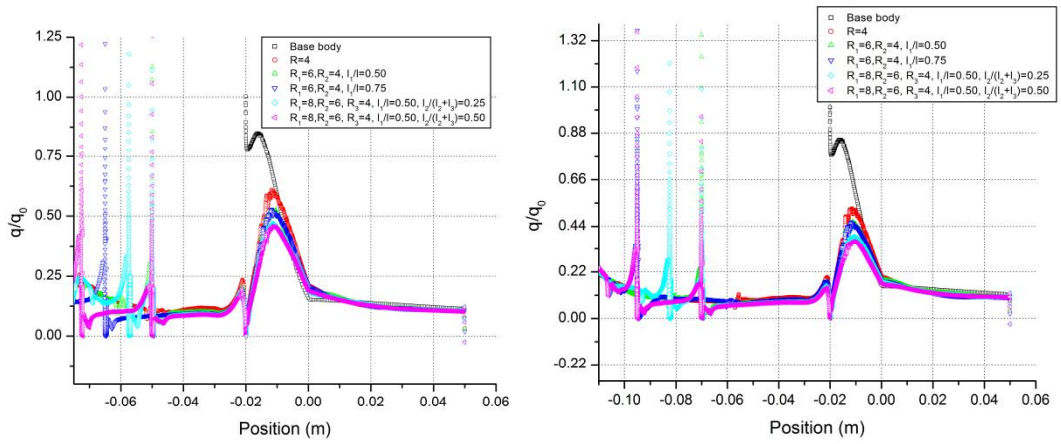

(c) Flat aerodisks, *l/D*=1.5 (d) Flat aerodisks, *l/D*=2.5

Fig. 5.48: Comparison of surface heat flux distribution for selected single and multiple disk spiked configurations with front disk size of *4 mm*

The superiority of multiple aerodisk spiked configuration over single aerodisk configurations in reducing peak reattachment heat fluxes is thus squarely established. The above statement is true more so for longer spikes with large *l/D* values. The reductions in peak reattachment heat fluxes also account for a reduced total heat transfer rates to the main body as shown in Fig. 5.49 which shows the normalized total heat transfer rates for selected hemispherical and flat aerodisk configurations with front disk radii of 4 *mm*.

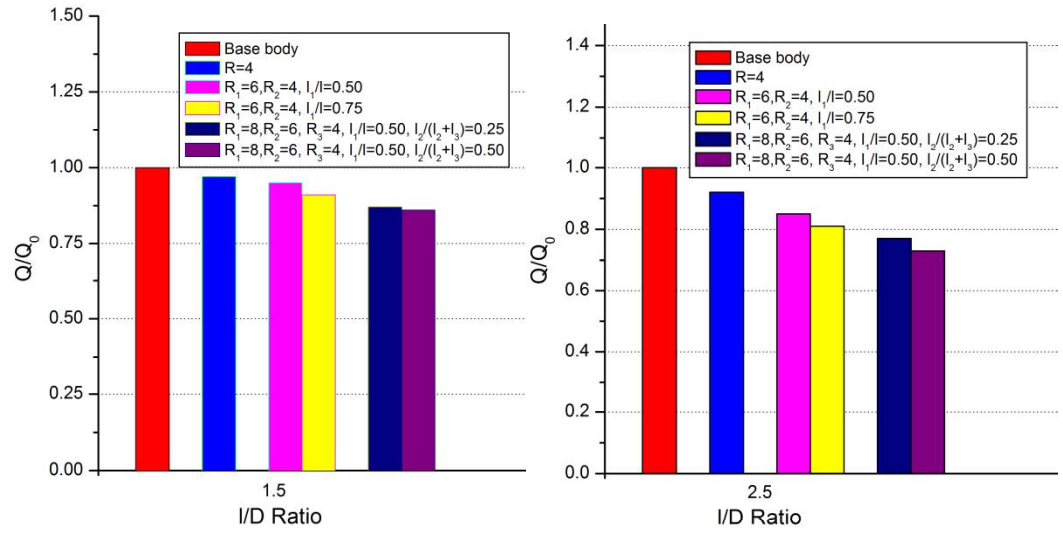

(a) Hemispherical aerodisks, *l/D*=1.5 (b) Hemispherical aerodisks, *l/D*=2.5

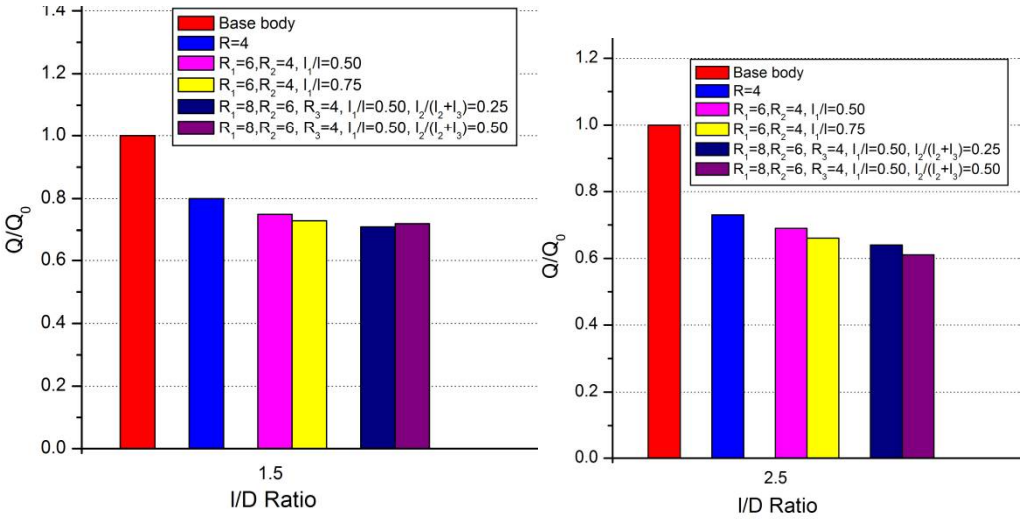

(c) Flat aerodisks, *l/D*=1.5 (d) Flat aerodisks, *l/D*=2.5

Fig. 5.49: Comparison of total heat transfer rates for selected single and multiple disk spiked configurations with front disk size of *4 mm*

For hemispherical aerodisk with *l/D*=1.5, the single disk configuration offers an insignificant reduction of 3% in total heat transfer rates while the configurations with two and three aerodisks offer reductions of up to 9% and 16% respectively. For longer aerospikes of *l/D*=2.5, these reductions go up to 8% for single

hemispherical aerodisk, 19% for double disk spiked configurations and 27% for the three hemispherical aerodisk configurations.

The reductions in total heat transfer rates to the main body are emphasized further for the flat aerodisk spiked configurations with the single aerodisk of size 4 *mm* and *l/D*=1.5 itself, giving out a reduction of 20% in total heat transfer rates. As the number of aerodisk is increased to two with same front disk radius and overall *l/D* of 1.5, the reductions scale up to 27% which further scales up to 31% for three flat aerodisk configurations. For an *l/D* ratio of 2.5, the reductions in total heat transfer rates provided by the flat aerodisks of front radius 4 *mm* goes up to 27% for single disk, up to 34% for double disks and up to 39% for the treble disk configurations.

The use of multiple aerodisk aerospikes at the nose of a blunt body certainly seems to be advantageous for the purpose of reduction of aerodynamic drag and heating. It is observed in the ambit of current research that two aerodisk configurations outperform single aerodisk configuration in terms of heat and drag reductions. The three aerodisk configurations however yield only a marginal reduction in aerodynamic drag over the two disk configurations. For reduction of heat fluxes and heat transfer rates though, the three disk configurations are extremely advantageous and give much larger reductions are compared to the two disk configurations. All the reductions provided by the multiple aerodisk configurations improve with increasing radii of the aerodisks except for very long aerospikes with a large disk sizes have diminished drag reductions. Among the shapes of disks investigated, the flat aerodisks are much superior to the hemispherical aerodisk in terms of both drag reduction and the reduction of local and total heat transfer rates to the main body but are associated with a very large local heat fluxes at the sharp edges of the disks. The flat triangular aerodisks performs almost same as the flat aerodisks with added advantage of not so high local heat fluxes at the aerodisks itself.